The Design of Light-Weight Trains

By R. EKSERGIAN,[1] PHILADELPHIA, PA.

New materials of construction have permitted the design of passenger trains of exceptionally light weight, which are capable of high speeds. The author discusses the economics of light-weight construction and deals with the relation of horsepower per ton to train performance under varying conditions of streamlining and weight. The importance of low-frequency spring reactions for light-weight cars is stressed. The paper then deals with the physical properties of stainless steel with consideration of the stability of thin-web structures.

It closes with the consideration of the major characteristics involved in the design of light-weight car structures as exemplified by the Burlington "Zephyr" in connection with which an effort was made to develop a rational basis of determining redundant reactions in the several indeterminate features involved in the structure.

1—ECONOMICS OF LIGHT-WEIGHT TRAINS

A PRIMARY difficulty in the development of motorized trains, particularly when propelled by self-contained units as is the case with Diesel- and gas-engine-electric drives, has been the limited power available per ton of train weight. On the power side advances have been made by the increase of rotative speeds, higher compression ratios, and better combustion performance, together with refinement in design. These have resulted in increased weight efficiencies for engine units as well as similar refinements and improved control, e.g., the differential and torque field control in the electric equipment.

Until lately, however, very little effort has been made in the reduction of equipment weight. Of the distinct light-weight class, there first appeared last year the Texas & Pacific train of stainless steel, next the aluminum Union Pacific train, and more recently the Burlington *Zephyr*. The last two have nearly comparable weights and similar performance, with approximately 600 engine horsepower and an operating efficiency of more than 4 hp per ton available at the rail.

To attain this performance and corresponding weight reduction and at the same time maintain the advantages of all-steel construction, stainless steel was selected for the *Zephyr* because of its excellent physical properties, good ductility, fatigue resistance, and resistance to corrosion. A special welding development has made it possible to use thin-web structural members, light gussets, and connections, which, with careful technical design, have resulted in a structure comparable in strength with present modern steel equipment, but with a reduction in weight in excess of 60 per cent. The use of articulated connections has eliminated two complete trucks in a three-car train and has achieved improved riding qualities.

Light-weight motorized trains offer distinct advantages for counteracting the present decline in passenger traffic that results from competition with the automobile and airplane. With light-weight trains, frequency of service can be established because of the relatively low cost and economy of operation. Faster schedules can be attained with more frequent stops because of rapid acceleration and the high-speed characteristics inherent in light-weight equipment. Terminal conditions are simplified and roundhouse attendance is greatly reduced.

Low Power Requirements

In what way does light-weight equipment make possible high speed, rapid acceleration, and increased frequency of service? Irrespective of the type of power—steam, gas, or Diesel engines—and the type of train, and neglecting for a moment the relative advantages of streamlining, the criterion of performance depends essentially on the horsepower per ton at the rail. Since both inertia and total train resistance increase with the tonnage of the train, the horsepower required for a given performance increases with the total weight of train. To obtain high speeds with rapid acceleration, it is necessary either to increase the horsepower capacity of the power plant or reduce the weight of the train itself. Aside from the obvious economic advantage of reducing the size of the power plant to a minimum, the demands for higher performance in acceleration and speed place a serious limitation in reasonable size of power plant for orthodox equipment. For instance, the usual three-car motor train, at a minimum of 70 tons per car, requires, for a performance similar to that of the *Zephyr*, a power plant developing at least 1100 hp at the rail, or an engine of from 1500 to 1600 hp, as compared with the *Zephyr* with its 660 hp. Again, to obtain the same performance as the *Zephyr's* with a six-car train, with light-weight construction at 30 tons per car, approximately 930 hp will be necessary at the rail, requiring an engine developing from 1200 to 1300 hp. With a similar heavy-weight train of 70-ton cars, 2150 hp would be required at the rail, or an engine developing 2900 hp. The former is entirely within the range of practicability, the latter would require a separate locomotive which, in turn, would considerably increase the size of the power plant and total weight of the train. For these reasons alone, consideration of minimum light-weight equipment is of vital importance for motorized trains.

Frequency of Service

Frequency of service ultimately depends upon the availability of train units, neglecting the limitation in trackage for freight and other service. Availability of service depends essentially on the ratio of days actually in service to the total assigned days and the schedule for any given assignment. Burlington statistics indicate, for present gas-electric equipment, that more than 90 per cent of the assigned days are covered. Even assuming more unfavorable conditions, the assignment efficiency of

[1] Consulting Engineer, Edward G. Budd Manufacturing Co. Mem. A.S.M.E. Dr. Eksergian was graduated from the Massachusetts Institute of Technology in 1914 with the degree of S.B. In 1915 he received the degree of M.S. from M.I.T. and from Harvard, and in 1928 the degree of Ph.D. from Clark University. From 1917 to 1919 he was engaged in research at M.I.T. and Harvard, leaving to enter the Ordnance Department of the U. S. Army, where, he was engaged in the theory and design of recoil systems and gun carriages, on which subject he wrote a book. From 1920 to 1929 he was a research engineer with the Baldwin Locomotive Works, Philadelphia, Pa., and acted also in the capacity of consulting engineer for the General Steel Castings Co. In 1929 he became consulting engineer for the E. I. du Pont de Nemours Co., Wilmington, Del. He was engaged by the E. G. Budd Mfg. Co. as consulting engineer in 1933.

Contributed by the Railroad Division and presented at the Semi-Annual Meeting, Denver, Colo., June 25 to 28, 1934, of The American Society of Mechanical Engineers.

Discussion of this paper should be addressed to the Secretary, A.S.M.E., 29 West 39th Street, New York, N.Y., and will be accepted until November 10, 1934, for publication in a later issue of Transactions.

motorized trains should be of fairly high order. With increased performance assignment can be materially increased. The *Zephyr* assignment covers a 500-mile schedule with frequent stops at roughly 15-mile intervals. With present steam equipment, schedule assignments are in general of much lower order, possibly ranging from 200 to 300 miles.

Low Operating Expense

From a purely economic point of view, light equipment is of fundamental importance in the reduction of the major operating, maintenance, and fuel charges. Both maintenance and fuel costs increase with the weight of the equipment, because a major element of cost is the maintenance of the power unit. Maintenance costs are roughly proportional to the rated horsepower-miles per unit. The cost per horsepower-mile obviously increases with smaller units; it is affected by the load factor, i.e., the ratio of average to peak horsepower, the type of power plant, and other variables. With heavy-weight steam locomotives it probably exceeds roughly \$0.0001 per horsepower-mile. With light steam power it may increase considerably. From Burlington statistics covering a variety of gas-electric equipment and assuming an average of 300 hp per unit, the cost per horsepower-mile is estimated roughly at \$0.0002, but this includes all other costs of train maintenance beyond the power plant. There are few or no statistics applicable to Diesel-engine units for rail service. However, in comparing the maintenance costs of motorized trains, it is evident that since the horsepower demand is proportional to train weight, savings in maintenance are in direct proportion to the weight of the equipment for comparable performance. In comparing light-weight motorized units with ordinary steam equipment, which requires about three times the horsepower but which meets roughly the same performance requirements, even with a cost per horsepower-mile for the motorized unit from $1^1/_2$ to 2 times greater, the savings in maintenance per train-mile should be from 50 to 25 per cent. In this latter competition the savings are even more drastically affected by the use of very light-weight equipment.

Low Fuel Costs

Fuel costs are an important element in total charges. It is evident that in comparing motor trains, fuel consumption varies with the horsepower of the unit and therefore in direct proportion to train weight. In the comparison of light-weight motorized units with heavy steam equipment for the same performance, in addition to reductions in horsepower ratios due to light weight, there is an additional advantage of low unit fuel costs for Diesel engines. With Diesel-engine-electric drives, the fuel consumption may be taken conservatively at 0.55 lb of fuel oil per hp-hr at the rail. Similarly, the fuel consumption of a steam locomotive at normal maximum horsepower may be estimated at 2.5 lb of coal per hp-hr at the rail. Because of the varying characteristics of the horsepower-vs.-speed curve of a steam locomotive, lower efficiency is realized, particularly in the lower speed ranges. In either case, in order to estimate the fuel consumption per mile it is necessary to estimate the horsepower-hours per mile which obviously varies greatly for different schedules. Moreover, the fuel consumption per horsepower-hour depends upon the relative efficiency, and this in turn depends upon the ratio of average to rated horsepower, i.e., the load factor.

The three-car motorized Burlington *Zephyr* under loaded operating conditions weighs 120 tons, including the power plant. The engine develops 660 hp, and deducting the power for auxiliaries and considering the overall efficiency of the electric drive, it delivers approximately 480 hp at the rail. The maximum performance characteristic is high, exceeding 4 hp per ton, and is approximately constant throughout the speed range. For a steam train to attain such a performance, but with heavy weight equipment at 70 tons per car or a train load of 210 tons, it would require over 1500 hp at the rail or about 1900 ihp. With stops 15 miles apart, the motor train would require roughly 8 hp-hr per mile as against 24 hp-hr per mile for the steam train. On the basis of fuel oil at \$0.03 per gallon, and coal at \$2.35 per ton, then per mile the costs of operation will be \$0.0165 and \$0.059 per mile for the motor and steam trains, respectively. Assuming a yearly mileage of 100,000, the saving in fuel amounts to \$4250 in favor of the motor train.

2—MECHANICS OF THE PERFORMANCE OF A TRAIN

The acceleration of a train is produced by the difference of the total tractive force ΣZ at the base of the motor truck and the resisting forces ΣF at the treads of the remaining truck wheels and the air resistance P_a. On grades there is in addition the gravity component $Mg \sin \alpha$, where M is the total mass of train, including all trucks, and α is the angle of gradient.

The equation of motion for the translation of the train is

$$\Sigma Z - \Sigma F - Mg \sin \alpha - P_a = M\ddot{x} \qquad [1]$$

where $\ddot{x} = \dfrac{dv}{dt} = v\dfrac{dv}{ds}$ is the translation acceleration. If Φ is the motor torque, γ the gear ratio, ϵ the motor and gear efficiency, $m_a k_a^2$ the moment of inertia of the armature, mk^2 the moment of inertia of the wheels, axles, etc., then if θ is the angular displacement and R the radius of the wheels, for the rotational motion

$$\epsilon\Phi\gamma - ZR = (m_a k_a^2 \gamma^2 + mk^2)\ddot{\theta}$$

and

$$Z = \epsilon\Phi\gamma/R - (m_a k_a^2 \gamma^2 + mk^2)\ddot{x}/R^2 \qquad [2]$$

In like manner, if Φ_R is the total friction torque per axle, consisting of bearing, rolling, flange, etc., friction moments

$$FR - \Phi_R = mk^2\ddot{\theta}$$

and

$$F = \frac{\Phi_R}{R} + \frac{mk^2}{R^2}\ddot{x} = F_R + \frac{mk^2}{R^2}\ddot{x} \qquad [3]$$

where F_R is the reduced friction force at the rail due to mechanical friction for the trucks other than the motor truck.

Substituting [2] and [3] in [1] we have

$$\Sigma\epsilon\Phi\frac{\gamma}{R} - \Sigma F_R - P_a - Mg \sin \alpha = \left(M + \Sigma m_a \frac{k_a^2\gamma^2}{R^2} + \Sigma m \frac{k^2}{R^2}\right)\ddot{x} \qquad [4]$$

From the rate of energy input to the train, i.e., the power equation, we have

$$\Sigma\epsilon\Phi\dot{\phi} - \Sigma\Phi_R\dot{\theta} - P_a\dot{x} - Mg \sin \alpha\, \dot{x} = \frac{d}{dt}\left[\frac{1}{2}(M\dot{x}^2 + \Sigma m_a k_a^2 \dot{\phi}^2 + \Sigma mk^2\dot{\theta}^2)\right] \qquad [5]$$

On differentiating the right-hand member, eliminating $\dot{x}$, and noting that $\phi = \gamma\theta$ for the angular motion of the armature, $\dot{\theta} = \dot{x}/R$ for the angular motion of the wheels, $\dot{x}$ being the velocity of the train at any instant, $\dfrac{d\dot{x}}{dt} = \ddot{x}$, the acceleration, we obtain Equation [4], which is the equation of motion of the train.

For the energy input to the train, we have the energy equation

$$\int (\Sigma\epsilon\Phi)d\phi - \int (\Sigma\Phi_R)d\theta - Mg\sin\alpha x = \tfrac{1}{2}(M\dot{x}^2 + \Sigma m_a k_a{}^2\dot{\phi}^2 + \Sigma mk^2\dot{\theta}^2) \ldots\ldots [6]$$

and

$$\int_0^x \left(\Sigma\epsilon\Phi\frac{\gamma}{R} - \Sigma F_R - P_a - Mg\sin\alpha\right)dx = \frac{1}{2}\left(M + \Sigma m_a k_a{}^2\frac{\gamma^2}{R^2} + \Sigma m\frac{k^2}{R^2}\right)v^2 \ldots\ldots [7]$$

On braking with a brake torque Φ_B, $F_R = \Phi_B/R$ and, neglecting Φ_R and P_a as small, with no gradient

$$\int_{x_1}^{x_2} F_R dx = \frac{1}{2}\left(M + \Sigma m_a k_a{}^2\frac{\gamma^2}{R^2} + \Sigma m\frac{k^2}{R^2}\right)v_1^2 \ldots [8]$$

where

$x_2 - x_1$ = the distance of braking
v_1 = the initial velocity.

In the various expressions we note additional terms for the rotational inertia of the train, which increases the translation inertia. For the equivalent inertia of the train, let

$$M_e = kM = M + \Sigma m_a\frac{k_a{}^2\gamma^2}{R^2} + \Sigma m\frac{k^2}{R^2}$$

where k varies from 1.1 to 1.2 and let

$Z_\phi = \Sigma\epsilon\Phi\gamma/R$ = motor tractive force at rail
$Z_R = \Sigma F_R + P_a$ = total train resistance.

Then the equation of motion of the train and the energy equation reduce to

$$\left.\begin{aligned} &Z_\phi - Z_R - Mg\sin\alpha = kM\ddot{x} \\ \text{and}\quad &\int_0^x (Z_\phi - Z_R - Mg\sin\alpha)\,dx = \frac{1}{2}kMv^2 \end{aligned}\right\} \ldots\ldots [9]$$

It is usual practise to express the acceleration in miles per hour per second as A, the velocity in miles per hour as V, and the displacement in feet as x, so that

$$\ddot{x} = 1.47A = 2.15V\frac{dV}{dx}$$

where

$$A = \frac{dV}{dt} = 1.47\,V\frac{dV}{dx}$$

The train weight is expressed in tons and the accelerating force in pounds per ton. Further, if G is the gradient in per cent, then $\sin\alpha = G/100$. If W is the weight of train in tons, $2000W = Mg$. Therefore

$$Z_\phi - Z_R - 2000\frac{G}{100} = \frac{1.47 \times 2000}{g}kWA$$

and

$$\frac{Z - Z_R}{W} \mp 20G = 91kA \ldots\ldots\ldots\ldots [10]$$

where

$$k = 1 + \Sigma\frac{W_a}{W}\frac{k_a{}^2\gamma^2}{R^2} + \Sigma\frac{w}{W}\frac{k^2}{R^2} = 1.1 \text{ (approx.)}$$

Therefore

Z_ϕ(per ton) $= Z_R$(per ton) $\pm 20G + 100A$ (lb per ton) [11]

which gives a condensed and generalized form for the motion of a train.

Power Relations

The horsepower H developed by the motors at the rail is

$$H = \frac{\Sigma\epsilon\Phi\phi}{550} = \frac{\Sigma\epsilon\Phi\frac{\gamma}{R}\dot{x}}{550} = \frac{Z_\phi V}{375}$$

$$\frac{375}{V}\left(\frac{H}{W}\right) - \left(\frac{Z_R}{W}\right) - 20G = 100A \ldots\ldots\ldots [12]$$

where

$\left(\frac{H}{W}\right)$ = the horsepower per ton at the rail

$\frac{Z_R}{W}$ = total train resistance, lb per ton.

Train Resistance and Streamlining

Train resistance may be divided into two primary components, (1) the resistance due to rolling and bearing friction, etc., and (2) wind resistance. At low and medium speeds the former is by far the greater component, and streamlining offers no particular advantage. With the higher speeds, air resistance becomes a large component of the total resistance and a material reduction of this component considerably reduces the total resistance.

For the mechanical resistance, i.e., rolling and bearing friction, etc., we have

$$\Phi_R = We + T_{bf} + T_{hf} + fq$$

where

$$F_R = \frac{\Phi_R}{R}$$

In the rolling-friction moment We, the offset of the rail reaction from the center of the journal is around 0.02 in. It may increase with bad track and speed. The bearing-friction moment $T_{bf} = \mu Wd/2$ where $\mu = 1/200$ (approx.), W = journal load, and e = diameter of bearing. With roller bearings $T_{bf} = 0.0025Wd/2$ (approx.). Flange friction moment fq depends upon the average lateral pressure and is difficult even to approximate.

It is well known that the resistance per ton increases with light-weight equipment. To take care of the aforementioned components, there are many train-resistance formulas with varying degrees of reliability. Undoubtedly one of the most accurate is the Davis formula. In this the mechanical friction per ton is

$$F_R = \frac{9.4}{\sqrt{w}} + \frac{12.5}{w} + kV \text{ (per ton)}$$

in which

$k = 0.09$, motor truck
$k = 0.03$, trailer truck

or a good approximation for axle loads exceeding 5 tons is

$$F_R = 1.3 + 29/w + kV \text{ (per ton)}$$

where $w = W/n$ = average weight per axle in tons.

With roller bearings, this resistance may be reduced as much as 20 per cent. Moreover, the high initial bearing friction, due to the complete breakdown of the oil film in the bearings under starting conditions, is eliminated.

The air-resistance component (2) is of interest particularly in the reduction of its value by streamlining. Without streamlining the air moves relative to the train with a velocity v. The mass affected per unit time is proportional to $\rho Av/g$, where ρ is the density of air, A the train cross-section, and v the velocity. The momentum in the air per unit time by the action of the train on the air is found to be approximately $\rho Av^2/2g$. With $\rho = 0.08$ lb per cu ft, $g = 32.2$ ft per sec per sec, and the reaction of the air on the train is approximately $P_a = \rho Av^2/2g = 0.00125 Av^2 = 0.0027AV^2$, where V is the speed in miles per hour and $v = 1.47V$.

In the Davis formula the head-end resistance is given as $0.0024V^2$. With more than one car there is an added factor for each car due to skin friction.

In aerodynamics, it is customary to express resistance in terms of drag coefficients, so that,

$$P_a = D_c A V^2$$

where D_c is the drag coefficient.

From wind-tunnel experiments conducted on small-scale models of the Burlington *Zephyr* at the Massachusetts Institute of Technology, the value of D_c for the model was found to be 0.0009917. A model of a conventional train was also tested, resulting in a drag $D_c = 0.002586$. It was estimated that D_c for the conventional car was 20 per cent low for full scale, and as both models were the same length it seemed reasonable to assume this factor would also apply to the full-scale value of the *Zephyr*, although actual tests proved that this factor was found to be overestimated. Therefore, for the streamlined *Zephyr*, $P_a = 0.0012AV^2$ lb. It is interesting to note that of the total air resistance, approximately two-thirds is due to skin friction, according to standard skin-resistance formula.

In the Davis formula air friction is given as $D_c = 0.00034$ for conventional trailing cars, which consists entirely of skin friction, turbulent resistance of projecting equipment, surface discontinuities between cars, etc. This may be considered side resistance. For three cars, this amounts to $D_c = 0.00102$. This is 85 per cent of the entire air resistance of the *Zephyr*.

For this reason, the importance of side resistance along a train increases with the length of train and may become of comparable importance with head-end resistance. It becomes of particular importance when head and tail end are well streamlined. Great care, therefore, should be given to the prevention of recesses, etc., in long trains.

For the *Zephyr* the complete formula for train resistance is

$$Z_R = 1.3 + 29/w + 0.0545V + 0.0012AV^2/wn \text{ (lb per ton)}$$

and for a conventional train of the same number of cars

$$Z_R = 1.3 + 29/w + 0.0545V + 0.0027AV^2/wn \text{ (lb per ton)}$$

where w is the average number of tons per axle and n is the total number of axles.

Generalized Performance Characteristics

The performance of any train depends on the available horsepower per ton at the rail and the total resistance per ton. Although the latter decreases somewhat with increased weight of train, in a first approximation it may be considered independent of the weight of the train for a considerable range of operating speeds. Therefore, in a first approximation, the performance depends essentially only on the available horsepower per ton at the rail and is fairly independent of the particular total weight of the train.

At very high speeds, however, the air-resistance component of the train resistance becomes of great importance. The air resistance, which depends upon the geometric configuration of the train, decreases with increased weight of the train, and at high speeds the total train resistance per ton is decreased, in general, with heavier trains. Moreover, the advantages of streamlining are not so great for heavy trains as for light trains.

An interesting comparison was made with the *Zephyr*, light and loaded. For the same total horsepower available, obviously the horsepower per ton for the light train is greater than for the loaded train. With 3.8 hp per ton for the loaded train as against 4.5 hp per ton for the light train, the same top speed was found. This is because the decreased air resistance per ton for the loaded train as against the increased air resistance per ton for the light train compensates for the differences in horsepower per ton for the two cases.

For close comparisons, particularly for estimating top speeds, it is always desirable in estimating performance characteristics to approximate closely the weight of train. At low speeds and in the more important acceleration zone, the particular train weight is not important.

The mean loaded weight of the *Zephyr* was taken at 120 tons. We might consider this as typical of light-weight, three-car trains.

For estimating performance characteristics for motorized trains, the following relation was used:

$$H_{(\text{ton})} = [1.3 + 29/w + k_1V + k_2SV^2/wn + 100A]V/375$$

where

$H_{(\text{ton})}$ = the horsepower per ton at the rail
V = velocity, mph
A = acceleration, mph per sec
S = cross-section of train, sq ft
$k_1 = \dfrac{0.09W_m + 0.03W_t}{W}$
W_m = weight on motor trucks
W_t = weight on trailer trucks
$W = W_m + W_t$ = total weight of train
$k_2 = 0.0004 + 0.00027N$ for streamlined trains[2]
N = total number of cars
$k_2 = 0.0024 + 0.00034N_t$ for conventional trains
N_t = number of trailer cars.

For constructing space-velocity curves

$$A = \frac{3.75\,H_{(\text{ton})}}{V} - 0.01\left(1.3 + 29/w + kV + k_2SV^2/wn\right)$$

but $A = 1.47V\dfrac{dV}{dx}$

$$\Delta V = \frac{0.255\,H_{(\text{ton})}}{V^2} - \frac{0.0068}{V}\left(1.3 + 29/w + k_1V + k_2SV^2/wn\right)\Delta S$$

where ΔV is the increment velocity in miles per hour corresponding to the increment displacement ΔS in fact.

Fig. 1 shows acceleration curves with differential rates of acceleration. The curves are based on *constant* horsepower throughout the speed range. Dotted lines indicate a conventional but light-weight train of 120 tons, not streamlined, and the solid lines are for a light-weight streamlined train.

With 4 hp per ton available at the rail and at 10 mph the acceleration is 1.5 mph per sec; at 50 mph it decreases to 0.2 mph per sec. To increase the acceleration to 0.5 mph per sec at 50 mph would require 8 hp per ton. When the tractive

[2] Arbitrarily increased by 20 per cent in scaling up from wind-tunnel tests.

force balances the train resistance, the acceleration A is zero, and we have the top speed condition. With the streamline train, assuming a maximum of 4.3 hp per ton, the maximum speed is 95 mph. Top speeds exceeding 100 mph have been

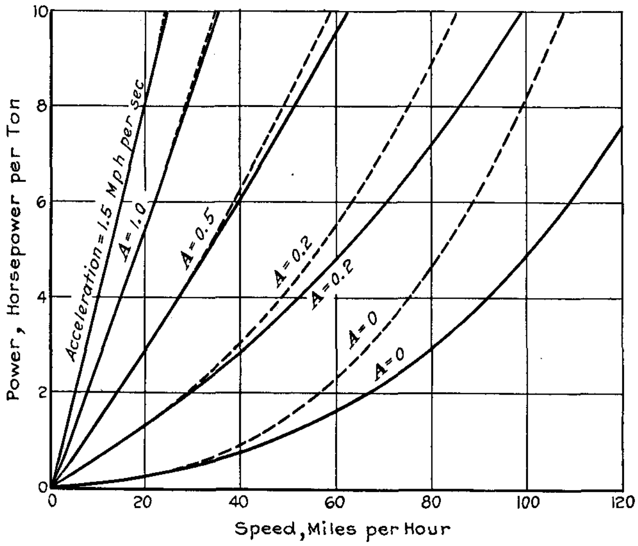

Fig. 1 Characteristics of Constant-Horsepower Train
(Relation between horsepower per ton and speed. Total weight, 120 tons.)

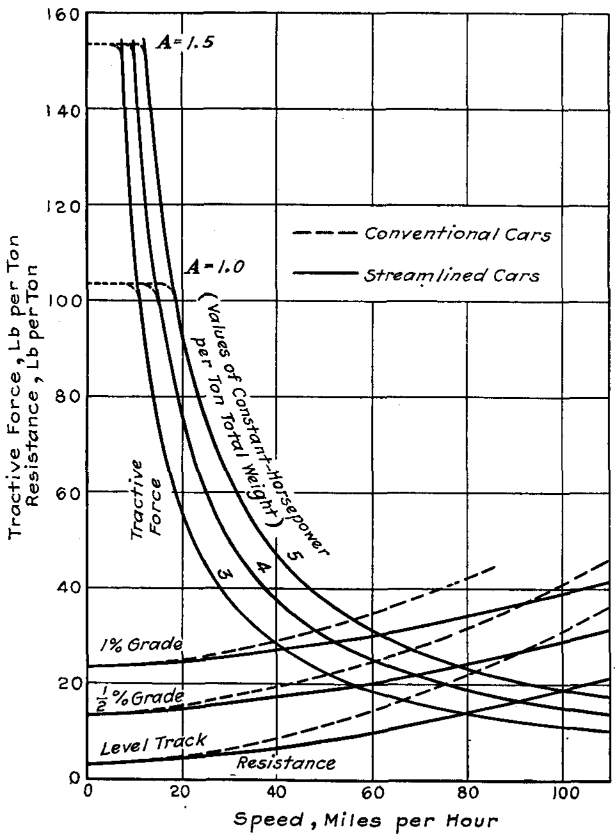

Fig. 2 Characteristics of Constant-Horsepower Train
(Relation between tractive force and resistance and speed. Total weight, 120 tons.)

reached with the *Zephyr* but the arbitrary 20-per cent increase of wind resistance over the values determined in the wind-tunnel tests account for this, and the figures, therefore, are on the conservative side. Without streamlining the maximum speed at 4.3 hp per ton is 78 mph. It is to be noted, however, that streamlining has very little effect on acceleration at the lower speeds.

Fig. 2 shows the relation between tractive force per ton and speed with constant horsepower throughout the speed range. Curves are plotted for 3, 4, and 5 hp per ton. Resistances per ton for level track and for grades of $^1/_2$ and 1 per cent are also plotted. Where the resistance curves intersect the tractive-force curves, a condition of equilibrium or limiting speed exists. The curves are plotted on the conservative side and actual performance should somewhat exceed these values. It is to be noted that if high initial acceleration is required, say at 1.5 mph per sec, the adhesion capacity must exceed 150 lb per ton. The solid lines refer to streamlined cars and the dotted lines to conventional cars. The curves are based on a total weight of 120 tons.

Fig. 3 shows the relation between acceleration and speed for constant-horsepower trains. The adhesion zone for all three cases was limited to 12 mph. Streamlining has very little effect on acceleration performance below 40 mph.

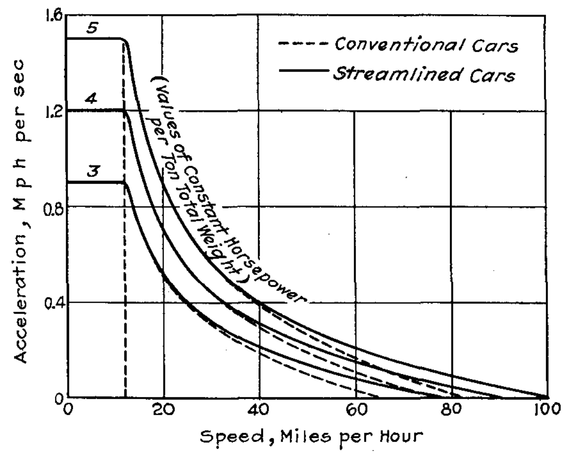

Fig. 3 Speed-Acceleration Characteristics of Constant-Horsepower Train

Fig. 4 shows distance-speed characteristics assuming constant horsepower throughout the speed range. Braking curves were taken at 2 mph per sec. A streamlined and a conventional train, of the same weight of 120 tons are compared on the basis of 4 hp per ton. Solid lines are for streamlined trains 3, 4, and 5 hp per ton.

For stops 2 miles apart, with 3 hp per ton, a speed of only 52 mph can be obtained. At 5 hp per ton, a speed of 62 mph is reached. The total time of the run is 190 sec at 3 hp per ton and 160 sec at 5 hp per ton, or somewhat more than 20 per cent in running time. It will be noted that no gain is effected by streamlining. With 15-mile stops, streamlining on the basis of 4 hp per ton results in a saving of $1^1/_3$ min. Limiting speeds can approximately be reached at 15-mile stops. Streamlining appears profitable for stops at intervals exceeding 12 miles.

Locomotive Haulage

It is of interest to compare locomotive units independently of the train. With trains comprising more than six cars, separate locomotive traction appears feasible because of the power required.

To estimate the size of the locomotive, it is necessary to make some assumption as to its weight efficiency. Present modern steam locomotives weigh from 100 to 130 lb per hp. The weight ratios of tenders with respect to the locomotive vary from 0.5 to 0.8. In Table 1 a locomotive weight efficiency of 100 lb per hp and a tender weight ratio of 0.75 have been used.

The weight efficiency of Diesel and special steam locomotives would be expected to vary considerably at the present time. A value of 140 lb per hp has been taken. It is likely that power plants as low as 120 lb per hp at the rail may be feasible.

In estimating indicated horsepower, the efficiency of transmission must be considered. With motorized units, it may vary from 0.75 to 0.8 and for steam locomotives the ratio of drawbar horsepower to indicated horsepower may be taken around 0.8.

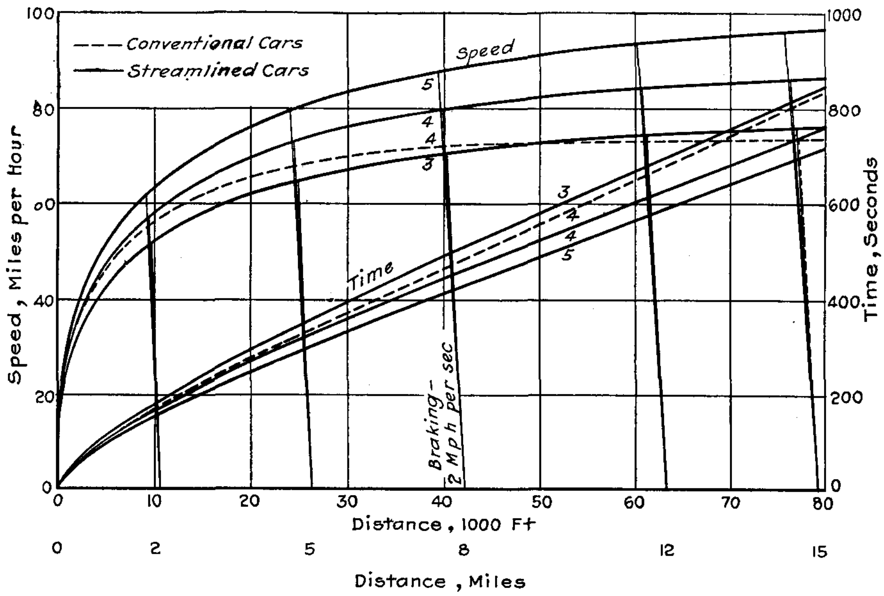

Fig. 4 Distance-Speed Characteristics of Constant-Horsepower Train
(Numbers on curves refer to values of constant horsepower per ton of total weight.)

Let W_t = weight of train in tons

W_L = weight of locomotive in tons

W_D = weight of tender in tons

W_P = $W_L + W_D$ = weight of power plant in tons

k = W_D/W_L = ratio of tender weight to locomotive weight

E = weight efficiency in lb per hp, H

so that

$$H = \frac{2000}{E} W_L \text{ (at rail)}.$$

The horsepower per ton for the train including locomotive and tender is

$$H_{(\text{ton})} = \frac{H}{W_t + W_P} = \frac{H}{W_t + (1 + k)W_L} = \frac{\frac{2000}{E} W_L}{W_t + (1 + k)W_L}$$

$$W_L = \frac{W_t H_{(\text{ton})}}{\frac{2000}{E} - (1 + k)H_{(\text{ton})}}$$

$$H = \frac{2000}{E} W_L$$

Expressed in terms of the power plant, i.e., for locomotive plus tender

$$W_P = \frac{W_t}{\frac{2000}{E(1 + k)H_{(\text{ton})}} - 1}$$

$$H = \frac{2000}{E(1 + k)} W_P$$

In the case of the Diesel power plant $k = 0$.

In order to survey the power requirements, Table 1 has been prepared. It is based on 4 hp per ton, which exceeds present steam performance by 33 per cent. Light-weight equipment is based on 30-ton and 35-ton loaded cars and heavy equipment on 70- and 85-ton cars. The horsepowers listed are the required horsepowers at the rail.

Table 1 and Fig. 5 are based on 4 hp per ton. Similar tables can be constructed for other performances. Heavy-weight trains in general require less horsepower per ton than light trains for attaining the same top speeds. Moreover, even with light-weight equipment but with longer trains, due to the decreased air resistance per ton, less horsepower per ton is required for sustained high speeds. But with acceleration, etc., the average performance is more nearly comparable with the same horsepower per ton.

Fig. 5 shows the weight and horsepower characteristics plotted against train weight for a high performance of 4 hp per ton. With steam locomotives, E is the locomotive weight efficiency in pounds per horsepower for the locomotive alone and k is the ratio of tender weight to locomotive weight, so that the combined weight efficiency of the locomotive and tender is $E(1 + k)$. With Diesel locomotives $k = 0$. In the case of motorized units $E(1 + k) = E$, since $k = 0$, and the power plant is considered to include engine and generator with auxiliaries together with motors on trucks. The total weight of the power plant of the *Zephyr* on the basis stated is approximately 55,000 lb, and with, roughly, from 480 to 500 hp at the rail, its weight efficiency E is 110 lb per hp, approximately. The train weighs, excluding the power plant, normally loaded, roughly, 30 tons per car.

From Fig. 5 will be noted the considerable reduction in horsepower for a 10-car light train at 210 tons compared with a similar heavy-weight train at 850 tons for any weight efficiency of power plant considered.

Due to the varying horsepower characteristics of steam locomotives against speed, the rated or normal maximum horsepower of steam locomotives must be increased to obtain a performance equivalent to the more nearly constant-horsepower performance of Diesel-electric power units.

From Table 1 and Fig. 5 the following features are of interest:

(1) The gain in the refinement of power-plant design in improved weight efficiencies is of small importance compared with the gain in the reduction of the horsepower capacity by the use of light-weight trains.

(2) Irrespective of power plant, whether motorized or locomotive haulage, the required horsepower of the plant for a given performance is practically directly proportional to the train weight.

(3) If the horsepower capacity of self-contained motorized units is limited to approximately 1200 hp at the rail, the field of motorized trains increases with light-weight equipment. Thus, with 30- to 35-ton cars, 6- to 8-car trains can be used. With heavy equipment motorized trains are practically excluded.

TABLE 1 HIGH-SPEED SERVICE PERFORMANCE

No. of cars	Motorized (Weight efficiency of power plant, 110 lb per hp) W_P	Horsepower at rail	Special steam or Diesel locomotive (140 lb per hp) W_P	Horsepower at rail	Steam locomotive (175 lb per hp) W_P	Horsepower at rail
	4 hp per ton—30-ton cars—light					
8	25.4	462	35.0	500	48.2	550
6	51.0	930	70.0	1000	96.4	1100
8	67.5	1225	93.2	1330	129.0	1470
10	84.5	1535	117.0	1680	161.0	1730
	4 hp per ton—35-ton cars—light					
3	29.6	538	40.6	580	56.5	645
6	59.2	1075	81.2	1160	113.0	1290
8	79.0	1435	108.0	1550	151.0	1725
10	98.8	1795	136.0	1950	188.0	2150
	4 hp per ton—70-ton cars—heavy					
3	59.2	1076	81.5	1170	113	1290
6	118.4	2150	163.0	2330	226	2500
8	158.0	2870	218.0	2980	302	3450
10	197.6	3590	272.0	3880	376	4300
	4 hp per ton—85-ton cars—heavy					
3	71.8	1310	98.6	1410	137	1570
6	143.6	2620	197.0	2820	274	3140
8	191.0	3470	263.0	3760	364	4160
10	240.0	4360	329.0	4700	455	5200

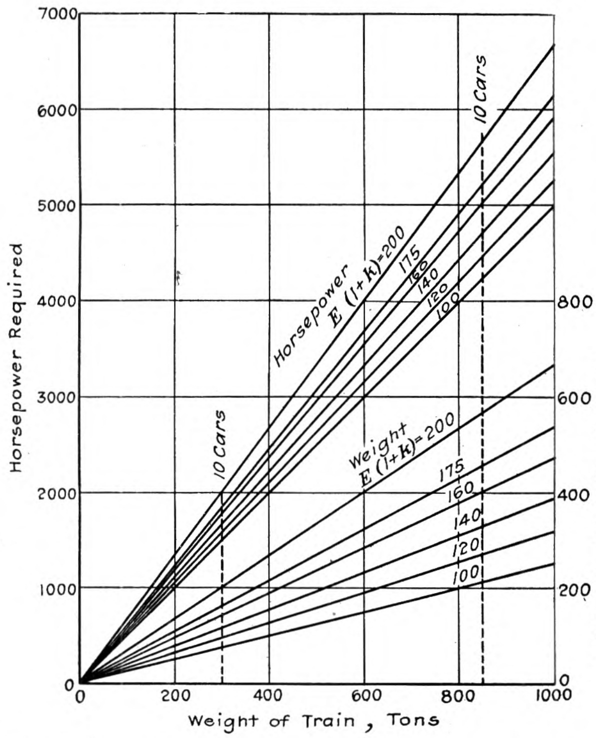

Fig. 5 Horsepower-Weight Characteristics of Constant-Horsepower Train

(Performance for 4 hp per ton of total weight. Total weight equals weight of train plus weight of power plant.)

Braking Characteristics

The braking of high-speed motorized trains presents a complicated problem. On the *Zephyr* each truck has individual brake cylinders. The brakes were designed for uniform braking throughout. Approximately 45 per cent of the entire braking of the train is effected on the leading motor truck. For maximum braking capacity and for the elimination of otherwise heavy pedestal loading, clasp brakes are used on all wheels. In addition, a retardation pendulum control is used which fixes the maximum retardation at 3.5 mph per sec, or any other setting, and thus prevents wheel slippage at the rail in stopping.

Essentially, the braking capacity is limited by the friction force at the rail, which, in turn, depends upon the coefficient of friction of the rail and the weight transfer, particularly under conditions of maximum retardation at the stop.

The forces on a wheel are shown in Fig. 6. The horizontal thrust H_t exerted by the pedestal on the journal bearing due to the inertia of the car is resisted by the tangential friction force F at the rail (neglecting the translation inertia of the wheels and axles). The rail-friction-force F is induced by the brake-shoe friction-couple $\mu_s BR$ which, neglecting the rotational inertia of the wheels, is just balanced by FR. Therefore, the retarding force $F = \mu_s B$, where μ_s is the coefficient of friction of the brake shoe and B the brake-shoe thrust.

It is convenient to consider F in terms of an equivalent coeffi-

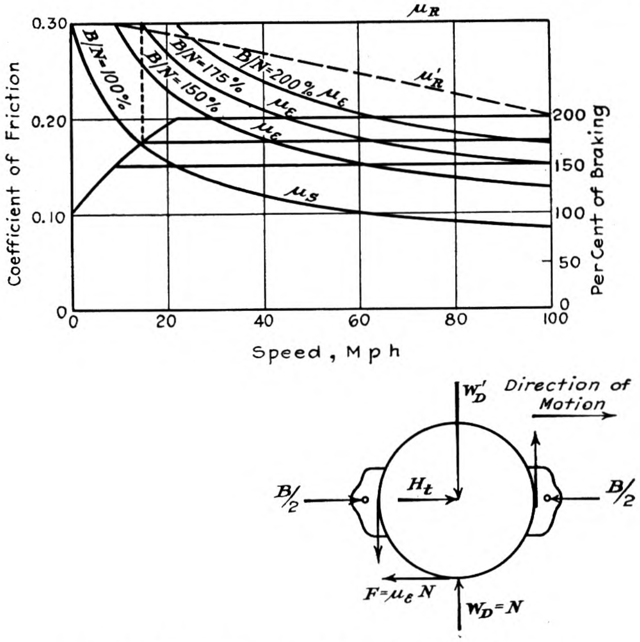

Fig. 6 Equivalent Rail Coefficients in Braking

($F \leqq \mu_R W_D \leqq 0.3 W_D$; $F = \mu_s B$ (approx.); $B =$ [per cent of braking] $\times$ $100 \times N$; $\mu_s \times \% W_D \leqq \mu_R W_D$; $\mu_s \times \% \leqq \mu_R$; μ_ϵ = equivalent rail coefficient; $\mu_\epsilon N = F = B\mu_s$; $\mu_\epsilon = B/N\mu_s = \% \mu_s$; $\mu \leqq \mu_R$.)

cient of rail friction μ_ϵ and the load at the rail $N = W_D$ = axle load at the rail. Then $F = \mu_\epsilon N$ or $\mu_\epsilon W_D$. Since

$$\mu_\epsilon N = F = \mu_s B, \qquad \text{then} \qquad \mu_\epsilon = \mu_s B/N = \mu_s B/W_D$$

The ratio B/N is the braking ratio or braking power, i.e.,

$$\frac{B}{N} = \frac{\text{total brake-shoe thrust}}{\text{rail-axle load}} = \text{per cent of braking power}$$

Evidently F is limited by the limiting friction at the rail, i.e., $F = \mu_R N$, where μ_R is the maximum coefficient of rail friction. Therefore, $F = \mu_\epsilon N < \mu_R N$ or $\mu_\epsilon < \mu_R$ to prevent slippage of the wheels at the rail. It is important to note that with the advent of weight transfer in braking, N is reduced over the static load at the rail, thereby reducing $F_{\max}$, the available retarding force at the rail.

It is well known that with sliding friction the coefficient of friction is reduced, decreasing with higher relative velocities. On the basis of experimental data with cast-iron brake shoes on steel wheels by Galton and Wichert, the coefficient of friction against speed translated into miles per hour is

$$\mu_s = \mu_0 \left(\frac{1 + 0.01395\,V}{1 + 0.07464\,V} \right)$$

$$\mu_0 = \mu_R = 0.3$$

The formula is at best a rough approximation. Brake-shoe friction coefficients are much affected by temperature and pressure. Increased friction coefficients are obtained with lower temperature and pressure. Clasp brakes inherently run cooler. The variation of μ_s against speed V in miles per hour is plotted in Fig. 6.

Now since $F = \mu_e N$, where $\mu_e = \mu_s B/N$ = per cent of μ_s it is of interest to plot the equivalent coefficient of rail friction for various braking ratios B/N. It is evident that $\mu_e = \%\ \mu_s$ cannot exceed μ_R at the rail without slippage, so that when $\%\ \mu_s$ equals μ_R occurs at a lower speed in the retardation, the braking ratio must be decreased, i.e., the per cent of braking $= \frac{\mu_R}{\mu_s} = \frac{0.3}{\mu_s}$. Thus with 200 per cent of braking, i.e., $B/N = 2.0$, braking release must occur at 23 mph. The reduction in braking ratios for the lower speeds is also shown in Fig. 6.

Two factors are of importance: (1) At the higher speeds, it is probable that the limiting rail coefficient of friction is reduced by vibration, rail joints, etc., and (2) the actual limit of friction force is reduced by weight transfer at the lower speeds. On the basis of a limit at the rail $\mu_R = 0.2$ at 100 mph, the dotted limiting line was drawn in. At all events, it appears that braking ratios exceeding 250 per cent at very high speeds are questionable without the possibility of incipient wheel slippage at the rail.

Moreover, braking ratios are limited by brake-shoe pressures which should not exceed from 20,000 to 25,000 lb. This is another advantage of clasp brakes with high braking ratios, which permit 200 per cent of braking for axle loadings up to 40,000 to 50,000 lb.

With light-weight equipment, not only are higher braking ratios possible but also higher shoe pressures, due to the shorter time of the stop and the inherent reduced kinetic energy. Thus the heat dissipated is reduced with resulting higher friction coefficients.

Weight Transfer

The subject of weight transfer is relatively simple. If a horizontal center-pin thrust H_t is exerted on the truck (the reaction of which retards the car body itself) and since the braking causes a total retarding force F at the wheel base which must exceed H_t by the local inertia force of the truck, there exists a couple $H_t h$ (h being the height of center pin above the rail) together with an additional small couple due to the inertia of the truck, which tends to increase the loads on the front wheels and decrease the loads on the rear wheels by an equal amount. Moreover, an additional change in loading takes place because of the decreased vertical loading at the center pin for trailing trucks and an increased loading for forward trucks due to the inertia couple of the car body itself. This latter, however, is relatively small because of the length between center pins and is practically eliminated with articulated constructions.

The following equation gives the weight transfer loading per axle. Let

W_c = total weight of car body,
$\ddot{x}$ = $1.47A$
A = mph per sec
h_c = height of center of gravity of W_c above center pins
L = length of car body between center pins
W = static load on center pin
w = weight of truck with center of gravity at height d above rail
ΔV = change in loading on center pin in braking
b = length of wheelbase
R = wheel radius
$\frac{w_w k_w^2}{g}$ = polar moment of inertia of wheels
$\frac{w_a k_a^2}{g}$ = polar moment of inertia of motor, if any
H_t = horizontal reaction at center pin
h = height of center pin above rail.

Then for the rear truck, assuming equal braking per truck

$$\Delta V = \frac{W_c h_c}{gL}\ddot{x}; \quad \text{and} \quad H_t = \frac{W}{g}\ddot{x} \text{ (approx.)}$$

The changes in axle rail loads are

$$\Delta N = \pm\left[\frac{H_t h}{b} + \frac{w}{g}\frac{d}{b}\ddot{x} + \frac{2(w_w k_w^2 - w_a k_a^2 r^2)}{gRb}\ddot{x}\right] - \frac{\Delta V}{2}$$

$$\therefore \Delta N = \pm\left[Wh + wd + \frac{2}{R}(w_w k_w^2 - w_a k_a^2 r^2) \pm \frac{W_c h_c b}{2L}\right]\frac{\ddot{x}}{gb}$$

In a first approximation the last two terms can be omitted and with articulations the last term is practically eliminated.

Table 2 shows the change in axle rail loads for different retardation rates. At 5 mph per sec the change in loading on the rear axle of the rear truck is nearly 13 per cent. In general, low center pins result in small weight transfer. Such was considered in the *Zephyr*.

TABLE 2 WEIGHT TRANSFER

	Truck 1		Truck 2		Truck 3		Truck 4	
Articulation reactions, lb.......	...	...	18,550	17,481	17,430	13,052	...	...
Static load, center plate, lb.	65,995		36,031		30,482		17,145	
Truck weight, lb.......	31,108		14,218		13,343		10,525	
	Rail axle loads, pounds							
Static......	48,551	48,551	25,125	25,125	21,912	21,912	13,835	13,835
A = 2.....	51,202	46,356	26,200	23,758	22,969	20,849	14,392	13,122
A = 3.....	52,443	45,327	26,696	23,126	23,458	20,358	14,646	12,794
A = 4.....	53,879	44,133	27,257	22,407	24,021	19,791	14,938	12,418
A = 5.....	55,231	43,009	27,781	21,737	24,551	19,261	15,207	12,071

NOTE: A is the acceleration in miles per hour per second.

3—TRUCKS

The trucks of high-speed light-weight trains require special consideration. For safety at high speeds and for riding comfort with light-weight equipment, it is essential to have considerable flexibility in the spring system, though consistent with sufficient stability for roll. Therefore, in the preliminary design of trucks, ample space and clearances must be provided for with flexible spring systems. Nosing or angular-vibration periods are very much affected by angular play in the truck. With the fixed lateral play, flange play, pedestal play, etc., the angular plays are considerably increased with short-wheelbase trucks, resulting in long periods or low-frequency angular vibrations, and the frequency of such vibrations becomes dependent to a great extent on the initial lateral-velocity disturbances set up by poor track, undulations, etc. Such velocity disturbances may result in severe lateral impact loadings. Moreover, particularly with motor trucks, self-induced vibrations are set up by the frictional forces at the wheelbase, resulting in larger amplitudes and lateral reactions with augmented angular plays. For these reasons it is highly desirable to use long-wheelbase trucks. Such wheelbases in no way interfere with tracking on curves and in fact are advantageous on spiral approaches. In the *Zephyr* a long wheelbase of eight feet was used on all trucks.

With high-speed trucks, wheel diameters should be limited approximately by the relation $P = 600\ d$, where d is the wheel diameter and P is the maximum wheel load in pounds. An extreme limit for the carrying capacity of a wheel is $P = 700\ d$.

In the design of the frame of a truck, low center-pin heights are desirable to reduce the weight transfer in braking and traction, as well as to lower the train height and to maintain reasonable heights of center of gravity of the car body above the center pins.

With swing bolsters, long hangers should be provided, and these result in low-frequency lateral and angular oscillations and, moreover, are effective in reducing lateral impacts transmitted to the car body.

It is highly desirable to maintain ample flexibility in coil springs with damping, in order to reduce rail impact soundings. While it is admitted all trucks are more or less non-equalized, the difficulty with so-called "non-equalized" trucks is the meeting of sufficient spring flexibility over the box and at the same time having sufficient load capacity. With equalized trucks, by means of equalizer beams, the variation in spring deflections due to rise and fall in the box is reduced, and the variation in loading is thereby reduced. For inside frame trucks with boxes inside wheel fits, rolling oscillations cause large changes in spring loading and the lateral stability is reduced.

For high-speed service equalized outside boxes with equalizer bars together with large flexibility in the spring system were used in the *Zephyr*.

Axles

No element in a train is of greater importance than the axles. Axles are subject to two types of loading. The first type is the normal loading, with approximately equal loads at journals and allowance for vertical oscillations. Such loadings result in an approximately constant bending moment between wheels, so that a complete reversal of stress takes place every revolution. Moreover, this loading condition is the average fatigue condition for reversal of stress. The working stress, therefore, should be consistent with the endurance limit of the axle steel. Ordinary carbon-steel axles have a tensile strength of approximately 75,000 lb per sq in., which gives a conservative endurance limit around 25,000 lb per sq in. An allowance of a stress-concentration factor of at least 2 should be made even with generous fillets. Moreover, at the press fit of the hub, an apparent reduction in fatigue strength should be provided for. Thus a maximum working stress of 8000 to 10,000 lb per sq in. would appear the limit to provide for such conditions. The second loading condition is dependent on extreme lateral loads, which give maximum stress conditions in the axle but not average conditions for fatigue. The following simplification of the Reuleaux method is convenient for estimating the strength of ordinary journal axles.

Referring to Fig. 7*a*, let

W = total rail axle load
W_1 = weight per axle of car body and truck parts above journals
W_a = weight of axle assembly, wheels, axle, etc.
w_a = weight of wheel
H_1 = kW_1 = lateral force per axle for car body and truck parts above journals
h_1 = height of center of gravity of car body and truck parts above the journals measured from center of axle
h = corresponding height of H_1 above rail = $h_1 + r$
r = radius of wheel
L = distance between journal-bearing centers
G = distance between wheel rail reactions = 59 in.

Then, for the journal loads P_1 and P_2

$$P_1 = \frac{W_1}{2} + \frac{H_1 h_1}{L};\quad P_2 = \frac{W_1}{2} - \frac{H_1 h_1}{L}$$

and for the wheel reactions at the rail,

$$N_1 = \frac{W}{2} + \frac{H_1 h + Hr}{G};\quad N_2 = \frac{W}{2} - \frac{H_1 h + Hr}{G}$$

where $W = W_1 + W_a$ and $H = H_1 + H_2$ = lateral reaction at rail. The bending-moment equation from journal center to rail center is $P_1 x$ and from rail center to the inside part of the axle, i.e., between wheel hubs, is

$$P_1 x - [N_1 - w_a]\left[x - \left(\frac{L-G}{2}\right)\right] + Hr$$

where x is measured from the center of the journal bearing.

In this method k is usually taken at 0.4, so that $H_1 = 0.4W_1$, $H_2 = 0.4W_1$, and $H = 0.4W$.

The critically stressed section is at the inside of the wheel hub so that with ordinary car axles in which the distance between hubs is 53¹/₄ in., and the rail pressures are at 59 in., we have

$$x = 0.5L - 26.63 \text{ (in.)}$$

and $x - 0.5(L - G) = 2.88$ in.

The stress at this section for the *Zephyr* was limited to 18,000 lb per sq in.

Motor Axles

In Fig. 7*b* let

L_1 = nose or suspension reaction of the motor on the truck frame
d_0 = horizontal distance from axle center to nose suspension
R = wheel radius
r_p = radius of pinion to pitch circle
r_g = radius of pitch circle of gear
r = r_g/r_p = gear ratio
W_m = total motor weight including housing, gears, etc., with qW_m suspended on axle and $(1 - q)W_m$ on nose suspension.

Then, if Φ is the motor torque and F the total traction force at the rail per axle

$$F = \Phi r/R;\quad L_1 = FR/d_0 \pm (1 - q)W_m = \Phi r/d_0 \pm (1 - q)W_m$$

Weight Transfer and Change in Loadings on Journals

In Fig. 7*b* let h be the height of center pin above rail, and $h - R$ the height above journal centers. If b is the length of the wheelbase, these will be reacting on the frame of the truck couples $L_1(b - 2d_0)$ and $H(h - R)$, which cause a change in loading on journals, as follows:

$$\Delta V = \frac{L_1}{b}(b - 2d_0) - \frac{H}{b}(h - R)$$

and since $H = 2F$

$$\Delta V = \frac{FR}{d_0}\left(\frac{b - 2d_0}{b}\right) - 2F\left(\frac{h - R}{b}\right) = \frac{\Phi\gamma}{Rb}\left[\frac{R}{d_0}(b - 2d_0) - 2(h - R)\right]$$

These augment the load on the leading journals and decrease the loads on the rear journals. Approximately, the two terms in the brackets cancel, so that the changes in journal and spring loads are practically negligible.

Considering the assembly of wheels, axles, and motor alone, and noting that the motor weights are included in the static weight at the rail

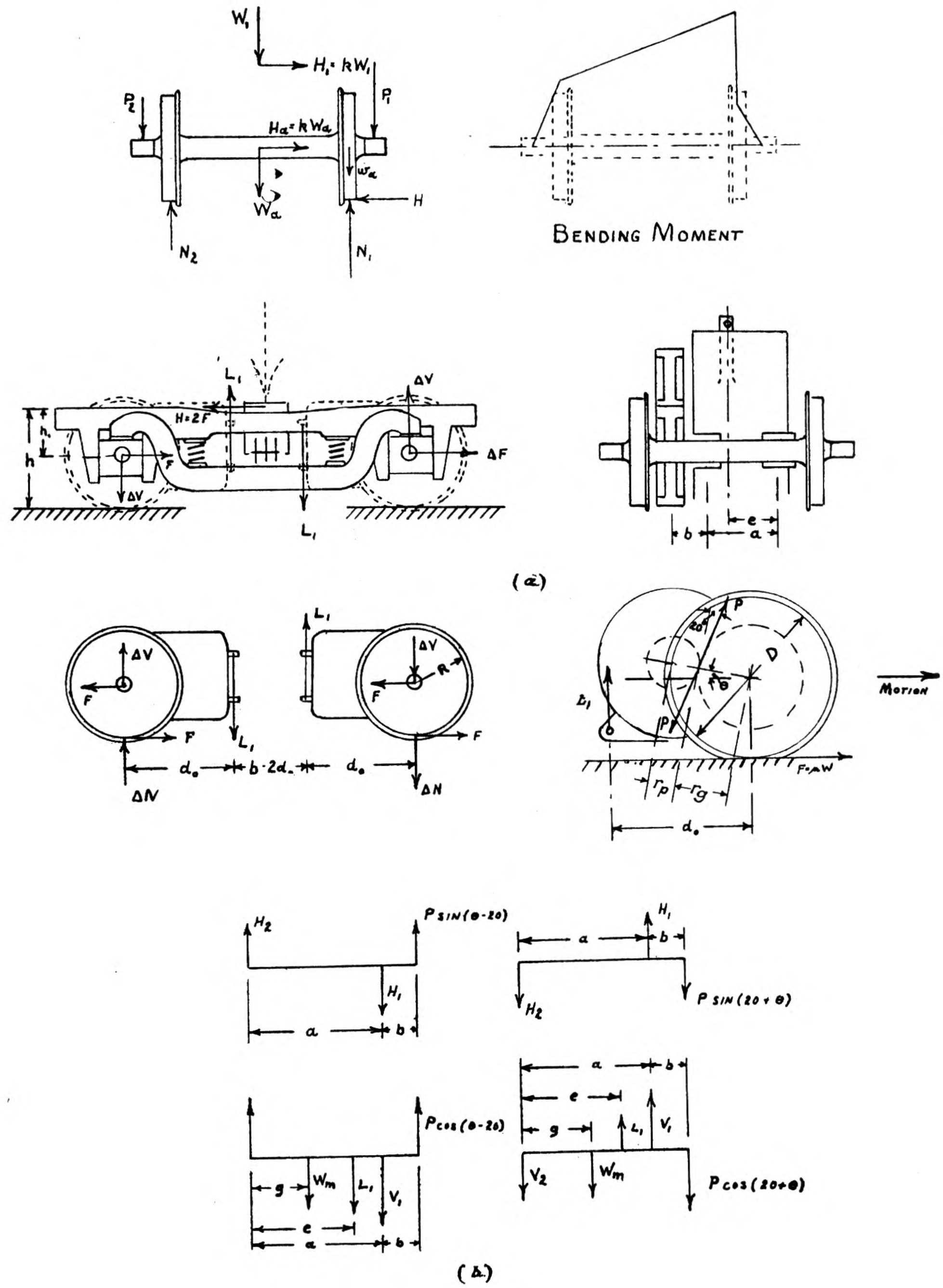

FIG. 7

$$\Delta N = \Delta V - L_1 = \frac{FR}{d_0}\left(\frac{b-2d_0}{b}\right) - \frac{2F}{b}(h-R) - \frac{FR}{d_0}$$

$$= -\frac{2Fh}{b} \text{ (leading)}$$

$$\Delta N = L_1 - \Delta V = \frac{FR}{d_0} - \frac{FR}{d_0}\left(\frac{b-2d_0}{b}\right) + \frac{2F}{b}(h-R)$$

$$= +\frac{2Fh}{b} \text{ (trailing)}$$

which agrees with over-all loadings on the total truck.

Motor Reactions on Axle

The motor reactions on the axle consist of the bearing reactions of the motor frame and the gear reaction, i.e., the armature-pinion reaction on the gear. Assume that the mutual reaction P between pinion and gear makes an angle of 20 deg, approximately, with respect to the tangent at the pitch-circle contact of pinion and gear.

If θ is the inclination of motor and axle center lines with the horizontal, then, considering the pinion, motor, and motor housing, the reactions on this system consist of the reactions of the axle at the journal bearings, the reaction of the gear on the pinion, and the nose reaction, together with the weights of these parts, W_m, approximately.

The reaction P between pinion and gear is

$$P = \frac{FR}{r_g \cos 20} = \frac{\Phi\gamma}{r_g \cos 20} = \frac{\Phi}{r_p \cos 20}$$

The horizontal reactions on the motor bearings are

$$H_1 = P\left(\frac{a+b}{a}\right) \sin (\theta \pm 20); \quad H_2 = P\frac{b}{a} \sin (\theta \pm 20)$$

and the vertical components on the motor bearings are

$$V_1 = P\left(\frac{a+b}{a}\right) \cos (\theta \pm 20) - L_1 \frac{e}{a} \pm W_m \frac{c}{a}$$

$$V_2 = P\frac{b}{a} \cos (\theta \pm 20) + L_1\left(\frac{a-e}{a}\right) \pm W_m\left(\frac{a-c}{a}\right)$$

where the plus and minus signs correspond to leading and trailing motor axles, respectively.

These reactions reversed are the reactions exerted by the motor housing and gear on the axle.

Finally, we have to consider the torsion moment, $0.5FR = 0.5\Phi\gamma$.

In the previous analysis the maximum motor torque and wheel traction per axle F is limited by the adhesion of the wheel, so that

$$F_{max} = \Phi_{max}\frac{\gamma}{R} = 0.33W$$

Brake Loads

During the application of single-shoe brakes an unbalanced thrust is exerted at the shoe $B = \% \times 100W$ where $\%$ is the per cent of braking power. This causes a horizontal bending moment between the hubs $B(L - G)/2$ in pounds, plus a small additional moment due to the wheel traction in braking. With clasp brakes, except for the latter, practically no braking stresses are imposed on the axle. This is one advantage of the clasp brakes.

Compounding Bending-Moment Diagrams

In general, the bending moment due to motor reactions is small compared with the loadings corresponding to the Reuleaux method. Moreover, the motor torque decreases at high speeds. Braking bending-moment diagrams occur in a horizontal plane and compound at right angles with the vertical bending moment by the Reuleaux method. It is questionable whether the two extreme loadings will occur at the same time.

For the reasons given, braking and motor reactions are usually neglected in the Reuleaux method. On the other hand, motor axles are subjected to considerable impact or vibratory loadings resulting from the deadweights of the motor suspension, and for this reason lower stresses should be used, both for the normal loadings and the Reuleaux method.

Spring Suspension

With light-weight equipment an over-all flexible-spring system is necessary: (1) It provides safety at the rail in high-speed service, (2) it takes care of the larger variation for heavy and light loading, and (3) it gives necessary riding comfort. But such spring flexibility should be designed with the limitation of preventing excessive roll.

From the point of view of safety at the rail, consider such a mass as the car body suspended on an equivalent spring of the same over-all deflection as the actual truck-spring system. With spring constant C_p for the bolster elliptic springs and C_c for the coil springs, then for a static load W the deflection is $\delta_1 = W/2C_p$ and $\delta_2 = W/4C_c$, so that the total deflection

$$\delta_s = W\left(\frac{1}{2C_p} + \frac{1}{4C_c}\right); \text{ and } C_E = W/\delta_s = \frac{2C_c + C_p}{4C_pC_c} \text{ (approx.)}$$

where C_E is the equivalent spring constant. Then the principal mode of vertical vibration is given by

$$M\ddot{y} = -C_E(y - y_0)$$

where $M = W/g$

y_0 = some periodic undulation disturbance at the rail, such as rail joints, etc.

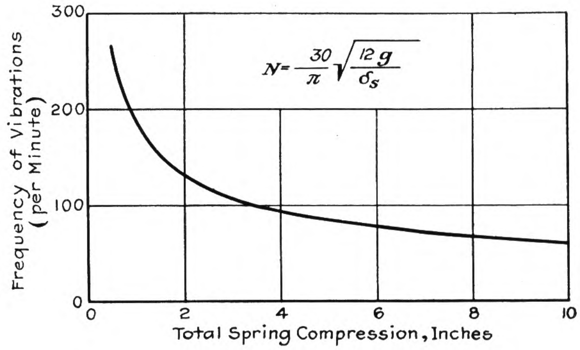

Fig. 8

Assuming

$$y_0 = A \sin pt$$

then

$$M\ddot{y} + C_E y = C_E A \sin pt$$

from which

$$y = \frac{C_E A \sin pt}{(C_E - p^2M)} = \frac{C_E A \sin pt}{M(w_c^2 - p^2)} \text{ (below the natural period)}$$

$$y = -\frac{C_E A \sin pt}{M(p^2 - w_c^2)} \text{ (at the higher speeds above the natural period)}$$

$$\text{where the natural period } w_c = \sqrt{\frac{C_E}{M}} = \sqrt{\frac{g}{\delta_s}} = \pi N/30$$

and N = the number of vibrations per minute.

Therefore, maintaining the frequency low as with large flexibility, the amplitudes of vibration become greatly reduced at high speeds. The change in rail pressure is

$$\Sigma N = C_E(y - y_0) = -\frac{p^2 C_E A \sin pt}{p^2 - w_c^2}$$

which is likewise reduced by keeping $w_c = \sqrt{\frac{g}{\delta_s}}$ low.

Fig. 8 shows the frequency N in vibrations per minute plotted against static spring deflection. An inspection of this plot shows that with over-all deflections of from 8 to 9 in., low frequencies of from 66 to 63 oscillations per minute are obtained; and with deflections at one-half these values as with light loads, the frequencies are approximately 90 per minute. Thus, by maintaining very flexible spring systems, changes of loading such as occur in light-weight equipment still maintain good riding even with light loads.

The same statements apply to angular vibrations.

Lateral and Angular Oscillation of Car Body With Combined Action of Swing Links and Spring System

While a car body has many degrees of freedom, the following is of interest in approximating the lower principle modes of vibration due to the interaction of the swing hangers with the spring system.

Assume a restoring moment Φ to be transmitted through the spring system. Neglecting the local inertias in the truck parts, then if C_p is the spring constant of the bolster elliptic springs, i.e., its load-deflection rate, and assuming the centers to be spaced laterally a distance a, the restoring moment is $\Phi = \frac{1}{2} C_p a^2 \phi_1$ where ϕ_1 is the relative angular deflection. If C_c is the spring constant for the coiled springs spaced laterally a distance L, then $\Phi = C_c L^2 \phi_2$. Then that part of the angular deflection of the bolster due to the springs alone is

$$\phi = \phi_1 + \phi_2 = \Phi\left(\frac{2}{C_p a^2} + \frac{1}{C_c L^2}\right)$$

and since

$$C_\phi = \Phi/\phi$$

then

$$C_\phi = \frac{C_p C_c a^2 L^2}{2C_c L^2 + C_p a^2}$$

Now the lateral restraint of the swing links due to vertical loading only is given approximately by

$$Q = \frac{W}{2}\left[\frac{y + d_0}{\sqrt{l^2 - (y + d_0)^2}} + \frac{y - d_0}{\sqrt{l^2 - (y - d_0)^2}}\right] = \frac{Wy}{l} \text{ (approx.)}$$

where W = center-pin load
l = length of hangers
d_0 = initial outward displacement at bottom of links.

Hence

$$C_y y = Q = \frac{W}{l} y$$

so that $C_y = W/l$.

Due to the swing of the hangers, the spring plank is raised, counteracting the roll on the springs. For small displacements from the neutral position, it "angles" by the amount $\psi = \frac{2 \tan B}{a} y$, where B is the outward angle of the initial spread of the hangers and a is the distance between spring centers. Due to rail depressions, the axles tilt by an angle θ_0 which is frequently of a periodic nature. There is also lateral play y_0 in the truck and at the flanges. Therefore, the relative angular displacement of the bolster in terms of the spring compression ϕ and the counter roll $\psi = K(y - y_0)$ is

$$\theta - \theta_0 = \phi - K(y - y_0)$$

where $K = \frac{2 \tan B}{a}$

and the compression in the spring system is

$$\phi = (\theta + Ky) - (\theta_0 + Ky_0)$$

If h is the height of the center of gravity above the bolster, M the mass of car body per truck, and I_g = polar moment of inertia about center of gravity, then the kinetic energy is

$$T = \tfrac{1}{2} M(\dot{y} + h\dot{\theta})^2 + \tfrac{1}{2} I_g \dot{\theta}^2$$

and the potential energy is

$$V = \tfrac{1}{2} C_y (y - y_0)^2 + \tfrac{1}{2} C_\phi [(\theta + Ky) - (\theta_0 + Ky_0)]^2 + Mgh \cos\theta$$

so that the equations of oscillation are

$$M(\ddot{y} + h\ddot{\theta}) = -C_y \cdot (y - y_0) - C_\phi K[(\theta + Ky) - (\theta_0 + Ky_0)] \ldots [13]$$

$$(I_g + Mh^2)\ddot{\theta} + Mh\ddot{y} = -C_\phi [(\theta + Ky) - (\theta_0 + Ky_0)] + Mgh\theta \ldots\ldots [14]$$

Assuming $\theta_0 = A \sin pt$ for period depressions in the track, and neglecting lateral play, and with $I = I_g + Mh^2$ for the moment of inertia of the car body about the bolster, then

$$M(\ddot{y} + h\ddot{\theta}) + (C_y + C_\phi K^2)y + C_\phi K\theta = 0 \ldots\ldots [15]$$

$$I\ddot{\theta} + Mh\ddot{y} + (C_\phi - Mgh)\theta + C_\phi Ky = C_\phi A \sin pt \ldots [16]$$

If we neglect the angling of the bolster because it is small compared with the spring system, then the amplitudes of vibration are

$$\theta_0 = \frac{(C_y - w^2 M)C_\phi A}{[C_y - w^2 M][(C_\phi - Mgh) - w^2 I] - w^4 M^2 h^2}$$

$$y_0 = \frac{wMhC_\phi A}{[C_y - w^2 M][(C_\phi - Mgh) - w^2 I] - w^4 M^2 h^2}$$

Conditions of large vibrations occur at the natural frequencies, i.e., when

$$[C_y - w^2 M][(C_\phi - Mgh) - w^2 I] - w^4 M^2 h^2 = 0$$

For high-speed service, it is important that such frequencies should be of low order. For the *Zephyr* (neglecting Mgh) the natural frequencies were found to be 79.5 and 170 oscillations per minute, the upper period being effectively damped.

Such frequencies are materially affected by both lateral and angular plays. In general, they are spread over a longer range and the periods are lengthened. They depend greatly on the initial lateral or angular disturbance. With high initial velocities the periods are shortened or the frequencies are raised, the spread in range is reduced, and they approach the natural frequencies with no plays.

In general, the frequencies are lowered by long swing links and flexible-spring systems, and in this way serious lateral and angular motion will not occur in the operating speeds. While damping is effected in the plate springs, it is very important also to have effective damping in the coiled springs. In this manner, periodic disturbances agreeing with the natural frequencies are effectively damped and reduce both lateral and angular vibrations. Such damping in the coiled springs should be relatively small to prevent impacts from being transmitted to the car body. Also, with damping in the coiled springs the ratio of deflections should be increased.

Reactions in Lateral and Angular Swing for Bolster and Spring System

In Fig. 9, assume a couple Φ due to the reaction of the side bearers, and a lateral force H, with center-pin loading W applied at the center pin of the bolster. From Fig. 9 the loads at the elliptical spring seats of the hangers are

$$P_1 = \frac{W}{2} + \frac{\Phi}{a} + \frac{Hh_1}{a}$$

$$P_2 = \frac{W}{2} - \frac{\Phi}{a} - \frac{Hh_1}{a}$$

where a is the lateral spread of the plate spring centers, and h_1 is the mean height from spring seats to center pin. If S_1 and S_2 are the tensions in the swing links, then

$$S_1 \cos\psi_1 = P_1 \quad \text{and } S_1 \sin\psi_1 = H_1, \text{ etc.}$$

and $$H = H_1 - H_2 = P_1 \tan\psi_1 - P_2 \tan\psi_2$$

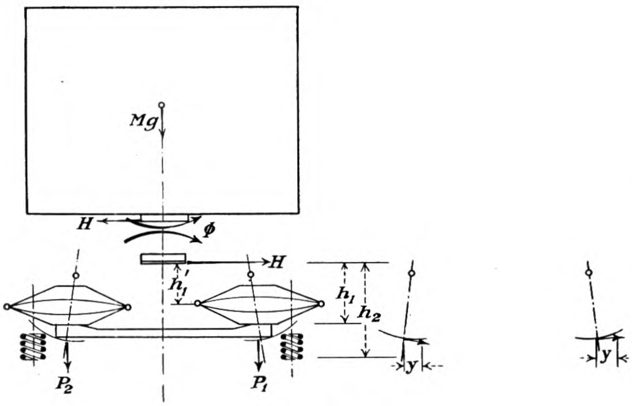

FIG. 9

where

$$\tan \psi_1 = \frac{d_0 + y}{\sqrt{l^2 - (d_0 + y)^2}}$$

$$\tan \psi_2 = \frac{d_0 - y}{\sqrt{l^2 - (d_0 - y)^2}}$$

d_0 = the outward initial lateral displacements
l = length of hangers.

Therefore, neglecting $(d_0 + y)^2$ as small compared with l^2, we have

$$H = \frac{Wy}{l} + \frac{2d_0}{la}(\Phi + Hh_1) \ldots\ldots\ldots\ldots [17]$$

For the angular displacements of the springs

$$\phi_1 = \frac{\Phi + Hh_1'}{C_1} \text{ (for the elliptic springs)}$$

$$\phi_2 = \frac{\Phi + Hh_2}{C_2} \text{ (for the coil springs)}$$

where h_2 is the height of the center pin above the axle and h_1' is the height of the center pin to the clip centers of the plate springs.

If C_p is the spring constant of elliptic springs spaced laterally a, and if C_c is the spring constant of the coiled spring spaced laterally L, then

$$C_1 = \tfrac{1}{2} C_p a^2 \text{ and } C_2 = C_c L^2$$

and the total angular deflection ϕ' for the spring system is

$$\phi = \phi_1 + \phi_2 = \left(\frac{1}{C_1} + \frac{1}{C_2}\right)\Phi + \left(\frac{h_1'}{C_1} + \frac{h_2}{C_2}\right)H \ldots [18]$$

Equations [17] and [18] can be written

$$\left.\begin{aligned} y &= A\Phi + BH \\ \phi &= C\Phi + DH \end{aligned}\right\} \ldots\ldots\ldots\ldots [19]$$

where

$$A = \frac{2d_0}{aW}; \quad B = \frac{1}{W}\left(l - \frac{2d_0 h}{a}\right)$$

$$C = \frac{1}{C_1} + \frac{1}{C_2}; \quad D = \frac{h_1'}{C_1} + \frac{h_2}{C_2}$$

From [19], Φ and H are linear functions of the lateral and angular deflections, i.e.

$$\Phi = \frac{Dy - B\phi}{AD - BC} \quad \text{and} \quad H = \frac{A\phi - Cy}{AD - BC}$$

or

$$\Phi = Py + Q\phi \quad \text{and} \quad H = E\phi + Gy \ldots [20]$$

Now the angular displacement of the bolster is $\theta = \phi - Ky$, where $K = \dfrac{2 \tan \psi_0}{a}$

ψ_0 = the initial angle of the swing links.

Hence

$$\left.\begin{aligned} \Phi &= (P + QK)y + Q\theta \\ H &= E\theta + (EK + G)y \end{aligned}\right\} \ldots\ldots\ldots\ldots [21]$$

If h is the height of the center of gravity of the car body above the center pin, and M is that part of its mass corresponding to the weight on the center pin, then, neglecting the interaction of the other center pin, or with symmetrical trucks for the primary modes of oscillation, the equations of motion are

$$\left.\begin{aligned} M(\ddot{y} + h\ddot{\theta}) &= -H \\ I\ddot{\theta} + Mh\ddot{y} &= -\Phi + Mgh\theta \end{aligned}\right\} \ldots\ldots\ldots\ldots [22]$$

if we neglect the secondary mass of truck. If I_g is the polar moment of inertia of the car body and $I = I_g + Mh^2$, the equations of oscillation are

$$\left.\begin{aligned} M\ddot{y} + (EK + G)y + Mh\ddot{\theta} + E\theta &= 0 \\ I\ddot{\theta} + (Q - Mgh)\theta + Mh\ddot{y} + (P + QK)y &= 0 \end{aligned}\right\} \ldots [23]$$

which gives a closer approximation for the two natural frequencies than in the previous analysis.

4—PHYSICAL PROPERTIES OF STAINLESS STEELS

The stainless steel used in the construction of the *Zephyr* is of the low-carbon chromium-nickel type. This steel is commonly known in the trade as 18-8. In the annealed state, the physical properties are roughly, ultimate strength, 85,000 lb per sq in., yield point, 40,000 lb per sq in., and elongation in 2 in., 65 per cent. This metal can be cold rolled to produce high tensile strength, but unlike most metals, a large portion of the ductility is retained. Tensile strengths as high as 150,000 lb per sq in. are obtainable with an elongation in 2 in. as high as 20 per cent. In light gages 0.010 in. thick, tensile strengths as high as 185,000 lb per sq in. may be obtained with adequate ductility.

Another important characteristic of this steel is that its most ductile condition is produced by rapid cooling from high temperatures. The value of this characteristic in welding becomes apparent at once when it is considered that after cooling from the necessary fusion temperature an extremely ductile weld results. Welds are regularly made which will not show a fracture under a shearing strain of 90 deg in torsion.

The early attempts at welding this metal resulted in difficulties due to the fact that certain metallurgical changes resulting in lowered corrosion resistance take place when the steel is heated to the range of temperatures 900 to 1500 F. The magnitude of the effect of these metallurgical changes is a function of time and temperature. It is obvious that during welding, certain zones near the fused portion of the weld must pass through this temperature range at a retarded rate.

The "shotweld" system, which was used in the construction of the *Zephyr*, is essentially a spot-welding process, but is so controlled as to give a minimum optimum-current control. Moreover, the time of current application is so short and so accurately controlled that the deleterious metallurgical changes mentioned do not take place. And further, in welding cold-rolled (high-tensile) stainless steel by the shotweld system, the extent of the annealed zones immediately surrounding the weld is held to a minimum. The kilowatt capacity increases with the gage of the material.

Obviously the shear strength of individual welds increases with the gage of the material and the size of the weld. With a thickness of 0.012 in., the minimum shear strength is approximately 300 lb, increasing to 1200 lb with material 0.04 in. thick. The unit shear value of welds is greater than 70,000 lb per sq in.

In the draw-rolling into sections, "spring back" is greatly reduced by the use of relatively sharp bends and by proper roll design. Sections, therefore, consist of a series of flat sides bounded by bends of relatively small radii.

Typical Sections Used in Construction

For struts under column compression with shotweld gusset connections, and ordinary limiting compressive stresses around 20,000 lb per sq in., values of l/ρ were not allowed to exceed 90. Somewhat lower values were used with maximum limiting compressive stresses of 25,000 lb per sq in.

A very important problem in the construction has been the local stability from buckling of thin strips in compressive members and thin webs in girders and beams for transverse loadings. It may be shown that the allowable critical compressive stress in a rectangular plate supported on four sides, as in a longitudinal side strip of a compressive member, is

$$f_{cr} = k\,\frac{\pi^2 E h^2}{12b^2(1-\mu^2)}$$

in which μ = Poisson's ratio

$$k = \left(\frac{a}{mb} + \frac{mb}{a}\right)^2$$

where m is an integer which corresponds to the number of waves in which the plates divide in buckling and is so chosen that k is a minimum, a the length, and b the width of rectangle under compressive loading. For long strips, $k = 4$ is a good approximation, and with $\mu = 0.3$, then

$$f_{cr} = \frac{108{,}500{,}000}{b^2/h^2}$$

where

$$\frac{b}{h} = \frac{\text{width of strip}}{\text{thickness of plate}} = \text{flat-pitch ratio.}$$

It is of considerable interest to note that complete experimental verification has been made with over 150 tests of various sections by Col. E. J. W. Ragsdale and A. G. Dean, in a very comprehensive study of this subject, which, however, indicates increasing edge stability due to more effective constraint. This effect is shown in Fig. 10.

Fig. 10 shows critical design compressive stresses plotted against flat-pitch ratios. Obviously, f_{cr} should not exceed the proportional limit taken in the plot at 80,000 lb per sq in., though at low values of b/h the ultimate strength has been demonstrated to approach very nearly the tensile strength of the material. For actual working stresses to allow for eccentricities and indeterminate boundary conditions, a factor of 2 to 3 should be used on the critical compressive stress. Flat-pitch ratios not exceeding 30 have been used with sections stressed to 25,000 to 30,000 lb per sq in. working compressive loadings, though somewhat higher values can be used.

In many cases, however, to maintain a low flat-pitch ratio with simple plane strips for the boundary of the section results in low values for the least radius of gyration ρ with correspondingly too high values for l/ρ for the column as a whole. To improve the section for the stability of the column requires, for maintaining low flat-pitch ratios, either a thickening of the plate or the addition of reinforcement strips. Central longitudinal corrugations are also found effective.

Because of lack of continuity of longitudinal shear with the shotweld reinforcement strips, the individual moments of inertia of the laminated strips are added in estimating the equivalent thickness, so that

$$I = \Sigma\,\frac{b_s h^3}{12} \quad \text{and} \quad h = \sqrt[3]{\frac{12I}{b}}$$

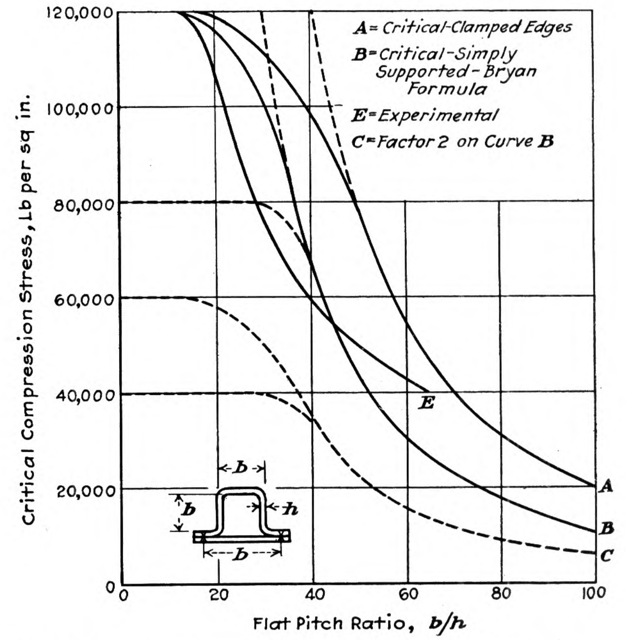

Fig. 10 Relation Between Critical Compressive Stress and Flat-Pitch Ratios, Stainless Steel

where b = width of plate
b_s = width of strip.

Reinforcement by central longitudinal corrugations is very effective in lowering flat-pitch ratios. In fact, long corrugations appear sufficiently effective to cause failure due to element flat-pitch rather than composite pitch for the side.

Weld spacing is taken at about 15 times the thickness of the minimum flange or strip, and at least 7 weld thicknesses from the edges of gussets. With flange strips around 15 times the minimum plate thickness in width, k is reduced to approximately 0.5 due to the unsupported edge, so that

$$f_{cr} = \frac{14{,}000{,}000}{b^2/h^2}$$

Thus with b/h equal to 15, ample stability is obtained with any working stress.

Transverse Loading of Beams

In the design of beams, the stability of the webs is of first importance because of the vertical and longitudinal shearing action. With vertical plate webs and assuming vertical stiffeners spaced a distance L apart, and with free depth d between flanges, then the critical shear stress is

$$f_{scr} = \frac{K}{d^2/h^2}$$

where $\frac{d}{h} = \frac{\text{free depth of beam}}{\text{plate thickness}}$ and K has the following values for L/d:

L/d	K	L/d	K	L/d	K	L/d	K
1.0	256×10^6	1.4	197×10^6	1.8	185×10^6	2.5	171×10^6
1.2	217×10^6	1.6	190×10^6	2.0	180×10^6	3.0	166×10^6

Because of the conjugate nature of the shear in the webs when the stiffener spacing is less than d, L/d is replaced in the table by d/L. In all cases the *Zephyr* beams have double webs. Limiting working stresses were maintained with a factor from 2 to 2.5 of the critical shearing stress.

With corrugated webs, both vertical and longitudinal corrugations have been used, the former being more common in the *Zephyr* construction in order to eliminate the use of vertical stiffeners. Longitudinal corrugated beams are substantially stronger than plane-web beams. In the applications of corrugated beams, sample tests have always been made with from 1.5 to 2 the normal loading condition.

Corrugated-Roof Strength

Over the baggage-door and step-well openings, the top and bottom chords must sustain the total shearing load together with secondary bending. The roof was reinforced with additional carlines for stiffeners, together with an inside plate welded to the longitudinal corrugations, and this reinforcement extended back two to three panels on either side of the openings. It is evident that in order that the roof may act as an integral heavy girder spanning the opening, the vertical shearing loads must be transmitted by reinforced corrugated curved webs.

It was estimated that the greater part of the shear transmitted by the corrugated curved web would be concentrated in an arc of 10 in. A test specimen was constructed as shown in Fig. 11. Vertical stiffeners assimilating the carlines were spaced $8^1/_2$ in., and the curvature with a 20-in. radius corresponded to that of the roof. The total maximum shear at the baggage-door opening is 16,000 lb, but this is divided between the roof and floor system.

Test No. 1. The 0.035-in. curved sheet was omitted and only the longitudinal corrugations were used in the webs. With a span of 51 in. loaded at the center, failure occurred at the flange welds at the center stiffener, corresponding to 750 lb (average) per weld, under a central loading of 27,000 lb. No failure occurred due to shearing or straight bending, though stresses of 26,700 lb per sq in. shear and 88,900 lb per sq in. bending were realized. The pulling out of the weld at the center stiffener was local in nature and due to the concentrated loading.

Test No. 2. In test No. 2, the 0.035-in. inside curved liner sheet was included. The 0.013-in. corrugations were $^1/_4$ in. deep, and the channel for top and bottom flanges was 0.05 by 2 in. In this case failure occurred by pure bending under a load of 31,000 lb with a shear stress of 13,150 lb per sq in. and a bending stress which caused failure at 111,300 lb per sq in. No accordian action or failure in the webs was observed.

Test No. 3. To assimilate drastic shear loading, the points of support were moved inward to a 17-in. total span and the structure was centrally loaded. In this test the 0.035-in. curved sheets and the 0.022-in. corrugations $^1/_2$ in. deep sustained a maximum load of 53,300 lb. The failure was not due to shear but occurred at the connection of the end stiffener to the web, with 1650 lb per weld. The shear stress exceeded 19,500 lb per sq in.

The shear in the roof is not likely to exceed 10,000 lb under the most drastic assumptions, so that ample strength was provided by the use of 0.04-in. reinforcement sheets $^1/_2$ in. deep, with 0.022-in. corrugations. In material of the thinnest gage no crimpling or shear failure has been observed. While much experimental work has been done on special applications, the data at this time are not in form to express in mathematical formulas.

Spot Welding and Shear Strength of Welds

Stainless steel of the 18-8 variety is normally a solid solution, that is the carbon, nickel, and chromium are dissolved in the iron. The maintenance of this condition is desirable for the prevention of corrosion and for increasing the resistance to fatigue.

If the metal is heated to between 950 F and 1550 F and held in this temperature range, carbide precipitation occurs, resulting in a change from a solid solution to an aggregate. The maximum precipitation occurs around 1200 F.

In the process of welding it is desirable that the heating and cooling be effected very rapidly through this temperature zone. In ordinary welding processes where a large mass of metal is affected in the fusion, the heating and cooling would be effected sufficiently slowly to cause a considerable amount of this precipitation. In the shotweld process the time element is sufficiently short so that the fusion is localized at the weld, resulting in very rapid cooling and the prevention, to a great extent, of the carbide precipitation in the surrounding zones.

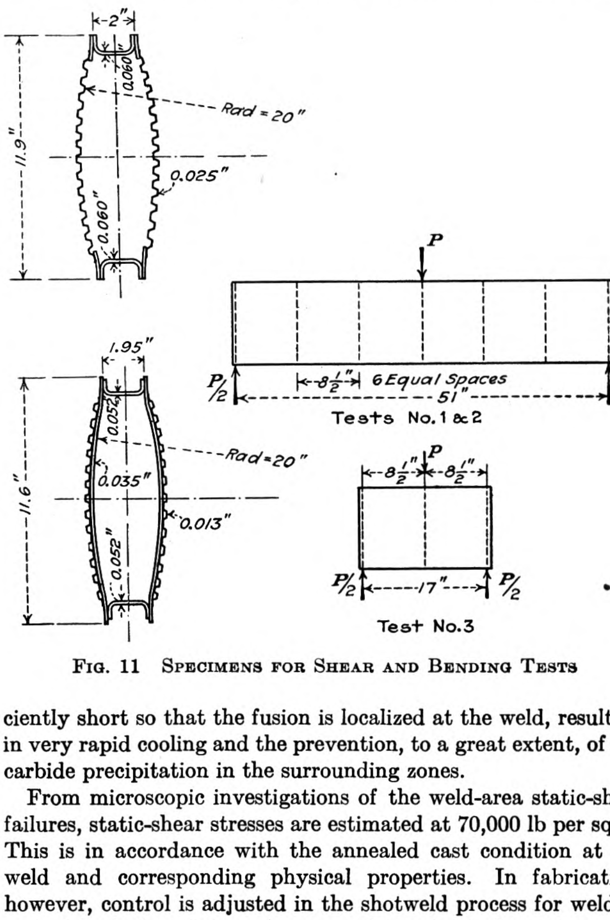

Fig. 11 Specimens for Shear and Bending Tests

From microscopic investigations of the weld-area static-shear failures, static-shear stresses are estimated at 70,000 lb per sq in. This is in accordance with the annealed cast condition at the weld and corresponding physical properties. In fabrication, however, control is adjusted in the shotweld process for welding material of the minimum gage, and the total shear stress per weld, which increases practically linearly with the gage of the material, is used in design. The static total shear per weld is approximately $f_{st} = 32{,}000\ h$, where h is the minimum gage of the material.

Depending upon the type of loading and stress-concentration allowance for secondary torsional-shear stresses and local bending allowance for fatigue, various factors of safety are used with this value.

With gussets subjected to secondary bending, torsional-shear stresses have been added to the straight-shear stresses.

Construction Details

Fig. 12 shows typical sections used in the *Zephyr* for posts, carlines, purlines, diagonals, the bottom chord or skid rail of the main side truss and the body panel, the belt rail and the body panel, and the roof or top rail and a portion of the corrugated roof. With heavy compression loads on the posts, the plate stability is strengthened by channel reinforcements, thus reducing

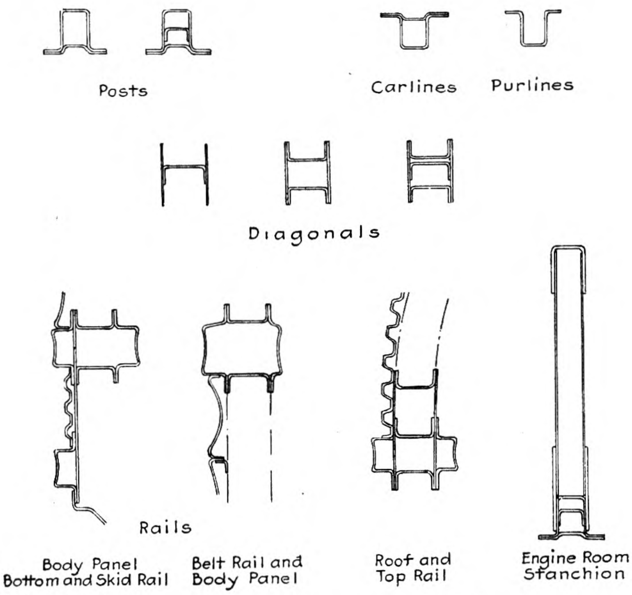

Fig. 12 Details of Stainless-Steel Sections

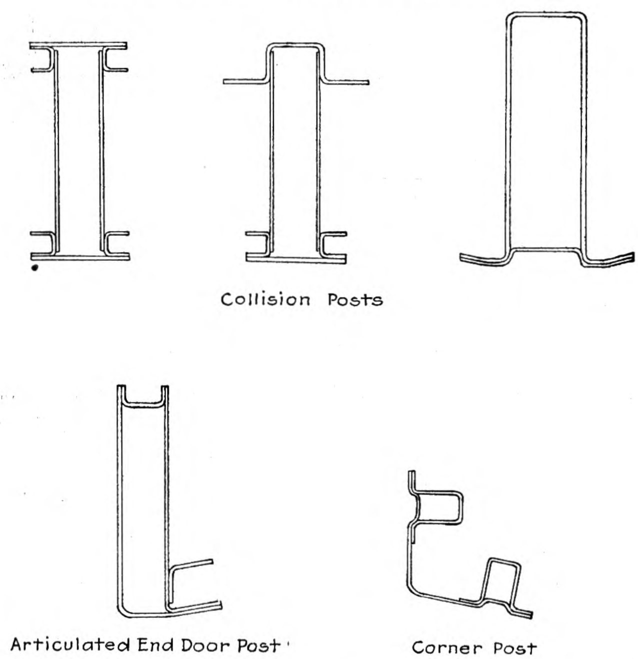

Fig. 13 Details of Stainless-Steel Sections

the flat-pitch ratio and augmenting the area of section. Such a reinforcement for a diagonal is also shown at the right.

Fig. 13 shows typical sections of collision posts used in the mail compartments and (at the right) for the front of train. Such posts are effective also as bulkhead reinforcements, having high resistance to bending. At the lower left is shown the cross-section of the main articulated-end door post. This post is designed for both longitudinal and lateral bending. At the bottom it connects with the articulated casting projections. A typical corner-post arrangement is shown at the right.

Fig. 14 shows the general scheme of maintaining connections

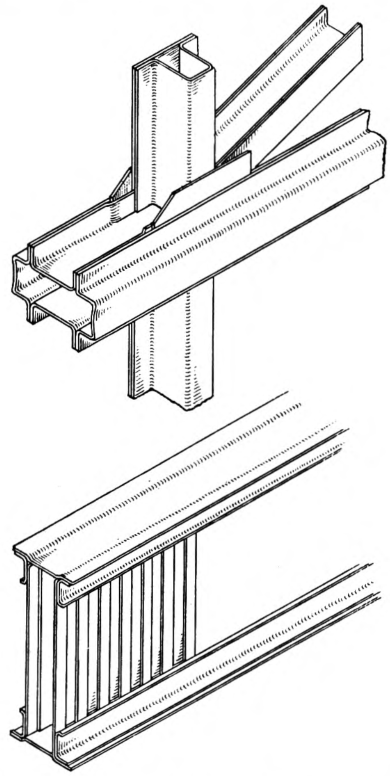

Fig. 14 Details of Structural Connections and Typical Web Girder

without eccentric loadings. A post fits within a main longitudinal rail, and symmetrical connections to diagonals are shown. The flange arrangements give effective reinforcements to webs and increase their stability. At the bottom is shown a typical corrugated-web girder with vertical corrugations.

BIBLIOGRAPHY ON STABILITY OF THIN SHEETS

(1) Bryan, G. H., Proc. Lond. Math. Soc., vol. 22.

(2) Timoshenko and Lessells, "Applied Elasticity."

(3) Southwall, R. V., and Skam, S. W., "On the Stability Under Shearing Forces of a Flat Elastic Strip," Proc. Roy. Soc., vol. 105.

(4) Wagner, H., "Plane Panel Frames of Very Thin Sheet," *Zeit. für Math.*, vol. 20 (1921).

(5) Wagner, H., "Flat Sheet Metal Girders With Very Thin Webs," N.A.C.A. (1931).

(6) Timoshenko, S., "Working Stresses for Columns and Thin-Walled Structures," A.S.M.E. Trans., 1933, paper no. APM-55-20.

5—ANALYSIS OF LIGHT-WEIGHT-CAR CONSTRUCTION

The use of stainless steel, which eliminates corrosion limitations, makes it possible to use thin-web beams designed to their stability strength. By the shotweld process, satisfactory connections of great lightness have been made. The stress-elongation curves of stainless steel differ from those of ordinary steels in having no strict demarcation at the yield point. The tensile properties of stainless steel, an 18-8 chrome-nickel alloy with carbon around 0.10 per cent, depend essentially on the degree of cold work. The average stock used has a minimum tensile strength of 150,000 lb per sq in., with minimum elongation of 2-in. specimens of from 12 to 20 per cent. The yield point, based on 0.1 per cent permanent set, approximates 120,000 lb per sq in., while the true elastic or proportional limit may be taken at 80,000 lb per sq in. The shear strength of individual spot welds increases with the gage of the material and the size of the weld, with a minimum static-shear strength of 70,000 lb per sq in. at the welds. Endurance values from preliminary tests so far made indicate, for complete alternation of stress, a limit at 20 per cent of the static weld strength.

When compared with ordinary carbon steels with tensile strength at 65,000 to 70,000 lb per sq in., it will be seen that this material has considerable stress capacity and that it possesses great opportunities of saving weight in connections as well.

In the design of the *Zephyr* relatively low stresses have been maintained. With the lowest proportional limit at 80,000 lb per sq in., a factor of from 3.2 to 4 was used in all major members, i.e., with a limiting working stress not exceeding 25,000 lb per sq in., corresponding to 16,000 lb per sq in. in low-carbon steel constructions. While the factor permits high-stress concentrations, secondary stresses have been estimated in all important members. Thus, with short members that have large moments of inertia, secondary bending moments have been estimated as well as the corresponding additional torsional-shear stresses in the gussets.

Considerable attention has been given to the stiffness of the car structure and to the corresponding stresses consistent with the deflection of the car as a whole and with local vibrations.

Essentially, a car is a beam or bridge supported at the center pins and proportioned to carry the dead and live loads. But, differing from a bridge, it must sustain heavy lateral and rolling loads which impose torsion loadings, together with large compressive loads consistent with reasonable collision capacity. Further, a continuous truss does not exist because of side-door openings, and considerable redundancy is introduced by them and the window panels.

In the conventional car, even with heavy center sills, the car body carries the greater part of the bending moment. With vertical panel posts between the windows, we have a very indeterminate type of structure with high redundancy resulting in secondary bending stresses in the posts. The roof itself is not greatly considered as a structural member.

In the structure of the *Zephyr*, the entire cross-section of the car is considered as a structural section, with compression in the roof as a top chord of the truss. Colonel Ragsdale aptly suggested that in relation to conventional car construction, the *Zephyr* was reminiscent of the transition from the old-time heavy-keel construction of ships to the plate-keel type with compression resistance in the deck.

In the *Zephyr* construction the shear loadings, which result in longitudinal shear forces that cause large secondary bending moments in panels between windows in conventional car construction, are carried in a more determinate way by diagonals in the truss.

The main side frames of the *Zephyr* cars are essentially Pratt trusses, in which advantage is obtained from diagonal members in tension and vertical posts as short-column compression members. Considerable lateral strength has been effected by making panel posts a part of a continuous frame bent or ring, which includes heavy roof carlines and an integral cross frame below the floor. Continuation of the truss scheme has been maintained under the belt rail at the window openings and the redundancy above them has been taken into consideration. In the main-truss analysis, only the roof rail and the floor rail have been considered for bottom and top chord members, respectively.

At door openings and step wells, generally, vertical shear loading has been combined with large bending moments to be transmitted by the upper and lower members. For such places, the roof itself was greatly reinforced as a heavy carrying beam and the reinforcement was extended to several panels either side of the opening. Deep longitudinal truss beams were inserted just inside of the steps and securely anchored to three panel points on either side of the step well.

A major problem in the design of the *Zephyr* is presented in the articulated type of construction used. While articulation reduces the weight of a train by the elimination of a truck for every connection, it imposes structural difficulties in increased bending moments and in the design of the end construction. Moreover, without light-weight construction, the use of articulated cars would be practically impossible structurally. The overhang effect of an 85-ton Pullman, with over-all length of 81 ft and truck centers of 56 ft, results in points of contraflexure between the trucks, providing a cantilever-bridge suspension between the points of contraflexure with an effective span reduced to 50 ft. Even with this span, the center bending moment, assuming an 85-ton car with distributed load, reaches a bending moment as high as 7,900,000 in-lb. If such a car were articulated at the ends, disregarding clearance difficulties, the bending moment for the same loading would increase to 20,300,000 in-lb. For this reason, articulation depends upon the specified length of the car, and hence, for longer spans, on light-weight construction.

Articulation Construction

The center-pin reaction, consisting of a vertical component, a lateral component, and a longitudinal thrust or tension component, is transmitted by a mild-cast-steel structure to stainless-steel trussed end frames, which, in turn, support the main side frames of the car body. The end frame itself consists of two vertical posts extending to the roof and riveted to the casting and to the side frames by a diagonal frame construction. Two horizontal legs of the casting connect the two main center sills.

While the end frames function mainly in carrying vertical loads from the casting to the side frames, they must also be designed for the unsymmetrical loading that results from lateral and rolling oscillations. In addition, the eccentricity of the center-pin bearings in a longitudinal direction with respect to the end frames throws considerable bending on the posts and a certain percentage is resisted by bending in the longitudinal sills. It is important to estimate the distribution of these moments. In the *Zephyr* more than 85 per cent of the center-pin-reaction bending moment is carried through the post and is resisted by a longitudinal reaction at the roof and the remainder is resisted by bending in the sills. With the New York Rapid Transit articulated train, a greater bending is resisted by the sills.

Power-Plant Support

The bed plate of the engine, generator, and auxiliaries is supported by an all-welded box of cromansil construction, which includes longitudinal girder supports for the engine and generator frames. The construction is shown diagrammatically in Fig. 15.

A feature of the design is the balancing of the entire structure including engine and generator over the truck bolster. In fact, the cross-bolster frame of the front car was included as the central cross member in this construction.

The main upward supporting forces acting on the stainless-steel side trusses react downward on the outer wings of the central cromansil cross member. The cross member was carefully designed for the lateral bending moments. A small un-

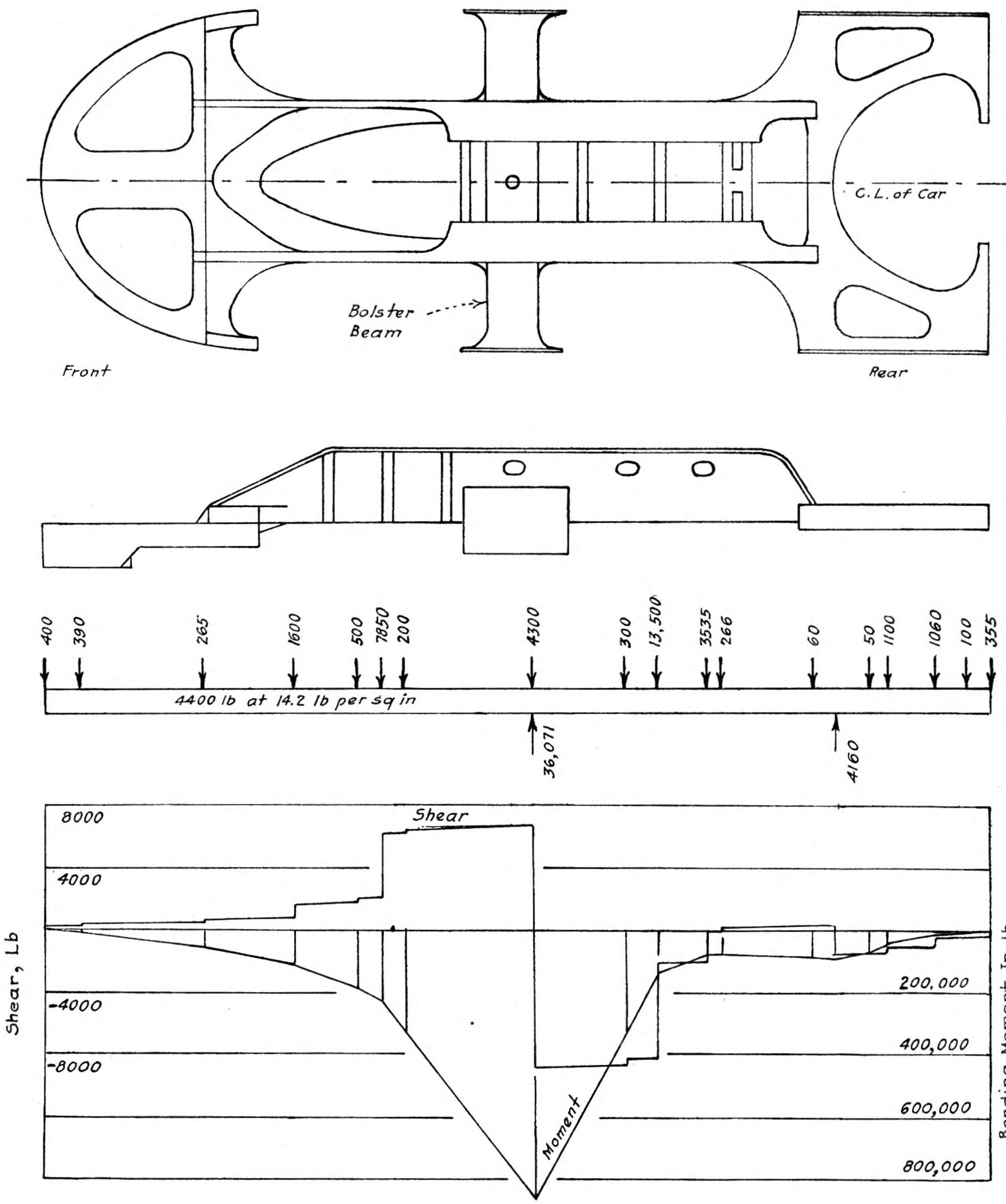

Fig. 15 Power-Plant-Support Shear and Bending-Moment Diagrams

balanced tipping reaction was taken by the side frames aft of the center pin.

Evidently the central supporting reaction consisted of the upward center-pin reaction of the truck and the downward reaction of the side-truss supports or their corresponding shear forces, a net loading of 36,000 lb. The distributed and concentrated loadings are shown in the diagram. From the bending-moment and shear diagrams, the frame structure was subjected to a maximum bending moment of 800,000 in-lb. The stiff girder supports of the engine and generator foundation were effective in giving a section modulus that was adequate for resisting this moment.

Bending-Moment and Shear Diagrams for Main-Side-Truss Loadings

A diagram of the front car is shown in Fig. 16 with the characteristic Pratt-truss diagonals. In the analysis special consideration was given to the redundant reactions at the mail- and baggage-door openings. Essentially, such openings must transmit the shear in the top and bottom chords which results in secondary bending stresses in these members. For this reason such openings were greatly reinforced and the entire roof was considered as the upper member.

The main side truss may therefore be considered as three separate trusses, with the intermediate supporting reactions consist-

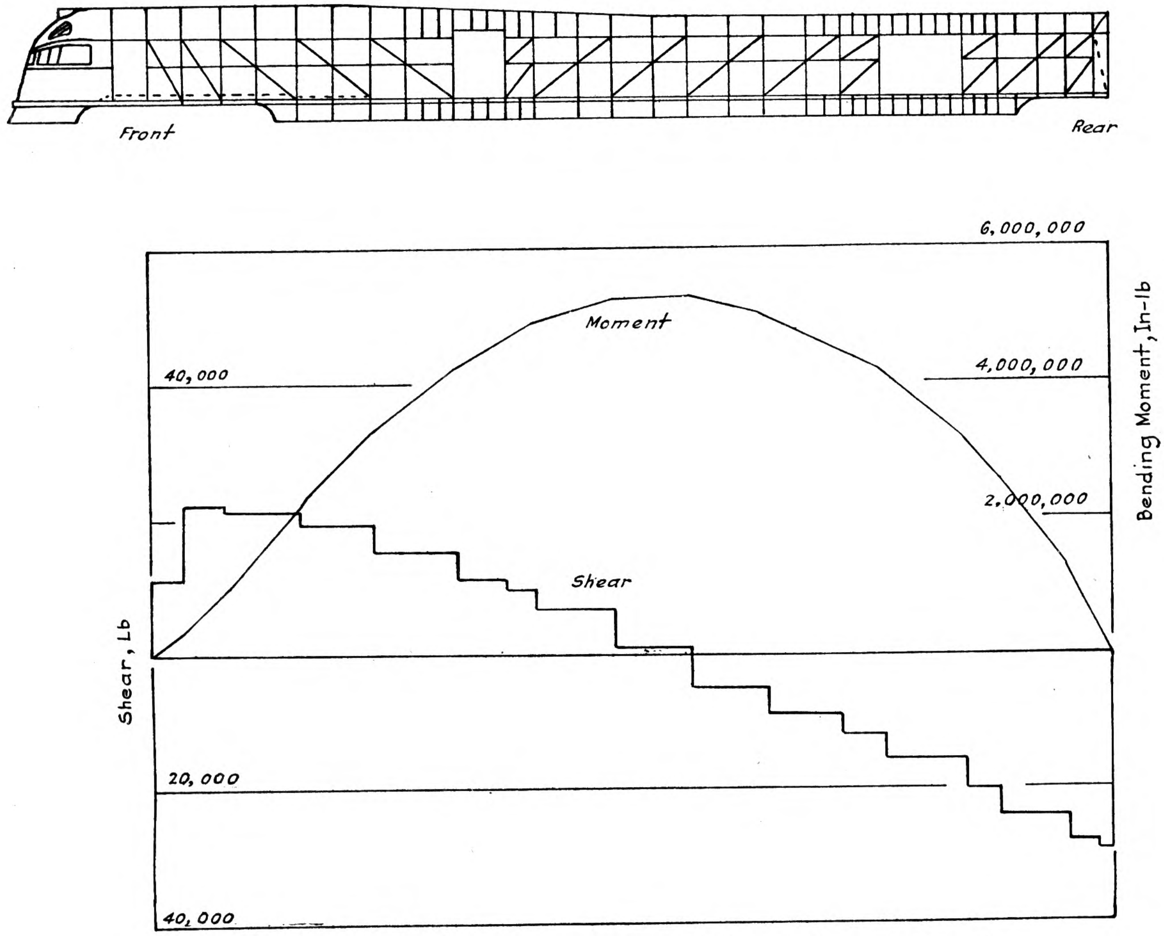

Fig. 16 Main-Side-Truss Shear and Bending-Moment Diagrams, Front Car

ing of the reactions of the openings, which are essentially a bending-moment couple and shear reactions distributed at the top and bottom members.

The bending moment in the front car with heavy baggage loading exceeded 5,000,000 in-lb.

The second car has a similar frame construction, Fig. 17, with reinforcements at its baggage-door and step-well opening. Here again there are essentially three component trusses, separated by the openings, that have intermediate supporting reactions corresponding to the reactions of the openings. At the rear, a special feature is the continuity of the diagonals below the belt rails at the window openings. The bending moment in this car also reaches a high value in excess of 5,000,000 in-lb.

The last car, Fig. 18, shows how the continuous diagonal scheme was maintained at the numerous window openings. The car structure was considerably redundant because of the upper members over the window openings. The step-well opening was subjected to considerable bending as shown in the bending-moment diagram. By the diagonal scheme used compression was maintained throughout the roof as a top chord.

Typical Analysis of Side Frames

As an example of the stress analysis for a side frame, the portion of the truss extending from the passenger-door opening of the rear car to the overhang at the rear beyond the rear truck has been chosen.[3] The structure is made redundant by the window openings, and simple statical considerations will show that it is redundant to three degrees. The applied loadings consist of the panel loadings and the overhang loads at the rear. The supporting reaction of the center pin is distributed on two cross-bolster beams, with equal upward reactions of 10,240 lb, as shown at the end of the diagram in Fig. 19. The shear reaction from the step-well opening divides in the ratio of the moments of inertia of the top and bottom chord members.

The supporting reaction at the rear end is determined from the external forces on the entire car. The bending moment and shear of the step-well reaction and the equality of the horizontal forces at the step well require three equations, which, when combined with the loads in the 48 truss members, give a total of 51 unknown quantities. On the other hand the 24 joints provide 48 equations for solution. The structure is therefore, a threefold redundant one, and the members with reactions X_a, X_b, and X_c were considered redundant.

The loads in the members are expressed as linear equations in terms of the applied loadings and the redundant reactions. We have, then

$$\Sigma \frac{T}{A} \frac{\partial T}{\partial X_a} L = 0; \quad \Sigma \frac{T}{A} \frac{\partial T}{\partial X_b} L = 0; \quad \Sigma \frac{T}{A} \frac{\partial T}{\partial X_c} L = 0$$

where the redundant members are included in the summations.

Cross-Beam Trusses

For supporting the floor structure and stiffening the structure as a whole, deep truss beams were used at panel points. Because of air-conditioning and electrical-wiring ducts and piping, the

[3] While a more complete analysis requires consideration of the interaction of the truss with the roof and floor system, in a first approximation a pure truss action was considered with roof rail and skid rail as top and bottom chords.

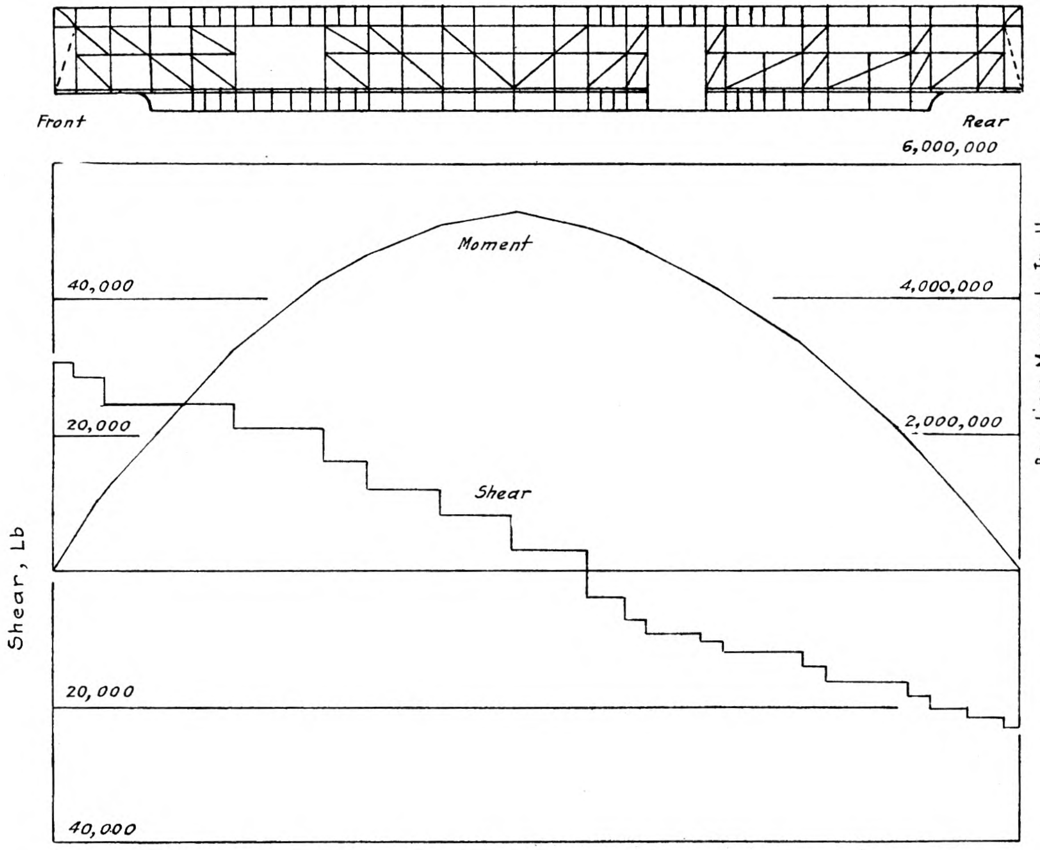

Fig. 17 Main-Side-Truss Shear and Bending-Moment Diagrams, Middle Car

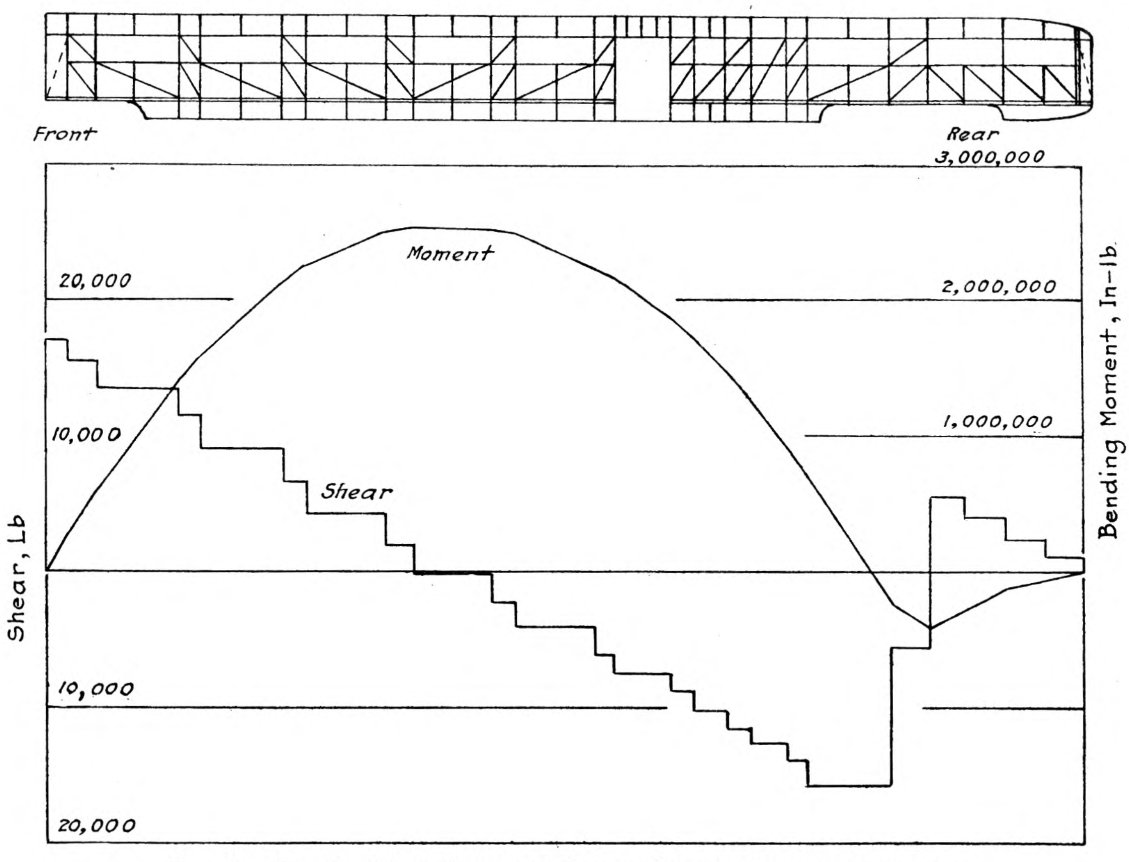

Fig. 18 Main-Side-Truss Shear and Bending-Moment Reactions, Last Car

$$\sum \frac{\partial W}{\partial X_a} = -1{,}265{,}390 + 53.18 X_a \qquad + 14.55 X_c = 0$$

$$\sum \frac{\partial W}{\partial X_b} = -357{,}575 \qquad + 41.07 X_b + 14.55 X_c = 0$$

$$\sum \frac{\partial W}{\partial X_c} = -477{,}608 + 14.55 X_a + 14.55 X_b + 16.48 X_c = 0$$

$$X_a = 23{,}619; \quad X_b = 8{,}478; \quad X_c = 643$$

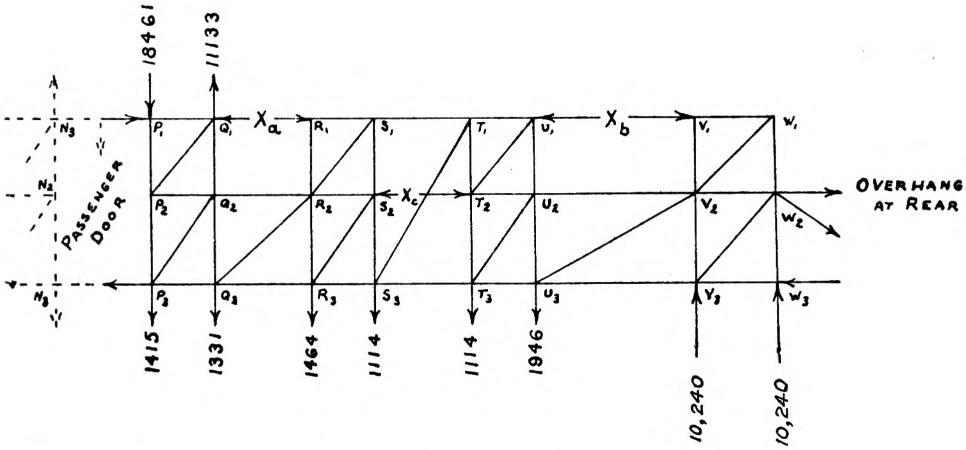

FIG. 19

central diagonal of the truss was frequently omitted. This imposed local bending on the top and bottom chords. In a first approximation, the entire bending was considered as acting only in the top beam and pure truss action below it.

For either symmetrical or unsymmetrical loading, the structure is redundant to one degree. The reactions between the top beam and the truss (see Fig. 20) are T_1, R_5, R_6, T_6, T_8, and T_5. Now the horizontal components of T_1 and T_5 with the center horizontal components T_8 and T_6 are equivalent to simple axial loadings on the top beam. For this reason, it is convenient to consider the truss as divided into a beam and a complete truss, the top chords of the latter taking the axial loadings of the beam, and the beam subjected only to bending due to the supporting forces and the vertical reactions between the truss and beam.

On this basis, for symmetrical loadings R was selected as the redundant reaction between truss and beam. The loadings in the truss members are of the form $T = KR$, so that $\frac{\partial T}{\partial R} = K$, and therefore

$$\Sigma \frac{T}{A} \frac{\partial T}{\partial R} L = R\, \Sigma K^2 \frac{L}{A} = 760.4R \qquad [24]$$

The center sills are spaced at distances of $b = 31$ in. and from the end supports a distance $a = 37.5$ in. The redundant supports of the truss on the beam act at the sills and end supports. For the differential coefficient of the bending energy of the beam with a uniform loading of w lb per in. with end supporting reactions $wl/2 - R$ and reactions R at the sills, where $l = 2a + b$, $I = 0.2$ in.^{4} for the beam, we have

$$\int \frac{M}{I} \frac{\partial M}{\partial R} dx = \left(a^2 b + \frac{2a^3}{3}\right) \frac{R}{I} - \left(\frac{5a^3}{6} + \frac{5a^2 b}{3} + ab^2 + \frac{b^3}{6}\right) \frac{wa}{2I} = 394{,}500 - 14{,}755{,}000w \qquad [25]$$

Hence

$$E \frac{\partial V}{\partial R} = 395{,}260R - 14{,}755{,}000w = 0$$

$$R = 37.3w$$

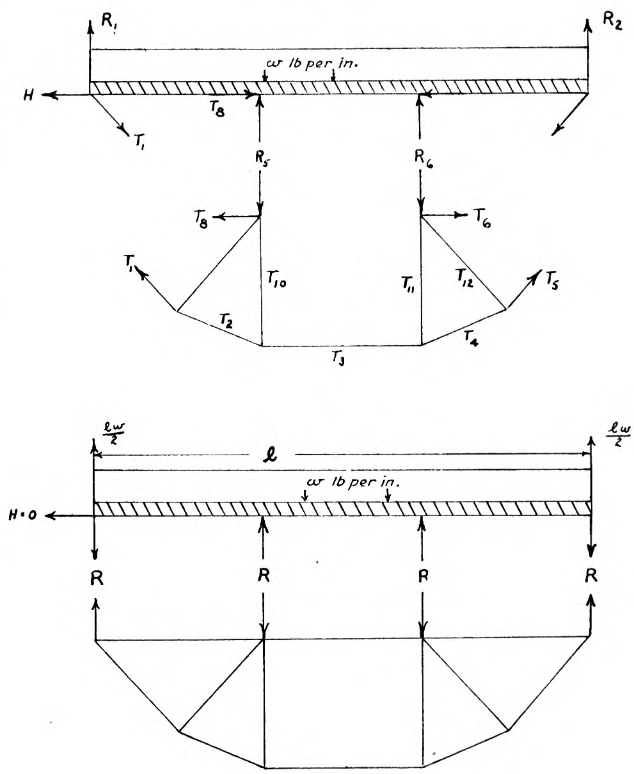

FIG. 20

The maximum bending moment occurs when the shear $S = 0$, i.e.

$$S = \frac{dM}{dx} = \frac{wl}{2} - R - wx = 0$$

Hence $$x = 15.7 \text{ in.}$$

and

$$M_{\max} = 246w \text{ in-lb}$$

Without a truss support the beam would be subjected to a bending moment of $2800w$ in-lb.

There are many cases in construction in which a beam is supported by a truss of proportions similar to those of the *Zephyr* cross truss. Since Equation [24] added to Equation [25] has very little effect on [25], it may be concluded that the truss is equivalent to continuous-beam supports with no appreciable deflection and with a uniform loading of w lb per in. and with two intermediate redundant supports spaced a distance a from the ends and b between each other. The reactions of the truss support are

$$R = \left(\frac{5a^3 + 10a^2b + 6ab^2 + b^3}{3a^2b + 2a^3}\right) wa$$

6—GENERAL END-TRUSS ANALYSIS

Two conditions were investigated, one with symmetrical loading increased by an impact factor of 26 per cent, and one for unsymmetrical loading caused by the roll of the car. In the latter, a lateral loading equal to 0.4 of the weight on the truck bolster per articulation, applied at the center of gravity of the car body, results in an increased loading on the right main frame and a decreased loading on the left side frame, or vice versa.

Therefore, in Fig. 21

$$W_R = \left(0.5 + \frac{0.4h}{L}\right) W_0 \text{ and } W_L = \left(0.5 - \frac{0.4h}{L}\right) W_0$$

h being the height of the center of gravity of the car body above the center pin, W_R the load on the right frame, W_L the load on the left frame, and L the cross spacing of the main side frames. With a rigid roof, the roll may be taken also in part by the torsional-shear reaction of the roof applied at the top of the end frame. This condition was investigated but was not considered as important to the end-frame loading as in the assumption above.

The roll is resisted by the side-bearing reaction $N_2 = \dfrac{0.4W_0h}{m}$ and $N_1 = W_0\left(1 - \dfrac{0.4h}{m}\right)$ is the center-pin reaction. These give the unsymmetrical loadings on the end truss and casting.

It was necessary to consider the lateral bending in the vertical posts and secondary bending in the horizontal short member a extending from the casting to the end frames, since the bending in this member and the torsion in the gusset were important. For the entire end frames, including both sides of the post, there are nine redundant reactions. Considerable simplification, however, was effected in the following manner. On either side of the end-door opening is a structure with five redundant reactions. The deflection due to the redundant tension Y is

$$\delta y_R = \frac{\partial V_e}{\partial Y}; \quad \delta y_L = \frac{\partial V_L}{\partial Y}$$

where $$\delta y_R = -\delta y_L$$

therefore

$$\frac{\partial V_R}{\partial Y} = -\frac{\partial V_L}{\partial Y}$$

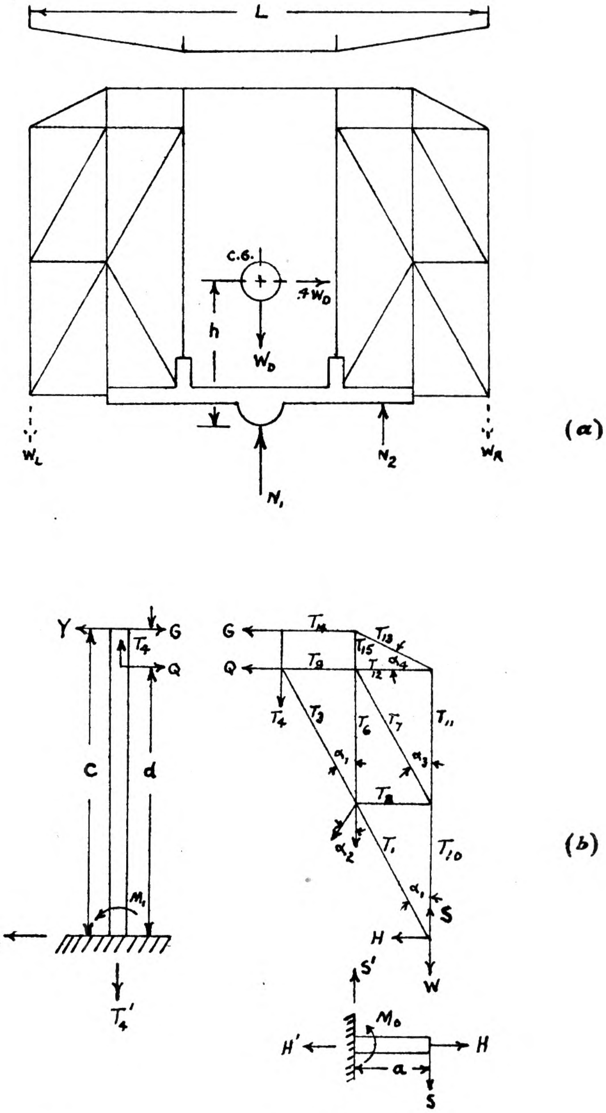

FIG. 21

where V_R is the elastic potential energy of the right frame corresponding to the loading W_R, and V_L is the potential energy for the left frame for the loading W_L.

The constraining bending moment of M_0 of the short horizontal member or skid rail extending from the side frame to the center-pin casting, the compression in this member H, the reactions G and Q on the post, and the redundant tension Y connecting the two parts of the end truss between the posts were taken as the redundant reactions. If T is a typical tension member, and if bending is considered in the post and short horizontal member extending from the casting, then, for the right truss with loading W_R

$$\Sigma \frac{T}{EA}\frac{\partial T}{\partial M_0} L + \Sigma \int \frac{M}{EI}\frac{\partial M}{\partial M_0} ds = 0$$

$$\Sigma \frac{T}{EA}\frac{\partial T}{\partial H} L + \Sigma \int \frac{M}{EI}\frac{\partial M}{\partial H} ds = 0$$

$$\Sigma \frac{T}{EA}\frac{\partial T}{\partial G} L + \Sigma \int \frac{M}{EI}\frac{\partial M}{\partial G} ds = 0$$

$$\Sigma \frac{T}{EA}\frac{\partial T}{\partial Q} L + \Sigma \int \frac{M}{EI}\frac{\partial M}{\partial Q}\, ds = 0$$

$$\Sigma \frac{T}{EA}\frac{\partial T}{\partial Y} L + \Sigma \int \frac{M}{EI}\frac{\partial M}{\partial Y}\, ds = \delta y_R$$

With similar equations for the left truss with loading W_L, the last equation takes the form

$$\Sigma \frac{T}{EA}\frac{\partial T}{\partial Y} L + \Sigma \int \frac{M}{EI}\frac{\partial M}{\partial Y}\, ds = \delta y_L$$

which, with the relation $\delta y_R = -\delta y_L$, gives eleven linear equations for the solution of the redundants M_0, H, G, and Q for the right and the left trusses, respectively, and for the mutual reaction Y between the two and the deflections δy_R and δy_L. The forms of the equations are obviously symmetrical for either part except for the substitution of the loading W_R and W_L. For symmetrical loading, $W_R = W_L$ and $\delta y_R = - \delta y_L = 0$.

For the solution it is necessary to express the tensions and bending moment in the post and horizontal beam as linear functions of the redundants and the applied loadings W_R or W_L.

Because of the relative length of the members compared with the gusset connection, the truss was considered as pin connected, the secondary bending of these members being of a small order. Due to the short horizontal member at the bottom connecting the casting to the side frames and the heavy gusset connection to the casting, this member, the skid rail, was considered as a cantilever extending from the casting to the side frame. It was considered important to estimate the secondary bending in the post itself in order to reduce the size of this member to the minimum as well as to allow for sufficient lateral stability.

Considering Fig. 21*b*, the inclinations of the diagonals of the end truss of the *Zephyr* are: $\alpha_1 = \sin^{-1} 0.4825$; $\alpha_2 = \sin^{-1} 0.441$; $\alpha_3 = \sin^{-1} 0.526$; $\alpha_4 = \sin^{-1} 0.635$, with the following values of L/A:

Member	L/A	Member	L/A	Member	L/A
1	43.25	6	33.75	11	59.6
2	37.9	7	39.75	12	16.5
3	38.5	8	20.80	13	36.8
4	8.5	9	14.75	14	25.5
5	42.2	10	66.80	..	..

For T_1 and S: $-H \csc \alpha_1 = -2.07H$; $S = S' = M_0/a = 0.053M_0$

For T_{10}: $T_{10} + T_1 \cos \alpha_1 + S = W$; $\therefore T_{10} = W - 0.053M_0 + 1.813H$

For S_1: $S_1c - M - Qe = 0$; $\therefore S_1 = Q - (Y - G) = \frac{1}{c}(M_1 + Qe)$

For M_1: $M_1 = (c - e)Q - c(Y - G) = 64.72Q - 80.22\,(Y - G)$

For T_{14}, T_{13}, and T_{12}: $T_{14} = G$; $T_{13} = T_{14} \sec \alpha_4 = 1.294G$; $T_{12} = -T_{14} = -G$

For T_{15}: $T_{15} = -T_{13} \sin \alpha_4 = -T_{14} \tan \alpha_4 = -0.821\,G$

For T_{11}: $T_{11} = T_{13} \sin \alpha_4 = 0.821G$

For T_7: $T_7 = (T_{10} - T_{11}) \csc \alpha_3 = 1.176W - 0.0624M_0 + 2.135H - 0.966G$

For T_9: $T_9 = T_{12} + T_7 \sin \alpha_3 = 0.6188W - 0.0328M_0 + 1.121H - 1.508G$

For T_8: $T_8 = -T_7 \sin \alpha_3 = 0.0328M_0 - 0.6188W + 0.508G - 1.121H$

For T_3: $T_3 = (Q - T_9) \csc \alpha_1 = 2.07Q + 0.068M_0 - 1.28W + 3.12G - 2.32H$

For T_6: $T_6 = T_{15} - T_7 \cos \alpha_3 = 0.053M_0 - W - 1.813H$

For T_4: $T_4 = - T_3 \cos \alpha_1 = 1.12W - 0.0595M_0 - 1.81Q - 2.74G + 2.03H$

For T_5: $T_5 \sin \alpha_2 + H + Q + G$; $T_5 = -2.268(H + Q + G)$

For T_2: $T_2 = S - W - T_5 \cos \alpha_2 - T_4 = 3.835Q + 0.1125M_0 - 2.12W + 4.765G$

These equations may be checked at any node of the structure. For bending in the post

$$M = (Y - G)x;\quad \frac{\partial M}{\partial Y} = x;\quad \frac{\partial M}{\partial G} = -x;\quad I = 4.73;\quad e = 15.5$$

and

$$M = (Y - G)(x + 15.5) - Qx;\quad \frac{\partial M}{\partial Y} = x + 15.5;$$

$$\frac{\partial M}{\partial G} = -(x + 15.5);\quad \frac{\partial M}{\partial Q} = -X;\quad I = 9.3;\quad d = 64.72$$

so that

$$\Sigma \int \frac{M}{I}\frac{\partial M}{\partial Y}\, ds = 263(Y - G) + 18{,}370(Y - G) - 13{,}208Q = 18{,}633(Y - G) - 13{,}208Q$$

$$\Sigma \int \frac{M}{I}\frac{\partial M}{\partial G}\, ds = -18{,}633(Y - G) + 13{,}208Q$$

$$\Sigma \int \frac{M}{I}\frac{\partial M}{\partial Q}\, ds = 9716Q - 13{,}208(Y - G)$$

For bending in the skid rail (horizontal member at the bottom of the truss)

$$M = Sx = 0.053M_0x;\quad \frac{\partial M}{\partial M_0} = 0.053x;\quad I = 0.961;\quad a = 18.87$$

$$\int \frac{M}{I}\frac{\partial M}{\partial M_0}\, ds = 6.54M_0$$

For the stresses in the members and the differential coefficients with respect to the several redundances, see Table 3.

Hence, for the axial loadings

$$\Sigma \frac{T}{A}\frac{\partial T}{\partial Q} L = T_2 \frac{\partial T_2}{\partial Q}\frac{L_2}{A_2} + T_3 \frac{\partial T_3}{\partial Q}\frac{L_3}{A_3} + T_4 \frac{\partial T_4}{\partial Q}\frac{L_4}{A_4} + T_5 \frac{\partial T_5}{\partial Q}\frac{L_5}{A_5} = 846.9Q + 22.69M_0 + 1079G - 120.4H - 427.25W$$

In like manner

$$\Sigma \frac{T}{A}\frac{\partial T}{\partial M_0} L = 22.696Q + 1.1644M_0 + 33.39G - 23.39H - 21.94W_R$$

$$\Sigma \frac{T}{A}\frac{\partial T}{\partial G} L = 1079.2Q + 33.34M_0 + 1627G - 349.45H - 628.57W_R$$

$$\Sigma \frac{T}{A}\frac{\partial T}{\partial H} L = -120.4Q - 23.39M_0 - 349.67G + 1111.9H + 440.7W_R$$

TABLE 3

		$\frac{\partial T}{\partial Q}$	$\frac{\partial T}{\partial M_0}$	$\frac{\partial T}{\partial G}$	$\frac{\partial T}{\partial H}$	$\frac{L}{A}$
$T_1 =$	$-2.07H$				-2.07	43.25
$T_2 =$	$3.835Q + 0.113M_0 + 4.765G - 2.12W$	3.835	0.113	4.765		37.9
$T_3 =$	$2.07Q + 0.068M_0 + 3.12G - 2.32H - 1.28W$	2.07	0.068	3.12	-2.32	38.5
$T_4 =$	$-1.81Q - 0.059M_0 - 2.74G + 2.03H + 1.12W$	-1.81	-0.059	-2.74	2.03	8.5
$T_5 =$	$-2.27Q \quad 2.27G - 2.27H$	-2.27		-2.27	-2.27	42.2
$T_6 =$	$0.053M_0 - 1.81H - 1.00W$		0.053		-1.81	33.75
$T_7 =$	$0.062M_0 - 0.966G + 2.13H + 1.17W$		0.062	-0.966	2.13	39.75
$T_8 =$	$0.033M_0 + 0.508G - 1.12H - 0.619W$		0.033	0.508	-1.12	20.80
$T_9 =$	$-0.033M_0 - 1.508G + 1.12H + 0.619W$		-0.033	-1.508	1.12	14.75
$T_{10} =$	$-0.053M_0 + 1.81H + 1.00W$		-0.053		1.81	66.80
$T_{11} =$	$+0.821G$			0.821		59.6
$T_{12} =$	$+1.00G$			1.00		16.5
$T_{13} =$	$1.294G$			1.294		36.8
$T_{14} =$	$1.00G$			1.00		25.5
$T_{15} =$	$-0.821G$			-0.821		17.18
$H =$	$+1.00H$				$+1.00$	30.2

and for the bending in the posts and skid rail

$$\Sigma \int \frac{M}{I} \frac{\partial M}{\partial Q} ds = 9716Q - 13{,}208(Y - G)$$

$$\Sigma \int \frac{M}{I} \frac{\partial M}{\partial M_0} ds = 6.54M_0$$

$$\Sigma \int \frac{M}{I} \frac{\partial M}{\partial G} ds = -18{,}633(Y - G) + 13{,}208Q$$

Also for the redundant Y

$$\Sigma \int \frac{M}{I} \frac{\partial M}{\partial Y} ds = 18{,}633(Y - G) - 13{,}208Q$$

On adding these equations, noting that

$$E\frac{\partial V}{\partial Q} = \Sigma\, T \frac{\partial T}{\partial Q} \frac{L}{A} + \Sigma \int \frac{M}{I} \frac{\partial M}{\partial Q} ds; \text{ etc.}$$

and including the compression resilience in the skid rail and the axial resilience in the post, then

$$10{,}562.9Q + 22.69M_0 + 14{,}287G - 120.4H - 13{,}208Y - 427.25\, W_R = 0$$

$$22.69Q + 7.70M_0 + 33.39G - 23.39H - 21.94W_R = 0$$

$$14{,}287.2Q + 33.34M_0 + 20{,}260G - 349.45H - 18{,}633Y - 628.57W_R = 0$$

$$-120.4Q - 23.39M_0 - 349.67G + 1111.9H + 440.7W_R = 0$$

$$18{,}633(Y - G) - 13{,}208Q = E\delta y_R$$

There is also a similar system of equations for the left side of the end truss in terms of additional redundants Q', M_0', G', H', the applied load W_L and the mutual reaction Y. These two systems of equations are related by the constraint condition $\delta y_R = -\delta y_L$.

The first four equations may be solved in terms of Y and W_R so that

$$H = 0.2095Y - 0.36218W_R$$
$$G = 0.8575Y - 0.02565W_R$$
$$M_0 = -3.3758Y + 1.6604W_R$$
$$Q = 0.10025Y + 0.06744W_R$$

and in a similar manner for the left side

$$H' = 0.2095Y - 0.36218W_L$$
$$G' = 0.8575Y - 0.02565W_L$$
$$M_0' = -3.3758Y + 1.6604W_L$$
$$Q' = 0.10025Y + 0.06744W_L$$

In addition

$$18{,}633(Y - G) - 13{,}208Q = E\delta y_R$$

and

$$18{,}633(Y - G') - 13{,}208Q' = E\delta y_L$$

but since

$$\delta y_R = -\delta y_L$$

$$18{,}633(Y - G) - 13{,}208Q + 18{,}633(Y - G') - 13{,}208Q' = 0$$

On substituting for G and Q, G', and Q'

$$Y = 0.155(W_R + W_L) = 0.155 \times 38{,}850 = 6023 \text{ lb}$$

With symmetrical loading, $W_R = W_L = W_0/2$

and $\quad 18{,}633(Y - G) - 13{,}208Q = 0$

whence $\quad Y = 6023$ lb.

Symmetrical Loading: With $W_R = W_L = {}^1/_2 \times 38{,}830 = 19{,}425$ lb

$Y = 6023$ lb	$Q = 1914$ lb
$G = 4667$ lb	$Y - G = 1356$ lb
$M_0 = 11{,}921$ in-lb	$H = -5772$ lb

The stresses in the truss in pounds are

$T_1 = 11{,}950$	$T_2 = -10{,}220$	$T_3 = 4070$	$T_4 = -2840$
$T_5 = -1{,}835$	$T_6 = -8{,}283$	$T_7 = 5345$	$T_8 = -2758$
$T_9 = -1{,}910$	$T_{10} = 9{,}293$	$T_{11} = 3840$	$T_{12} = -4667$
$T_{13} = 6{,}040$	$T_{14} = 4{,}667$	$T_{15} = -3840$	

$$S = M_0/a = 632 \text{ lb}$$

For Lateral Loading Only: $\Delta W = 0.4 \times 13{,}208 = 5158$ lb; $Y = 0$

$$H = -1868;\ G = -132;\ M_0 = 8562 \text{ in-lb};\ Q = 348$$

The stresses in the truss in pounds are

$T_1 = 3860$	$T_2 = -9280$	$T_3 = -1380$	$T_4 = 1212$
$T_5 = 3750$	$T_6 = -1324$	$T_7 = 1674$	$T_8 = -866$
$T_9 = 1018$	$T_{10} = 1324$	$T_{11} = -108$	$T_{12} = 132$
$T_{13} = -171$	$T_{14} = -132$	$T_{15} = 108$	

$$S = 0.053M_0 = 454 \text{ lb}$$

On combining the lateral and symmetrical loading, the unsymmetrical loading is determined. Algebraically, the lateral loading adds to the symmetrical loadings on the right side and subtracts on the left, as in Table 4.

For the bending in post and skid rail with combined symmetrical and lateral loading:

Maximum bending moment at the bottom of the post = $64.72Q_R - 80.22(Y - G_R) = 27{,}500$ in-lb

Maximum bending moment at the top of the casting = $53.7Q_R - 69.2(Y - G_R) = 12{,}800$ in-lb

Maximum bending moment at the roof rail = $15.5(Y - G) = 23{,}000$ in-lb

Maximum bending moment in skid rail $M_0 = 20{,}483$ in-lb.

The critical lateral bending stresses in the post at the top of the casting are 7960 lb per sq in. and at the roof rail are 14,600 lb per

TABLE 4

Member	Right side, lb	Left side, b	Critical, lb	Area, sq in.	Max. stress, lb per sq in.
T_1	15,810	8090	15,810	0.9036	17,500 T
T_2	—19,500	— 940	—19,500	0.9036	21,600 C
T_3	2690	5450	5450	0.9036	6,050 T
T_4*	— 1628	—4052	— 4052	4.7300	858 C*
T_5	1915	—5585	— 5585	0.9036	6,190 C
T_6	— 9617	—6969	— 9617	0.9036	10,600 C
T_7	7019	3671	7019	0.9036	7,770 T
T_8	— 3644	—1872	— 3644	0.906	4,030 C
T_9	— 892	—2928	— 2928	1.143	2,560 C
T_{10}	9617	6969	9617	0.512	19,500 T
T_{11}	3732	3948	3848	0.512	7,720 T
T_{12}	— 4535	—4799	— 4799	1.143	4,180 C
T_{13}	5869	6211	6211	0.662	9,400 T
T_{14}	4535	4799	4799	0.662	7,240 T
T_{15}	— 3732	—3948	— 3948	0.9036	4,370 C
H*	— 7640	—3904	— 7640	0.622	12,300 C*

* Axial compression in post and skid rail.

sq in. The maximum bending stress in the skid rail is 37,200 lb per sq in. and without the lateral stress and a bending moment of 11,921 in-lb the bending stress is 20,483 lb per sq in. Since the lateral loading is far in excess of what would occur in practise and yield takes place in the gussets, such stresses were not considered excessive. Moreover, considering secondary bending, the factor of safety can be lowered.

The analysis proved the initial postulate that important bending loads are thrown both on the post and skid rail, so that the assumption of a simple truss action would have been erroneous.

Deflection of End Truss

For the articulation analysis, it is important to estimate the potential energy of the end trusses. The elastic energy stored in the end truss is $V = {}^1/_2 Wy$, where y is the deflection corresponding to the main-side-frame load W, i.e., the load transmitted to the articulated center-pin casting.

To calculate y, it is possible to estimate the cantilever deflection of the horizontal skid-rail beam under the shear reaction $S = M_0/a$, where a is the length of the beam and M_0 the constraining bending moment at the fixture on the center-pin articulated casting. Then, for the symmetrical loading

$$y = \frac{Sa^3}{3EI} = \frac{M_0 a^2}{3EI} = \frac{11{,}921 \times 18{,}875^2}{3 \times 28 \times 10^6 \times 0.961} = 0.0527 \text{ in.}$$

As an additional check on the entire analysis, it is also noted that

$$y = \frac{\partial V}{\partial W} = \Sigma \frac{T}{EA} \frac{\partial T}{\partial W} L + \Sigma \int \frac{M}{EI} \frac{\partial M}{\partial W} ds$$

Considering the members in which W appears explicitly, and noting the disappearance of the bending terms since W does not appear, the following relations hold:

Member	$T \frac{\partial T}{\partial W} \frac{L}{A}$
T_2	$-308Q - 9.05M_0 + 170W - 383G$
T_3	$-100Q - 3.35M_0 + 63W - 154G + 114H$
T_4	$-17Q - 0.58M_0 + 11W - 26G + 19H$
T_6	$-1.79M_0 + 34W + 61H$
T_7	$-2.29M_0 + 55W - 45G + 100H$
T_8	$-0.42M_0 + 8W - 7G + 14H$
T_9	$-0.30M_0 + 6W - 14G + 10H$
T_{10}	$-3.54M_0 + 67W + 121H$

Whence

$$\Sigma T \frac{\partial T}{\partial W} \frac{L}{A} = -425Q - 21.95M_0 + 414W - 629G + 439H.$$

On substituting for Q, M_0, W, G, and H corresponding to the symmetrical loading of the end truss,

$$Ey = \Sigma T \frac{\partial T}{\partial W} \frac{L}{A} = 1497.7; \quad y = 0.0534 \text{ in.}$$

which agrees with the previous value.

The potential energy of the end truss is, therefore

$$V = {}^1/_2 \times 19{,}425 \times 0.053 = 514.8 \text{ in-lb.}$$

7—ANALYSIS OF ARTICULATED-END CONSTRUCTION

In the *Zephyr* because of the necessary outward projection of the center pin with respect to the plane of the end frames, eccentric loadings due to both vertical and horizontal reactions result in a moment which is resisted in greater part by a horizontal reaction from the roof, which, in turn, causes bending in the post. However, since the center sills are rigidly connected to the end castings, it was considered important to estimate accurately the percentage of bending moment transmitted by the sills resulting from the eccentric loadings.

The major reactions are shown in Fig. 22 where (*a*) is a longitudinal elevation of the post, (*b*) the center sills, (*c*) the projection of the end frame, and (*d*) the redundant portion of the side frame.

Redundancy

To estimate the redundancy, we note first that the projected reactions on the end frame are functions of the load S, transmitted by the end frame from the center-pin casting to the main side frames, and also that the reactions $R_5 = R_6$ transmitted from the roof to the side frames are functions of P_0. The stresses in the end frame are all functions of S_1 while the end-post reaction on the roof P_0 is assumed to be localized by reactions R_5 and R_6 at the first panel. We thus eliminate considering the end frame and roof for estimating redundancy, these being merely transmitting members.

The reactions H and V at the center pin and the panel loads are the applied loads on the system. The unknown reactions are the roof reaction on the post P_0 the loading S_1 transmitted by the end frame to the side frames, the constraining bending moment, shear and tension (or compression) in the sills, M_0, S_0, and T_0, respectively, at the section adjacent to the casting, the tension (or thrust) T_1 and the reactions R_1 and R_2 transmitted by the floor cross frames to the bottom chords of the side truss, a total of eight unknown reactions. But in addition there are the unknown loads in the truss members for the redundant portion of the truss, a total of 21 members. There are, therefore, 29 unknown quantities. The available equations are 3 for the post system (*a*), 3 for the sills (*d*), and 24 for the main side truss with 12 joints (*c*), or a total of 30 equations. But three of these are used for determining the reactions of the remaining portion on the redundant portion of the side truss, so we have but 27 independent equations for determining the 29 unknowns enumerated. We have, therefore, two redundant reactions. The bending moment at the sill M_0 and the roof reaction on the posts P_0 were chosen as such.

Reaction of Remaining Portion of the Truss on the Articulated Redundant Part

The redundant portion of the structure affected by M_0 and P_0 extends to panel section F. In the panel F-G is the baggage-door opening which in itself introduces additional redundancy. However, the following approximation has been made. The roof and floor beam must carry the total shear, resulting in secondary bending in these members. While these openings have been

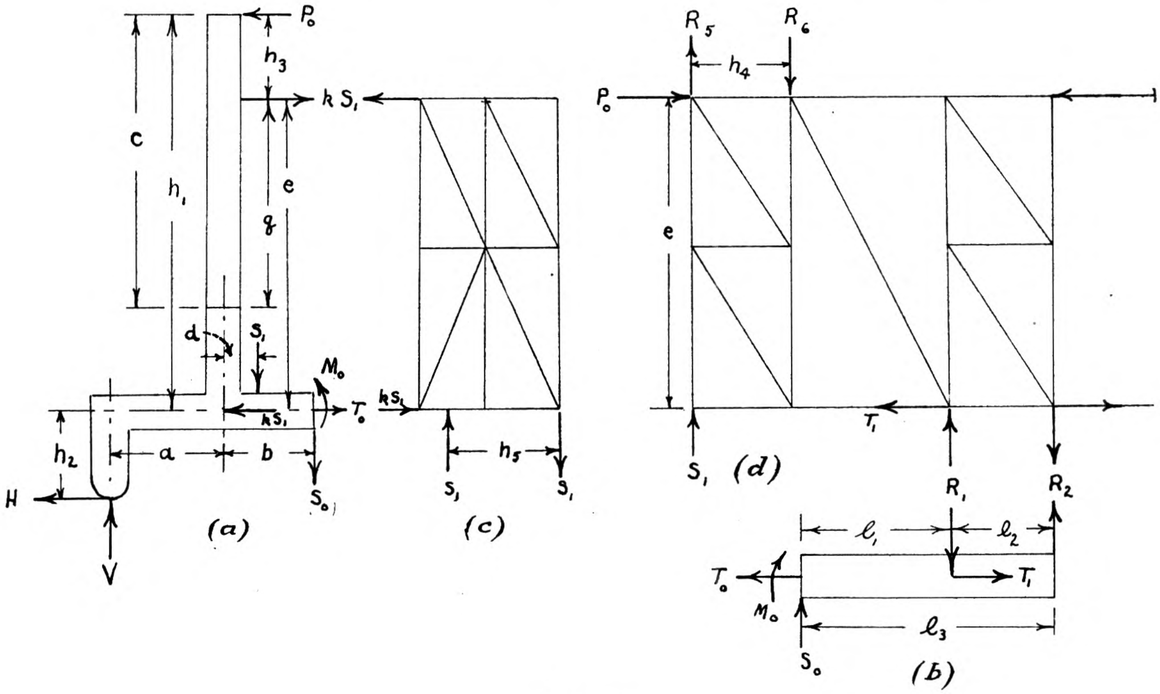

FIG. 22

analyzed more rigidly, for the articulation analysis, due to the preponderance of shearing action, points of contraflexure were assumed midway in panel *F-G* and the shear components for the upper and lower members were adjusted in the ratio of the moments of inertia for these members.

The horizontal components in the top and bottom members at the points of contraflexure in panel *F-G* are, with the maximum bending moment at this section, taken at 3,760,000 in-lb and a dynamic maximum drawbar load $H = 35{,}000$ lb, as follows:

$$H_1 = \frac{3{,}760{,}000}{66.63} + \frac{35{,}000 \times 10.44}{66.63} = 62{,}000 \text{ lb}$$

$$H_2 = \frac{3{,}760{,}000}{66.63} + \frac{35{,}000 \times 77.07}{66.63} = 97{,}000 \text{ lb}$$

On the assumption that $V_1/V_2 = I_1/I_2$

$$V_1 = (V - \Sigma W)I_1/I; \quad V_2 = (V - \Sigma W)\, I_2/I; \quad I = I_1 + I_2$$

then $V_1 = 8470$ lb and $V_2 = 7646$ lb.

From these the *equivalent reactions* on the redundant portion may be estimated, assuming that the bending constraints are concentrated in the two panels adjacent to the baggage-door opening. Therefore $P_1 = 17{,}070$ lb and $H_1 = -62{,}000$ are concentrated at the top, and $P_3 = 15{,}396$ lb and $H_2 = 97{,}000$ concentrated at the bottom of section *F*, and $P_2 = 8600$ lb at the top and $P_4 = 7750$ lb at bottom of section *E*.

EXPRESSION OF THE PRINCIPLE INTERNAL REACTIONS BETWEEN THE PARTS IN TERMS OF REDUNDANTS M_0 AND P_0

To express the elastic energy of the system in terms of the redundant reactions M_0 and P_0 and the applied loading, the following relations of the internal mutual reactions between the parts consisting of the center-pin casting and vertical post, the projected end frame, the main side frames, and the center sills, where the reactions between the center sills and side frames are transmitted by the floor cross frames are noted. See Fig. 22.

For T_1 and T_0: $T_1 = T_0 = H + P_0$

For S_1: $\quad S_1 = V - S_0$

For S_0:

$$S_0 = \frac{P_0h_1 - k_1S_1e - S_1d + M_0 - Va - Hh_2}{b} = \frac{P_0h_1 - (ke + d + a)V + M_0 - Hh_2}{b - ke - d}$$

For R_1 and R_2: $\quad R_1 = \dfrac{M_0 + S_0l_3}{l_2}; \quad R_2 = R_1 - S_0 = \dfrac{M_0 + S_0l_1}{l_2}$

For R_5 and R_6: $\quad R_5 = R_6 = \dfrac{h_3}{h_4} P_0$

Assuming $H = 35{,}000$ lb and $V = 30{,}850$ lb and numerical dimensions for Fig. 22 as follows: $h_1 = 94.63$ in.; $h_2 = 10.44$ in.; $h_3 = 28$ in.; $h_4 = 21$ in.; $h_5 = 6.06$ in.; $l_1 = 62.06$ in.; $l_2 = 31.56$ in.; $l_3 = 93.62$ in.; $a = 10.44$ in.; $b = 26$ in.; $c = 72$ in.; $d = 0$ in.; $e = 66.3$ in.; and letting

$$C_1 = b - ke - d = 19.94; \; q = C - h_3 = 44 \text{ in};$$

then

$$\begin{aligned}
S_1h_5 &= kS_1e, \\
k &= h_5/e = 0.091 \\
T_1 &= T_0 = P_0 + 35{,}000 \\
S_0 &= 4.47P_0 + 0.0502M_0 - 44{,}000 \\
S_1 &= -4.74P_0 - 0.0502M_0 + 74{,}850 \\
R_1 &= 14.04P_0 + 0.1805M_0 - 130{,}600 \\
R_2 &= 9.32P_0 + 0.1305M_0 - 86{,}600 \\
R_5 &= R_6 = 1.33P_0
\end{aligned}$$

To determine the redundant reactions M_0 and P_0 we have

$$\frac{\partial V}{\partial M_0} = \frac{\partial V_A}{\partial M_0} + \frac{\partial V_B}{\partial M_0} + \frac{\partial V_C}{\partial M_0} + \frac{\partial V_D}{\partial M_0} + \frac{\partial V_E}{\partial M_0} = 0$$

$$\frac{\partial V}{\partial P_0} = \frac{\partial V_A}{\partial P_0} + \frac{\partial V_B}{\partial P_0} + \frac{\partial V_C}{\partial P_0} + \frac{\partial V_D}{\partial P_0} + \frac{\partial V_E}{\partial P_0} = 0$$

where V_A = elastic energy of the post
V_B = elastic energy of the center sills
V_C = elastic energy of the floor cross frames

V_D = elastic energy of the main side frames in the redundant region

V_E = elastic energy of the end truss.

Therefore

$$E\frac{\partial V}{\partial M_0} = \left[\Sigma\int\frac{M}{I_V}\frac{\partial M}{\partial M_0}ds\right]_A + \left[\Sigma\int\frac{M}{I_s}\frac{\partial M}{\partial M_0}ds\right]_B$$

$$+\left[\Sigma\frac{T}{A}\frac{\partial T}{\partial M_0}L\right]_C + \left[\Sigma\frac{T}{A}\frac{\partial T}{\partial M_0}L\right]_D + \left[E\frac{\partial V_E}{\partial M_0}\right]_E = 0. \quad [26]$$

$$E\frac{\partial V}{\partial P_0} = \left[\Sigma\int\frac{M}{I_V}\frac{\partial M}{\partial P_0}ds\right]_A + \left[\Sigma\int\frac{M}{I_s}\frac{\partial M}{\partial P_0}ds\right]_B$$

$$+\left[\Sigma\frac{T}{A}\frac{\partial T}{\partial P_0}L\right]_C + \left[\Sigma\frac{T}{A}\frac{\partial T}{\partial P_0}L\right]_D + \left[E\frac{\partial V_E}{\partial P_0}\right]_E = 0. \quad [27]$$

For the Vertical Posts: From Fig. 22a

$$M = P_0x; \quad \frac{\partial M}{\partial P_0} = x; \quad \frac{\partial M}{\partial M_0} = 0 \quad \text{from 0 to } h_3$$

$M = P_0(x + h_3) - kS_1x$ from 0 to q with the origin at h_3

$$= P_0(x + h_3) - kx\left(V - \frac{P_0h_1 - (ke + d + a)V + M_0 - Hh_2}{C_1}\right)$$

$$\frac{\partial M}{\partial M_0} = \frac{kx}{C_1}; \quad \frac{\partial M}{\partial P_0} = x + h_3 + \frac{kh_1x}{C_1}; \quad C_1 = b - ke - d$$

The mean moment of inertia of the posts (per pair of posts) about a transverse axis is $I_v = 99.5$ in.^{4} Hence

$$\left[\Sigma\int\frac{M}{I_v}\frac{\partial M}{\partial M_0}ds\right]_A = 0.0059M_0 + 3.08P_0 - 8770 = \frac{\partial V_A}{\partial M_0}$$

$$\left[\Sigma\int\frac{M}{I_v}\frac{\partial M}{\partial P_0}ds\right]_A = 3.1M_0 + 1783.5P_0 - 4{,}640{,}000 = \frac{\partial V_A}{\partial P_0}$$

For the Center Sills: From Fig. 22c

$M = M_0 + S_0x$ from 0 to l_1

$$= M_0 + \left(\frac{P_0h_1 - (ke + d + a)V + M_0 - Hh_2}{C_1}\right)x$$

$$\frac{\partial M}{\partial M_0} = 1 + \frac{x}{C_1}; \quad \frac{\partial M}{\partial P_0} = \frac{h_1x}{C_1}; \quad C_1 = b - ke - d$$

$M = R_2x$ from 0 to l_2

$$= \left[\frac{M_0}{l_2} + \frac{l_1}{l_2}\left(\frac{P_0h_1 - (ke + d + a)V + M_0 - Hh_2}{C_1}\right)\right]x$$

$$\frac{\partial M}{\partial M_0} = \frac{x}{l_2} + \frac{l_1}{l_2}\frac{x}{C_1}; \quad \frac{\partial M}{\partial P_0} = \frac{h_1l_1x}{l_2C_1}$$

The moment of inertia of the center sills (per pair of sills) is I_s = 18.4 so that

$$\left[\Sigma\int\frac{M}{I_s}\frac{\partial M}{\partial M_0}ds\right]_B = 34.4M_0 + 2215P_0 - 20{,}600{,}000 = \frac{\partial V_B}{\partial M_0}$$

$$\left[\Sigma\int\frac{M}{I_s}\frac{\partial M}{\partial P_0}ds\right]_B = 2216M_0 + 146{,}500P_0 - 1{,}360{,}000{,}000 = \frac{\partial V_B}{\partial P_0}$$

For the Floor Cross Frames: A standard floor cross truss as at stations E and F, and loaded with a reaction R is shown in Fig. 23. Here

$$\Sigma T\frac{L}{A}\frac{\partial T}{\partial R} = 380.2$$

Therefore, at stations E and F

$$\Sigma T\frac{L}{A}\frac{\partial T}{\partial R_1} = 380.2R_1 = 68.6M_0 + 5340P_0 - 49{,}600{,}000$$

$$\Sigma T\frac{L}{A}\frac{\partial T}{\partial R_2} = 380.2R_2 = 49.6M_0 + 3545P_0 - 32{,}950{,}000$$

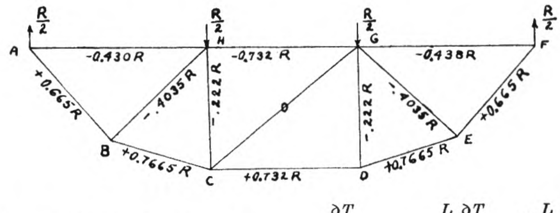

Member	Length	Area	L/A	$\frac{\partial T}{\partial R}$	$\frac{L}{A}\frac{\partial T}{\partial R}$	$T\frac{L}{A}\frac{\partial T}{\partial R}$
A–B	25.8	0.1896	136.0	0.665	90.5	60.2R
B–C	21.5	0.3699	58.2	0.7665	44.6	34.2R
C–D	31.0	0.3699	83.8	0.732	61.3	44.9B
D–E	21.5	0.3699	58.2	0.7665	44.6	34.2R
E–F	25.8	0.1896	36.0	0.665	90.5	60.2R
F–G	37.5	0.3432	109.2	—0.438	—47.8	21.0R
G–H	31.0	0.3432	90.3	—0.732	—66.0	48.3R
H–A	37.5	0.3432	109.2	—0.438	—47.8	21.0R
B–H	28.2	0.1896	148.8	—0.4035	—60.0	24.2R
C–H	25.625	0.3230	79.3	—0.222	—17.6	3.9R
C–G	40.0	0.1896	211.0	0	0	0
D–G	25.625	0.3230	79.3	—0.222	—17.6	3.9R
E–G	28.2	0.1896	148.8	—0.4035	—60.0	24.2R

$$\Sigma T\frac{L}{A}\frac{\partial T}{\partial R} = 380.2R$$

FIG. 23

Now

$$\Sigma T\frac{L}{A}\frac{\partial T}{\partial M_0} = \Sigma T\frac{L}{A}\frac{\partial T}{\partial R_1}\frac{\partial R_1}{\partial M_0} + \Sigma T\frac{L}{A}\frac{\partial T}{\partial R_2}\frac{\partial R_2}{\partial M_0}$$

$$\Sigma T\frac{L}{A}\frac{\partial T}{\partial P_0} = \Sigma T\frac{L}{A}\frac{\partial T}{\partial R_2}\frac{\partial R_2}{\partial P_0} + \Sigma T\frac{L}{A}\frac{\partial T}{\partial R_2}\frac{\partial R_2}{\partial P_0}$$

But $R_1 = 14.04P_0 + 0.1805M_0 - 130{,}600$

$R_2 = 9.32P_0 + 0.1305M_0 - 86{,}600$

$$\text{Whence } \frac{\partial R_1}{\partial M_0} = 0.1805; \quad \frac{\partial R_2}{\partial M_0} = 0.1305; \quad \frac{\partial R_1}{\partial P_0} = 14.04; \quad \frac{\partial R_2}{\partial P_0} = 9.32$$

$$\text{and } \left[\Sigma T\frac{L}{A}\frac{\partial T}{\partial M_0}\right]_C = 0.1805\,(68.6M_0 + 5340P_0 - 49{,}600{,}000)$$

$$+ 0.1305(49.6M_0 + 3545P_0 - 4{,}300{,}000)$$

$$= 18.87M_0 + 1426.5P_0 - 13{,}250{,}000 = \frac{\partial V_C}{\partial M_0}$$

$$\left[\Sigma T\frac{L}{A}\frac{\partial T}{\partial P_0}\right]_C = 14.04(68.6M_0 + 5340P_0 - 49{,}600{,}000)$$

$$+ 9.32\,(49.6M_0 + 3545P_0 - 4{,}300{,}000)$$

$$= 1425M_0 + 107{,}900P_0 - 1{,}003{,}000{,}000 = \frac{\partial V_C}{\partial P_0}$$

For the Main Side Truss: The redundant portion of the structure affected by M_1 and P_1 extends to panel F. (See Fig. 24.) The reaction of the remaining portion of the truss on the redundant portion is equivalent to reactions H_1 and H_2 with P_1 and P_3 at section F and P_2 and P_4 at section E. The reaction transmitted by the end frame is the supporting force S_1 at the panel B_1. The reaction transmitted by the roof consists of the post-reaction P_0 applied at B_3 and the forces $R_5 = R_6$ applied at B_3

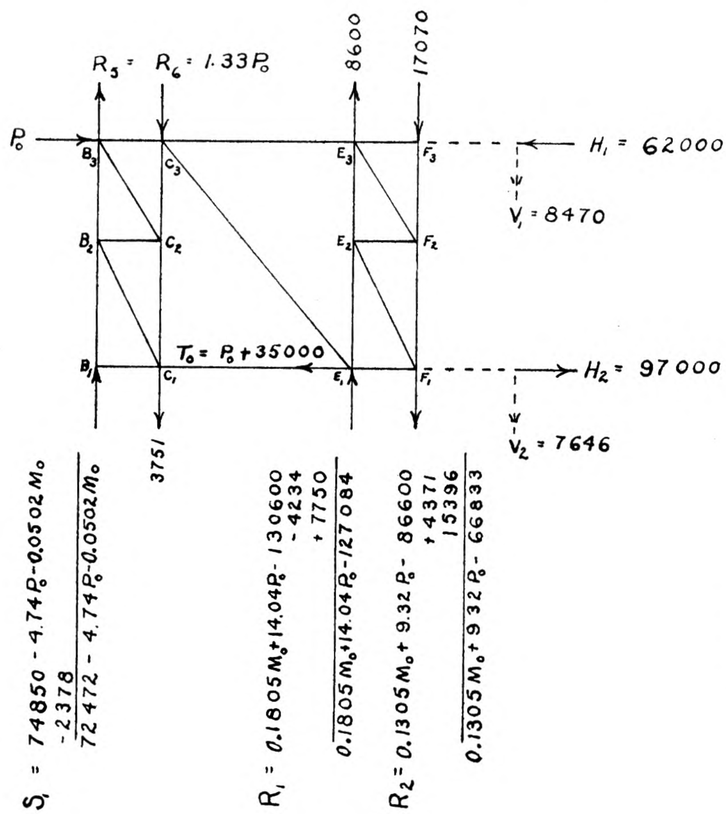

FIG. 24

and C_3, which arise on account of the eccentricity of the post reaction on the roof with respect to the top rail of the truss. Finally, there are the reactions from the center sills which are transmitted by the cross floor frames at panels E and F. These consist of the horizontal shear force of the cross transom and are equal to the tension (or thrust) T_1 applied at E, together with the vertical constraining reactions of the sills and transmitted by the cross members as vertical shear forces R_1 at E and R_2 at F. In addition, there are the dead loads at panels B, C, E, and F.

It is evident that the stresses in the truss can be readily expressed in terms of S_1, P_0, R_5, and R_6, and T_1, R_1, and R_2, together with the applied loads.

But $S_1R_5 = R_6$, and T_1, R_1, and R_2 are all functions of M_0 and P_0, that is

$$S_1 = -4.74P_0 - 0.0502M_0 + 74{,}850$$

$$R_5 = R_6 = 1.33P_0; \; T_1 = P_0 + H = P_0 + 35{,}000$$

$$R_1 = 14.04P_0 + 0.1805M_0 - 130{,}600$$

$$R_2 = 9.32P_0 + 0.1305M_0 - 86{,}600$$

and the applied loads are

$$H_1 = 62{,}000; \; H_2 = 97{,}000 \text{ lb}$$

$$P_1 = 17{,}070; \; P_2 = 8600; \; P_3 = 15{,}396; \; P_4 = 7750 \text{ lb}$$

and the panel loads

$$W_B = 2378; \; W_C = 3751; \; W_E = 4234; \; W_F = 4371 \text{ lb}$$

The loads in the various members in terms of M_0 and P_0 are given in Tables 5 and 6.

$$\left[\Sigma \frac{T}{A} \frac{\partial T}{\partial M_0} L\right]_D = 118.97P_0 + 1.579M_0 - 1{,}171{,}259$$

$$\left[\Sigma \frac{T}{A} \frac{\partial T}{\partial P_0} L\right]_D = 9097.4P_0 + 119.013M_0 - 92{,}364{,}410$$

For the End Truss: Due to the obliquity of the end truss which makes an angle of approximately 10 deg with a transverse plane, its action must be considered in the articulation analysis. We are concerned with the projection of the end truss in a longitudinal plane for determining the equilibrium of forces as well as its deflection in estimating the effect of its flexibility in the system.

The reactions in the end-truss analysis were assumed in the oblique plane of the truss. The projections of the external reactions acting on the end frame are the load of the side frame S_1 and a corresponding supporting load S_1 from the articulated casting which form an overturning couple S_1h_5. This is balanced by a couple kS_1e. Hence

$$S_1h_5 = kS_1e \text{ and } k = \frac{h_5}{e} = 0.091$$

Because of the small obliquity of the end truss, the elastic energy stored in the post as in the end-truss analysis may be considered as the transverse component of the elastic energy in the post. Thus the elastic energy of the end frame includes the transverse bending elastic energy of the post.

The elastic energy of the end truss is

$$V_E = \Sigma \frac{1}{2} \frac{T^2L}{AE} = \frac{1}{2} S_1y$$

Now S_1 is a function of the redundants M_0 and P_0, so that

TABLE 5 REDUNDANT PART OF SIDE FRAMES AT ARTICULATED ENDS

Member	Length	Area	L/A	Load
B_1–B_2	36.13	2.0476	17.65	$+4.74P_0 + 0.0502M_0 - 72{,}500$
B_2–B_3	30.5	2.0476	14.9	$+2.89P_0 + 0.0230M_0 - 33{,}200$
B_1–C_1	21.0	3.708	5.67	0
B_2–C_1	41.8	1.687	24.8	$-2.140P_0 - 0.0315M_0 + 45{,}500$
B_2–C_2	21.0	1.812	11.59	$+1.075P_0 + 0.0158M_0 - 22{,}840$
B_3–C_2	37.0	1.687	21.95	$-1.892P_0 - 0.0278M_0 + 40{,}250$
B_3–C_3	21.0	8.172	2.57	$+0.075P_0 + 0.0158M_0 - 22{,}840$
C_1–C_2	36.13	1.262	28.6	$+1.85P_0 + 0.0272M_0 - 35{,}549$
C_2–C_3	30.5	1.262	24.15	$+3.41P_0 + 0.0502M_0 - 68{,}749$
C_1–E_1	61.0	3.708	16.45	$-1.075P_0 - 0.0158M_0 + 22{,}840$
C_3–E_1	90.4	1.807	50.0	$-6.43P_0 - 0.0680M_0 + 93{,}200$
C_3–E_3	61.0	8.172	7.46	$+4.39P_0 + 0.0017M_0 - 85{,}800$
E_1–E_2	36.13	1.544	23.4	$-9.29P_0 - 0.1303M_0 + 58{,}100$
E_2–E_3	30.5	1.544	19.75	$-4.24P_0 - 0.0597M_0 + 31{,}600$
E_1–F_1	31.56	3.708	8.50	$-4.405P_0 - 0.0619M_0 + 120{,}740$
E_2–F_1	48.0	1.687	28.5	$+6.71P_0 + 0.0940M_0 - 36{,}100$
E_2–F_2	31.56	1.812	17.4	$-4.39P_0 - 0.0617M_0 + 23{,}800$
E_3–F_2	44.0	1.687	26.1	$+6.12P_0 + 0.0861M_0 - 33{,}200$
E_3–F_3	31.56	8.172	3.86	$-62{,}000$
F_1–F_2	36.13	1.0238	35.25	$+4.27P_0 + 0.0599M_0 - 39{,}633$
F_2–F_3	30.5	1.0238	29.8	$-17{,}070$

TABLE 6 DIFFERENTIAL COEFFICIENTS OF ELASTIC ENERGY FOR REDUNDANT PART OF SIDE FRAMES

Member	$T\frac{L}{A}\frac{\partial T}{\partial M_0}$	$T\frac{L}{A}\frac{\partial T}{\partial P_0}$
B_1–B_2	$4.20P_0 + 0.0444M_0 - 64{,}100$	$396.5P_0 + 4.20M_0 - 6{,}060{,}000$
B_2–B_3	$0.991P_0 + 0.0079M_0 - 11{,}380$	$124.5P_0 + 0.991M_0 - 1{,}430{,}000$
B_1–C_1	0	0
B_2–C_1	$1.67P_0 + 0.0246M_0 - 35{,}500$	$113.8P_0 + 1.674M_0 - 2{,}415{,}000$
B_2–C_2	$0.197P_0 + 0.00289M_0 - 4{,}180$	$13.4P_0 + 0.197M_0 - 285{,}000$
B_3–C_2	$1.155P_0 + 0.01695M_0 - 24{,}570$	$68.75P_0 + 1.155M_0 - 1{,}671{,}000$
B_3–C_3	$0.003P_0 + 0.01064M_0 - 929$	$0.01444P_0 + 0.003M_0 - 4{,}410$
C_1–C_2	$1.441P_0 + 0.0212M_0 - 27{,}600$	$98.1P_0 + 1.44M_0 - 1{,}878{,}000$
C_2–C_3	$4.13P_0 + 0.0607M_0 - 83{,}200$	$280.7P_0 + 4.13M_0 - 5{,}660{,}000$
C_1–E_1	$0.28P_0 + 0.00411M_0 - 5950$	$19.0P_0 + 0.2795M_0 - 405{,}000$
C_3–E_1	$21.825P_0 + 0.231M_0 - 316{,}500$	$2065P_0 + 21.85M_0 - 30{,}000{,}000$
C_3–E_3	$2.02P_0 + 0.0284M_0 - 39{,}500$	$143.6P_0 + 2.023M_0 - 2{,}810{,}000$
E_1–E_2	$28.3P_0 + 0.395M_0 - 177{,}100$	$2015P_0 + 28.3M_0 - 12{,}610{,}000$
E_2–E_3	$5.0P_0 + 0.0703M_0 - 37{,}300$	$355P_0 + 5.0M_0 - 2{,}640{,}000$
E_1–F_1	$2.31P_0 + 0.0323M_0 - 63{,}200$	$165P_0 + 2.31M_0 - 4{,}520{,}000$
E_2–F_1	$18.0P_0 + 0.252M_0 - 96{,}500$	$1284P_0 + 18.0M_0 - 6{,}900{,}000$
E_2–F_2	$4.71P_0 + 0.0661M_0 - 25{,}550$	$335P_0 + 4.71M_0 - 1{,}816{,}000$
E_3–F_2	$13.75P_0 + 0.1935M_0 - 74{,}600$	$978P_0 + 13.75M_0 - 5{,}310{,}000$
E_3–F_3	0	0
F_1–F_2	$8.99P_0 + 0.1265M_0 - 83{,}600$	$642P_0 + 9M_0 - 5{,}950{,}000$
F_2–F_3	0	0
Total	$118.972P_0 + 1.5785M_0 - 1{,}171{,}259$	$9097.36P_0 + 119.0125M_0 - 92{,}364{,}410$

$$\frac{\partial V_E}{\partial M_0} = \frac{\partial V_E}{\partial S_1}\frac{\partial S_1}{\partial M_0} = \Sigma \frac{T}{AE}\frac{\partial T}{\partial S_1}\frac{\partial S_1}{\partial M_0} L$$

$$\frac{\partial V_E}{\partial P_0} = \frac{\partial V_E}{\partial S_1}\frac{\partial S_1}{\partial P_0} = \Sigma \frac{T}{AE}\frac{\partial T}{\partial S_1}\frac{\partial S_1}{\partial P_0} L$$

where $T_1 = \alpha_1 Q' + \alpha_2 M_0' + \alpha_3 G' + \alpha_4 H' + \alpha_5 S_1$

$$T_2 = b_1 Q' + b_2 M_0' + b_3 G' + b_4 H' + b_5 S_1, \text{ etc.}$$

$$S_1 = -4.74P_0 - 0.0502M_0 + 74{,}850$$

and

$$\frac{\partial T_1}{\partial S_1} = \alpha_5; \quad \frac{\partial T_2}{\partial S_1} = b_5, \text{ etc.}$$

$$\frac{\partial S_1}{\partial M_0} = -0.0502; \quad \frac{\partial S_1}{\partial P_0} = -4.74$$

where Q', M_0', G', and H' are the redundant reactions in the end truss and are solved in the "End-Truss Analysis."

A much simpler method is to estimate the deflection y, which is likewise the deflection of the cantilever skid rail extending from the casting to the side frame. The shear for the cantilever (assumed) skid rail is $S' = M_0'/a$, where a is the length of the skid rail, so that

$$y = \frac{S'a^3}{3EI_R} = \frac{M_0'a^2}{3EI_R}$$

where I_R = moment of inertia of the skid rail.

Then for a pair of trusses

$$S' = M_1'/a = 0.02855S_1/2$$

and with $a = 18.875$ in.

$$I_R = 0.961; \quad E = 28 \times 10^6$$

$$y = \frac{2.38}{10^6}\frac{S_1}{2}$$

so that the elastic energy is

$$V_E = 2\left(\frac{1}{2}y\frac{S_1}{2}\right) = C_2\frac{S_1^2}{2}$$

where $C_2 = 1.19 \times 10^{-6}$

Then $\dfrac{\partial V_E}{\partial M_0} = C_2 S_1 \dfrac{\partial S_1}{\partial M_0}; \quad \dfrac{\partial V_E}{\partial P_0} = C_2 S_1 \dfrac{\partial S_1}{\partial P_0}$

with $S_1 = -4.74P_0 - 0.0502M_0 + 74{,}850$

and $\dfrac{\partial S_1}{\partial M_0} = -0.0502; \quad \dfrac{\partial S_1}{\partial P_0} = -4.74$

$$\left[E\frac{\partial V}{\partial M_0}\right]_E = 0.084M_0 + 7.91P_0 - 125{,}300$$

$$\left[E\frac{\partial V}{\partial P_0}\right]_E = 7.93M_0 + 748P_0 - 11{,}810{,}000$$

Summation of the Component Elements of the Articulation System

For $E\dfrac{\partial V}{\partial M_0} = E\left(\dfrac{\partial V_A}{\partial M_0} + \dfrac{\partial V_B}{\partial M_0} + \dfrac{\partial V_C}{\partial M_0} + \dfrac{\partial V_D}{\partial M_0} + \dfrac{\partial V_E}{\partial M_0}\right) = 0$

$$54.936M_0 + 3771.45P_0 - 35{,}155{,}330 = 0$$

For $E\dfrac{\partial V}{\partial P_0} = E\left(\dfrac{\partial V_A}{\partial P_0} + \dfrac{\partial V_B}{\partial P_0} + \dfrac{\partial V_C}{\partial P_0} + \dfrac{\partial V_D}{\partial P_0} + \dfrac{\partial V_E}{\partial P_0}\right) = 0$

$$3771M_0 + 266{,}028.5P_0 - 2{,}471{,}814{,}400 = 0$$

Hence

$$M_0 + 70.546P_0 - 655{,}480 = 0$$
$$M_0 + 68.652P_0 - 639{,}934 = 0$$

From which $P_0 = 8173$ lb and $M_0 = 78{,}908$ in-lb.

From these values, the stresses in all parts of the articulated end, including stresses in the redundant portion of the side truss, can be estimated. The moment due to the eccentricity corresponding to the moments of the center-pin loads H and V about the intersection of the center line of the post and sill, with the loadings assumed, is 688,000 lb. This is counteracted by the bending moments of the post and sill and the shear moments at the legs of the casting. The bending moment transmitted to the sills amounts to 11 per cent, and for the post, 67 per cent of the total eccentricity moment. With bumping loads, H is reversed but is opposed by the moment of the vertical center-pin reaction.

Such analysis, though at best an approximation, gives a closer insight into the interactions taking place in the articulated end.

8—BAGGAGE-DOOR AND STEP-WELL OPENINGS

Longitudinal Bending

The upper and bottom chord members at the door openings must transmit the total shear and bending moment because no diagonals are possible in such panels. Large secondary bending and shear stresses are sustained by these members.

In the analysis the roof itself, which is reinforced through the opening and several panels back on either side of the opening, has been considered as an effective upper member. Likewise the equivalent beam of the floor system has been taken as the bottom chord.

It has been pointed out that the roof and floor systems are essentially continuous beams with elastic supports, the reactions of which are mostly redundant actions from the intervening truss system. On this basis it is to be noted that oscillations of the bending moment extend along the entire roof and floor system, while the oscillations are considerably augmented at the openings. If it is considered that the oscillations are damped to small amplitude at three panels on either side of opening, the structure may be analyzed between these terminal sections, which include the openings, where the applied forces consist of the bending moments and the shears acting at the terminal sections and exerted by the remaining parts of the truss. The redundancy even for this is considerable. Thus on this assumption there are seven redundant reactions at the main baggage-door opening. An analysis was made on this basis for a first approximation of the bending moment and shear distribution. A more precise approximation may be found elsewhere in this paper under the heading "Indeterminate Features of Construction."

Three cases will be considered. Case 1 is that of an opening that carries principally a shear loading only, Fig. 25*a*, and the bending moment of which is of small order. Such conditions occur when the opening is adjacent to the articulation support.

In this case points of contraflexure occur at the center of the panel C, and the shearing loads divide as the moments of inertia, i.e., $S_1/S_2 = I_1/I_2$, with $S_1 + S_2 = S$, so that

$$S_1 = S\frac{I_1}{I_1 + I_2}$$

and

$$S_2 = S\frac{I_2}{I_1 + I_2}$$

The maximum bending moment at A or B is $S_1 a$, and at A' or B' it is $S_2 a$.

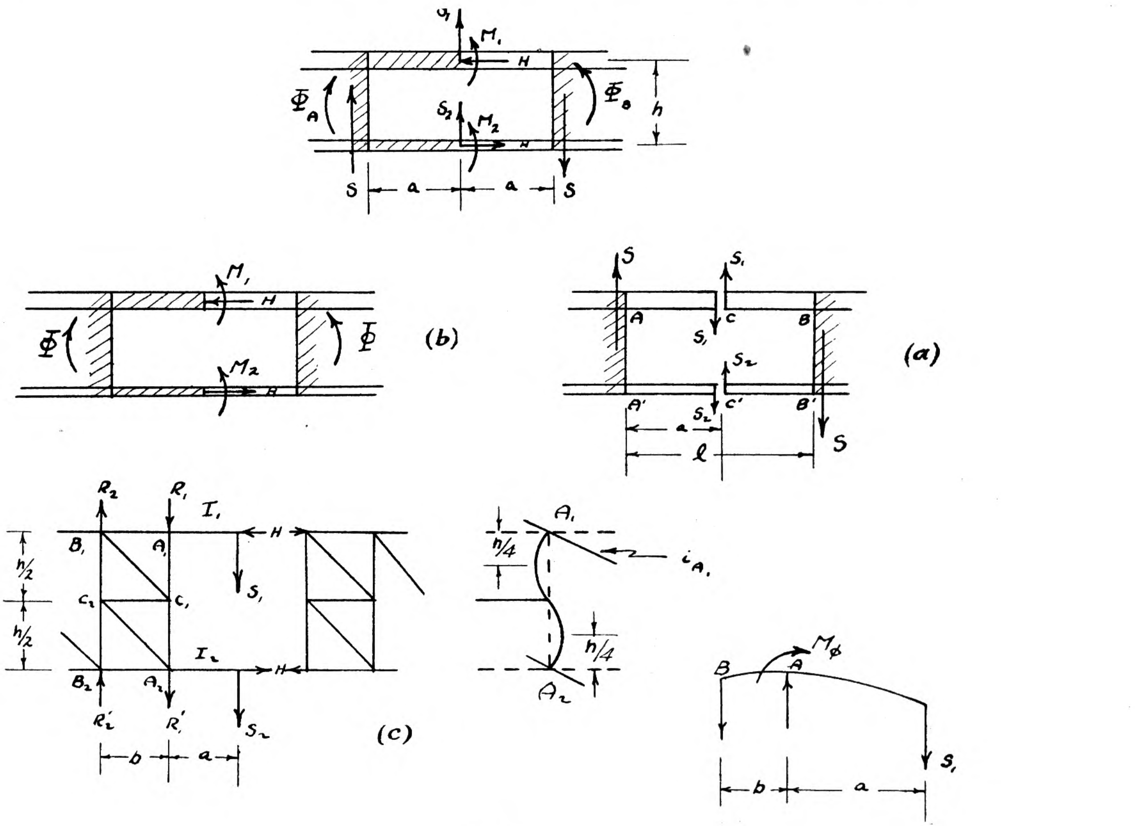

FIG. 25

Case 2 is that of an opening which transmits pure bending only (Fig. 25*b*). No point of contraflexure occurs in the panel. Such conditions would occur for an opening at the center of the car under symmetrical loadings.

Let Φ = total bending moment transmitted
M_1 = secondary bending in upper member
M_2 = secondary bending in lower member
H = axial horizontal thrusts in the two members.

Assuming the center of gravity of the top and bottom chords separated by a vertical distance h, and with I_1 and A_1 for the upper and I_2 and A_2 for the lower moments of inertias and areas, then, we have a structure with two redundant reactions, say M_1 and H. Since $M_1 + M_2 + Hh = \Phi$

$$M_2 = \Phi - M_1 - Hh; \quad \frac{\partial M_2}{\partial M_1} = -1; \quad \frac{\partial M_2}{\partial H} = -h$$

On equating to zero the differential coefficients of the elastic energy of the upper and lower chords with respect to the redundants M_1 and H and simplifying

$$M_1\left(\frac{1}{I_1} + \frac{1}{I_2}\right) + \frac{Hh}{I_2} = \frac{\Phi}{I_2} \qquad [28]$$

$$M_1\frac{h}{I_2} + H\left(\frac{h^2}{I_2} + \frac{1}{A_1} + \frac{1}{A_2}\right) = \frac{\Phi h}{I_2} \qquad [29]$$

Case 3 is that of an opening transmitting both shear and bending (see Fig. 25*c*).

Let Φ = the bending moment at the center of the panel
S = total shear

then

$$S_2 = S - S_1$$

and

$$M_2 = \Phi - M_1 - Mh$$

where M_1, H, and S_1 are the redundant reactions.

For the upper member, we have, on either side of the mid-section

$$M = M_1 + S_1(a - x); \quad \frac{\partial M}{\partial M_1} = 1; \quad \frac{\partial M}{\partial S_1} = a - x$$

and

$$M = M_1 - S_1(a - x'); \quad \frac{\partial M}{\partial M_1} = 1; \quad \frac{\partial M}{\partial S_1} = -(a - x')$$

and likewise for the bottom chord

$$M = M_2 + S_2(a - x) = \Phi - M_1 - Hh + (S - S_1)(a - x)$$

$$\frac{\partial M}{\partial M_1} = -1; \quad \frac{\partial M}{\partial S_1} = -(a - x); \quad \frac{\partial M}{\partial H} = -h$$

and

$$M = M_2 - S_2(a - x) = \Phi - M_1 - Hh - (S - S_1)(a - x)$$

$$\frac{\partial M}{\partial M_1} = -1; \quad \frac{\partial M}{\partial S_1} = (a - x)_1 \quad \frac{\partial M}{\partial H} = -h$$

On substituting in the equations

$$\Sigma \int \frac{M}{EI_1}\frac{\partial M}{\partial M_1}dx + \Sigma \int \frac{M}{EI_2}\frac{\partial M}{\partial M_1}dx = 0$$

$$\Sigma \int \frac{M}{EI_1}\frac{\partial M}{\partial H}dx + \Sigma \int \frac{M}{EI_2}\frac{\partial M}{\partial H}dx + \frac{2Ha}{EA_1} + \frac{2Ha}{EA_2} = 0$$

$$\Sigma \int \frac{M}{EI_1} \frac{\partial M}{\partial S_1} dx + \Sigma \int \frac{M}{EI_2} \frac{\partial M}{\partial S_1} dx = 0$$

Then, by integrating and simplifying

$$M_1 \left(\frac{1}{I_1} + \frac{1}{I_2}\right) + \frac{Hh}{I_2} = \frac{\Phi}{I_2} \quad [30]$$

$$M_1 \frac{h}{I_2} + H \left(\frac{h^2}{I_2} + \frac{I}{A_1} + \frac{1}{A_2}\right) = \frac{\phi h}{I_2} \quad [31]$$

$$S_1 \left(\frac{1}{I_1} + \frac{1}{I_2}\right) = \frac{S}{I_2} \quad [32]$$

which, with the static relations

$$S_2 = S - S_1 \text{ and } M_2 = \Phi - M_1 - Hh$$

gives the bending moments, shears, and axial loading at the center section of the panel. It is to be noted that the points of contraflexure are no longer at the center but are shifted from it, depending upon the relative magnitude of the shear and bending moment.

Method of Superposition

The shearing loads divide according to case 1, which agrees with Equation [32]. Likewise Equations [28] and [29] for case 2 agree with Equations [30] and [31] of case 3. It is convenient, therefore, to estimate the shear loads for upper and bottom chord as for case 1 with pure shear action. Then, if a bending moment is transmitted through the panel to superimpose the secondary bending and axial loads according to Equations [30] and [31], we may readily estimate the reactions of the truss constraints on either side of the panel.

On solving [30] and [31], the secondary bending moments for the top and bottom members are

$$M_1 = \frac{\Phi}{\left(1 + \frac{I_1}{I_2}\right) + \frac{h^2}{I_2}\left(\frac{A_1A_2}{A_1 + A_2}\right)} \text{ (in-lb)} \quad [33]$$

$$M_2 = \Phi \left[1 - \frac{1}{\left(1 + \frac{I_1}{I_2}\right) + \frac{h^2}{I_2}\left(\frac{A_1A_2}{A_1 + A_2}\right)} - \frac{1}{1 + \frac{(I_1 + I_2)}{h^2A_1A_2}(A_1 + A_2)}\right] \text{(in-lb)} \quad [34]$$

$$H = \frac{\Phi}{h + \frac{I_1 + I_2}{hA_1A_2}(A_1 + A_2)} \text{ (lb)} \quad [35]$$

From a direct inspection of these equations, it will be noted that by increasing I_2, the bending moment in the upper chord or roof is decreased, so that to reduce bending stresses in the roof it is necessary to have deep longitudinal beams well connected as far back as two or three panels on either side of the opening in the floor system. This was carried out in the *Zephyr*.

The method is useful in estimating the constraint reactions brought on the truss on either side of the openings. While such reactions are distributed several panels back, a drastic loading assumption would be to assume the constraint reactions localized to one panel adjacent to the openings. It is also necessary to investigate the maximum bending moment in the vertical posts adjacent to the openings, approximately.

The slope i_A at A_1 can be approximated as follows (see Fig. 25*c*):

Let M_ϕ be the very small bending constraint offered by the post. Then for the redundant part of the top chord A_1B_1

$$M = R_2x = \left(\frac{S_1a + M_\phi}{b}\right) x; \quad \frac{\partial M}{\partial M_\phi} = \frac{x}{b}$$

Then $$i_{A1} = \int_0^b \frac{(S_1a + M_\phi)}{b^2} x^2dx = \frac{S_1ab}{3EI_1}$$

with $M_\phi = 0$.

Also $i_{A2} = \dfrac{S_2ab}{3EI_2}$, so that, since $\dfrac{S_1}{S_2} = \dfrac{I_1}{I_2}$; $i_{A1} = i_{A2}$ (approx.).

With the belt-rail constraint, the post will bend approximately as indicated, so that

$$\frac{M_p\left(\frac{h}{4}\right)^2}{2EI_p} = i_A; \quad M = \frac{32EI_p}{h^2} i_A; \quad I_p = \text{moment of inertia of}$$
the post.

Torsional Strength Through Step Wells and Openings

Because of rolling inertia couples, lateral forces, and jacking conditions, openings such as those through step wells must transmit large torsional loads which are superimposed on the main longitudinal bending loads previously discussed.

The characteristics for transmitting torsion depend greatly on the bulkhead partitions at either end of the step well. For instance, if the bulkheads are very rigid, a pure torque is applied by the truss to the openings. In this case, the roof takes a considerable share of the torsion. On the other hand, without any partition whatsoever, the torsional effect is manifested by a couple exerted on the main side frames, increasing the loading on one side frame and decreasing the loading on the other side frame. This torsional effect for the latter condition must be resisted at the opening by an increase of vertical shear loading for the longitudinal stringer or beam adjacent to the steps, and also at the center sills to a less extent, with a corresponding decrease for the members on the other side, while an additional resisting couple is exerted by vertical shear loadings of the roof rails. It is to be particularly emphasized that the roof rails continue as an integral part of the upper chord of the main truss, so that even without a partitition they are effectively brought into action. A little consideration will show that the shearing forces resisting torsion for either case, result in bending stresses which are superimposed on the main longitudinal bending stresses.

The two extreme cases discussed are shown in Fig. 26*a* and *b*, the actual case being a partial effect of both actions.

While the transverse shear forces at the roof and floor system are an effective couple, and also materially reduce the vertical shear forces causing bending in the longitudinal floor stringers and roof rail, their action postulates a rigid bulkhead partition. For this reason it was considered important that the torsional strength of the step well should be independent of the relative strength of the bulkhead and it was assumed that the entire torsional loading was resisted by vertical shear forces at points midway between partitions in the step well. The additional deep longitudinal step-well beams adjacent to the step well and extending back for two panels on either side of the well were designed to sustain the heavy torsional loads and relieve to a considerable extent the torsional vertical shear loadings in the roof rails.

Assuming, therefore, torsional loading resisted by vertical shear forces at points midway between partitions in the step well (Fig. 26*c*)

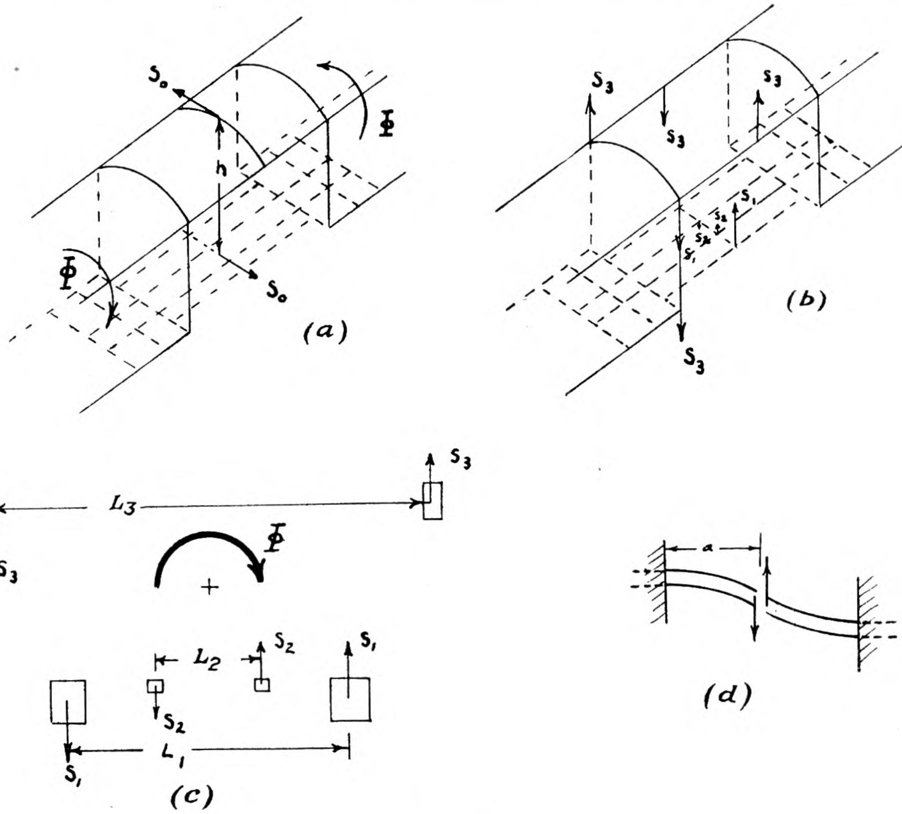

Fig. 26

where T = total torsional moment transmitted
L_1 = lateral distance between center sills
L_2 = lateral distance between longitudinal side step-well beams
L_3 = lateral distance between roof rails.

Then, the shear reactions at the points of contraflexure midway between the partitions are proportional to their lateral distances out and to the moments of inertias

$$S_1 = kL_1I_1; \quad S_2 = kL_2I_2; \quad \text{and } S_3 = kL_3I_3$$

so that the moments of resistance are

$$T = S_1L_1 + S_2L_2 + S_3L_3 = k(L_1^2I_1 + L_2^2I_2 + L_3^2I_3)$$

$$k = \frac{T}{I_1L_1^2 + I_2L_2^2 + I_3L_3^2}$$

$$S_1 = \frac{TL_1I_1}{I_1L_1^2 + I_2L_2^2 + I_3L_3^2}; \quad S_2 = \frac{TL_2I_2}{I_1L_1^2 + I_2L_2^2 + I_3L_3^2}$$

$$S_3 = \frac{TL_3I_3}{I_1L_1^2 + I_2L_2^2 + I_3L_3^2}$$

The bending moment resulting from torsion for any of the members has the form Sa (Fig. 26*d*), which is superimposed on the longitudinal bending.

9—INDETERMINATE FEATURES OF CONSTRUCTION

The assumption of a simple truss action for the main side frame is at best but a crude approximation of the actual action taking place in the car body. While the roof and belly were reinforced to the equivalent of heavy girders over and adjacent to the openings, it must be appreciated that more or less secondary bending exists throughout the entire roof and belly structure even for the non-reinforced portions.

The beams for the roof and belly structure are essentially continuous with considerably augmented moments of inertia at the approaches and over the openings and with the intervening truss reacting on these elements. An analysis along these lines for the entire car structure would obviously result in considerable redundancy. It is easy to see that the stiffness of the roof and belly reinforces the structure as a whole, reduces the deflections, and decreases, in general, the stresses in the truss, but at the expense of secondary bending in both roof and belly.

The secondary bending and shear loadings become of particular importance over door openings. It is appreciated that a thorough analysis would require consideration of the entire structure. However, due to the fact that the moments and shears are considerably augmented over and adjacent to the openings but gradually become damped to small values several panels away from such openings, a first approximation for secondary bending is to consider a portion of the structure including the opening and from two to three panels back on either side of the opening.

On this basis a study has been made, first, in the approaches two panels back on either side of the opening, and next, for one panel back on either side of the opening. In either case, the secondary bending at the terminal sections for the roof and belly was considered negligible.

For the case of two panels on either side of the opening, Fig. 27, case 1, shows a typical structure with the roof truss and belly separated. The applied loadings consist of the panel loadings and the reaction of the remaining truss on this portion, at one terminal section. At the other terminal section the reaction of the remaining truss consists of three elements, the bending moment, the total shear, and the equality of the axial loads for roof and belly. In addition, there are 18 truss members and 16 inter-

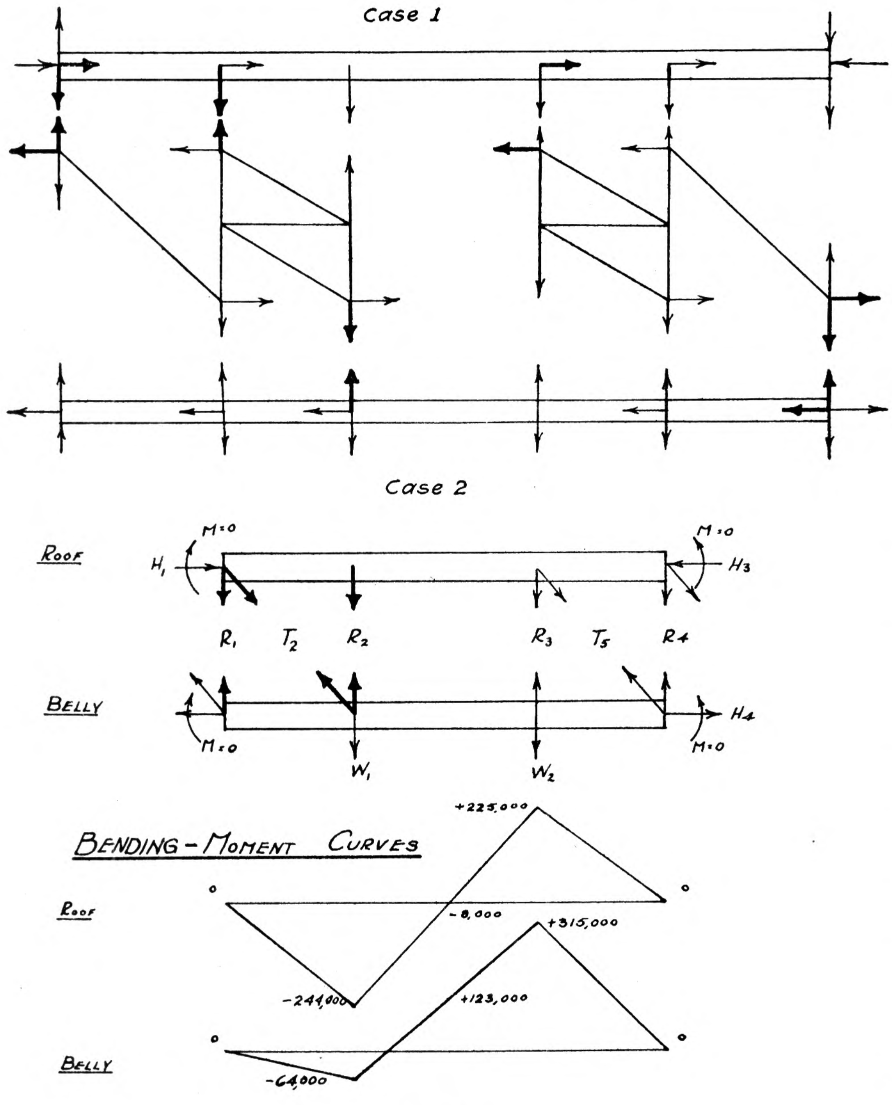

Fig. 27

actions between the roof and belly, respectively. Thus there is a total of 37 unknown quantities. For solution there are 12 joints or 24 equations with the six equilibrium equations for roof and belly, respectively, or a total of 30 equations. There are, therefore, seven redundant reactions. These are shown by heavy-lined vectors in Fig. 27.

For a crude approximation, the analysis for one-panel approaches is shown in Fig. 27, case 2. In this case, truss deflections have a marked effect on the distribution of secondary bending in both roof and belly. The applied loadings consist of the panel point loads, and the reaction of the remaining portion of the car structure at the terminal sections. However, the reactions at one terminal section must be determined from the three equations of equilibrium for the external forces, from which are determined the horizontal components H_3 and H_4 and the diagonal tension T_4. The truss reactions on the roof and belly consist of the reactions of the diagonal and vertical members of the truss within the terminal sections, a total of six unknowns. There are, however, six condition equations for the equilibrium of the roof and belly, respectively, but of these, three equations are required for the determination of the external forces. There are, then, but three equations for the determination of the six unknown internal reactions. The system, therefore, is redundant to the third degree.

The reactions R_1, T_2, and R_2 were chosen as the redundant reactions. For the determination of these reactions, the differential coefficients of the elastic energy for the truss roof and belly with respect to these redundants must be equated to zero.

The first terms apply for the truss members and axial components in roof and belly, and the second terms apply for the bending in roof and belly.

For an actual study, an approximation was made for the baggage-door opening in the *Zephyr*. The panel loads were taken at 2000 lb each and the bending-moment and shear reactions of the remaining portion of the truss at the forward terminal section consisted of 3,500,000 in-lb and 15,000 lb, respectively. The distance between the neutral axes of the roof and the belly is 70 in. The shear loading was taken by the tension in the diagonal. The moments of inertia of the roof and the belly are 2000 in.^{4} and 1000 in.^{4}, respectively. The panel spacings are 65 in. across the door and 30 in. across the bays. Areas of all of the truss members were taken at 1.5 sq in. and those of the roof and the belly at 15 sq in. each.

On expressing the loadings in the truss members and axial components in the roof and belly, as well as the bending moments, in terms of the applied loadings and the redundant reactions by the use of the condition equations of equilibrium for the various parts, and integrating for the differential coefficients for the bending in roof and belly, then, on summing up for the various differential coefficients with respect to the respective redundants, we have

$$1886.1R_1 + 1259.6R_2 + 1366.4T_2 + 14{,}121{,}000 = 0$$
$$1259.7R_1 + 933.5R_2 + 947.4T_2 + 9{,}893{,}000 = 0$$
$$1368.6R_1 + 947.4R_2 + 1168.5T_2 + 5{,}896{,}000 = 0$$

from which $R_1 = -17{,}126$ lb, $R_2 = -15{,}373$ lb, $T_2 = 27{,}476$ lb, and the stresses in the members were determined.

Bending-Moment Diagram for Roof and Belly

The bending moments in the roof and belly for case 2 are shown in Fig. 27. It will be noticed that the effect of the truss deflection causes unsymmetrical location of the points of contraflexure in the door opening for the top and bottom members, respectively, and a shifting toward the points of diagonal attachments. The shear forces were found to divide approximately in the ratio of the moments of inertia of roof and belly, respectively.

From a construction point of view we should infer from this analysis that, in order to obtain more symmetrical conditions of bending at door openings, it is desirable to cross-brace the approaching bays at the openings.

Secondary Bending in Truss Members

In order to show the relative importance of secondary bending for heavily gusseted short members and the relief of such stresses with longer members, the simple structure of Fig. 28 was analyzed. It consisted of a cantilever beam with a heavy tie member loaded at the end. The system has three redundants, M_0, S_0, and T_0, i.e., the bending moment at the joint, the transverse-shear reaction of the diagonal at the joint, and the axial tension along the diagonal.

If δ is the inclination of the diagonal, a and b the lengths of diagonal and horizontal members, I_a and I_b the corresponding moments of inertia, and A_a and A_b the areas of sections, then, for an applied load P_1

$$\begin{aligned} AM_0 + BS_0 + CT_0 &= K_1P \\ BM_0 + DS_0 + ET_0 &= K_2P \\ CM_0 + ES_0 + FT_0 &= K_3P \end{aligned}$$

where

$$A = \frac{a}{I_a} + \frac{b}{I_b};\; B = -\left[\frac{a^2}{2I_a} + \frac{b^2 \cos\delta}{2I_b}\right];\; C = \frac{b^2 \sin\delta}{2I_b}$$

$$D = \frac{a^3}{3I_a} + \frac{b^3\cos^2\delta}{3I_b} + \frac{b\sin^2\delta}{A_b};\quad K_1 = \frac{b^2}{2I_b}$$

$$E = \left(\frac{b}{A_b} - \frac{b^3}{3I_b}\right)\sin\delta\cos\delta;\; K_2 = -\frac{b^3}{3I_b}\cos\delta$$

$$F = \frac{b^3}{3I_0}\sin^2\delta + \frac{a}{A_a} + \frac{b\cos^2\delta}{A_b};\quad K_3 = \frac{b^3}{3I_b}\sin\delta$$

From these equations M_0, S_0, and T_0 were determined.

Three designs, with moments of inertia $I_a = I_b$ of 0.1754, 0.2301, and 0.3206 in.[4] were considered so that the ratios of a/I_a are 172.8, 131.5, and 94.5, respectively, and b/I_b = 124.0, 95.6, and 68, respectively.

The bending M_0 at the load joint was found to have values of 354, 479, and 669 in-lb, thus consistently increasing with decreased ratios of a/I_a and b/I_b. Likewise the bending moment at the fixed end of the diagonal member increased by 221, 262 to 345 in-lb, and the bending moment at the fixed end of the horizontal member increased much more rapidly from 1172, 1527 to 2089 in-lb. The axial stresses were practically unaffected retaining these simple statical values.

The stresses in the longer diagonal member were very little affected by secondary bending but the compression in the horizontal was materially increased by bending.

From this it can be concluded that secondary bending at the gusset connections, particularly for short members, may result in high stress concentrations in the gussets unless due allowance is made for additional torsional-shear stresses. This is particularly true for short horizontal members with diagonal trussing. It was considered an important problem in the articulated end-frame truss.

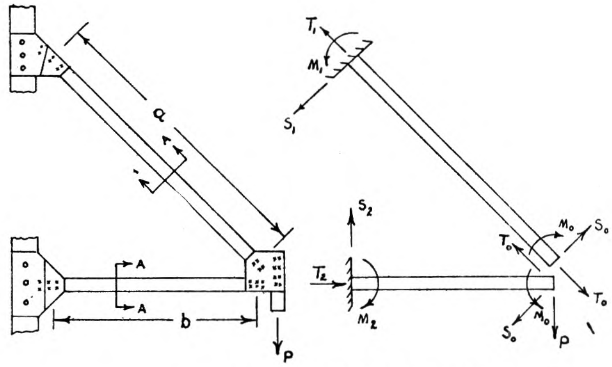

Section A-A

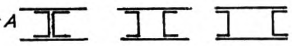

$I_a = I_b$	0	0.1754	0.2301	0.3206
a/I	∞	172.8	131.5	94.5
b/I	∞	124.0	95.6	68.0
M_0	0	354	479	669
M_1	0	221	262	345
M_2	0	−1172	−1527	−2089
S_0	0	4.4	7.15	10.7
$T_0 = T_1$	7070	6978	6949	6904
T_2	5000	4936	4918	4889
Stress in Diagonal Member				
Bending	0	1880	1710	1610
Axial	15,040-T	14,820-T	14,790-T	14,700-T
Maximum	15,040-T	16,700-T	16,500-T	16,310-T
Stress in Horizontal Member				
Bending	0	10,000	9940	9780
Axial	10,640-C	10,500-C	10,470-C	10,400-C
Maximum	10,640-C	20,500-C	20,410-C	20,180-C

Fig. 28

The Deflection of Car Structure and Interaction With Heavy Center Sills or Longitudinal Floor Girders

At each panel point there is a redundant reaction between the car truss and center sill or floor girder. Evidently with a long truss such a system would be very indeterminate. For this reason the following approximate method is useful in determining the common deflection curve and the interactions between the car truss and girder. The common deflection curve can be represented by the trigonometric series

$$y = a_1 \sin\frac{\pi x}{l} + a_2 \sin\frac{2\pi x}{l} + a_3 \sin\frac{3\pi x}{l}\ldots$$

The potential energy of the total system, including both truss and girder, is

$$V = \frac{EI_1}{2}\int_0^l \left(\frac{d^2y^2}{dx^2}\right) dx + \frac{EI_2}{2}\int_0^l \left(\frac{d^2y}{dx^2}\right)^2 \ldots\ldots [36]$$

where the equivalent moment of inertia of the truss is I_1 and for the girder I_2. Also

$$\frac{d^2y}{dx^2} = -\frac{\pi^2}{l^2}a_1 \sin\frac{\pi x}{l} - \frac{4\pi^2}{l^2}\sin\frac{2\pi x}{l}\ldots \text{etc.}$$

On squaring and noting terms as $\int_0^l \sin\frac{n\pi x}{l}\sin\frac{m\pi x}{l}\,dx = 0$

while $\int_0^l \sin^2\frac{n\pi x}{l}\,dx = \frac{l}{2}$

we have from [36]

$$V = \frac{E(I_1 + I_2)^4}{4l^3}\sum_{n=1}^{n=\infty} n^4a^2 \ldots\ldots\ldots\ldots [37]$$

Now the variations of the deflection at panel points are

$$\delta y_1 = \delta a_1 \sin\frac{\pi x_1}{l} + \delta a_2 \sin\frac{2\pi x_1}{l}\ldots\text{(at panel 1)}$$

$$\delta y_2 = \delta a_1 \sin\frac{\pi x_2}{l} + \delta a_2 \sin\frac{2\pi x_2}{l}\ldots\text{(at panel 2)}$$

The work of the extraneous forces on the system equals the change in the elastic energy of the system, hence

$$W_1\delta y_1 + W_2\delta y_2 \ldots \int w dx \delta y = \delta V$$

and $$W_1\left(\sin\frac{\pi x_1}{l}\,\delta a_1 + \sin\frac{2\pi x_1}{l}\,\delta a_2 \ldots\right) + W_2\left(\sin\frac{\pi x_2}{l}\,\delta a_1 + \sin\frac{2\pi x}{l}\,\delta a_2 \ldots\right) + \int_0^l w\sin\frac{\pi x}{l}\,dx\,\delta a_1 + \int_0^l w\sin\frac{2\pi x}{l}\,dx\delta a_2 = \frac{\partial V}{\partial a_1}\,\delta a_1 + \frac{\partial V}{\partial a_2}\,\delta a_2 \ldots\ldots [38]$$

Due to the independence of the coordinates a_1, a_2, etc., we have, finally

$$\left(W_1\sin\frac{n\pi x_1}{l} + W_2\sin\frac{n\pi x_1}{l}\ldots\frac{2l}{n^*\pi}\,w\right) = \frac{E(I_1+I_2)\pi^4}{2l^3}\,n^4a_n$$

$$\therefore a_n = \frac{2\left(W_1\sin\frac{n\pi x_1}{l} + W_2\sin\frac{n\pi x_2}{l}\ldots + \frac{2l}{n^*\pi}\,w\right)l^3}{n^4\pi^4E(I_1+I_2)}$$

where n^* applies to odd harmonics only. The deflection curve is, therefore

$$y = \frac{2l^3}{\pi^4E(I_1+I_2)}\sum_{n=1}^{n=\infty}\left(W_1\sin\frac{n\pi x_1}{l} + W_2\sin\frac{n\pi x_2}{l}\ldots + \frac{2l}{n^*\pi}\,w\right)\sin\frac{n\pi x}{l}$$

In a first approximation, taking the first term in the series, we have for the approximate deflection curve

$$y = \frac{2l^3}{\pi^4E(I_1+I_2)}\left(w_1\sin\frac{\pi x_1}{l} + W_2\sin\frac{\pi x^2}{l}\ldots\frac{2l}{\pi}\,w\right)\sin\frac{\pi x}{l}$$

where W_1, W_2, etc., are the panel loads at x_1 and x_2, and w is the dead load per inch run.

For the reactions between the truss and girder, neglecting the distributed load w, or assuming it concentrated at the panel points, we have

$$\left(R_1\sin\frac{n\pi x_1}{l} + R_2\sin\frac{n\pi x_2}{l}\ldots\right) = \frac{\pi^4EI_2n^4a_n}{2l^3}$$

$$\left(W_1\sin\frac{n\pi x_1}{l} + W_2\sin\frac{n\pi x_2}{l}\ldots\right) = \frac{\pi^4E(I_1+I_2)n^4a_n}{2l^3}$$

Hence

$$\left(\frac{R_1}{I_2} - \frac{W_1}{I_1+I_2}\right)\sin\frac{n\pi x_1}{l} + \left(\frac{R_2}{I_2} - \frac{W_2}{I_1+I_2}\right)\sin\frac{n\pi x_2}{l}\ldots\ldots = 0$$

so that

$$R_1 = W_1\left(\frac{I_2}{I_1+I_2}\right);\ R_2 = W_2\left(\frac{I_2}{I_1+I_2}\right);\ \ldots\text{etc.}$$

and the loadings on the truss structure alone are

$$(W_1 - R_1);\ (W_2 - R_2);\ \ldots\text{etc.}$$

It is therefore evident that with a deep truss and large I_1 the reactions of center sills, unless very deep, have no appreciable effect on the truss. The same arguments apply to the roof structure in parallel with the truss.

GENERAL CONCLUSIONS

The comparative study of standard heavy-weight railway equipment with that of streamlined light-weight construction amply justifies the conclusion that streamlined light-weight trains may be used to advantage by the railroads of the United States. Greater economy, higher performance, greater safety, greater relative strength, and improved comfort will obtain by this radical departure from standard practise.

The analyses of the various construction elements indicate the sound engineering upon which this development rests. Larger units of greater capacity to meet the varied requirements of railroad operation may well be developed along similar lines.

ACKNOWLEDGMENTS

The *Zephyr* was designed and constructed by the Hi-Tensile Division of the Edward G. Budd Manufacturing Company under the direction of F. H. Russell, and is a product of its Engineering Department, composed of Col. E. J. W. Ragsdale, chief engineer, and the following associate engineers: Walter Dean, Albert Dean, Stanford Landell, and William J. Mayer. The assistance of Joseph Winlock, director of the Metallurgical Laboratories of the Budd Company has been of constant value. To these gentlemen and their staffs, the author is indebted.